

University of New Hampshire

University of New Hampshire Scholars' Repository

Doctoral Dissertations

Student Scholarship

Fall 2020

DEMOGRAPHY OF A RECOVERY: TRACKING THE REBOUND OF LITTLE BROWN BAT (MYOTIS LUCIFUGUS) POPULATIONS

Katherine Ineson

University of New Hampshire, Durham

Follow this and additional works at: <https://scholars.unh.edu/dissertation>

Recommended Citation

Ineson, Katherine, "DEMOGRAPHY OF A RECOVERY: TRACKING THE REBOUND OF LITTLE BROWN BAT (MYOTIS LUCIFUGUS) POPULATIONS" (2020). *Doctoral Dissertations*. 2529.

<https://scholars.unh.edu/dissertation/2529>

This Dissertation is brought to you for free and open access by the Student Scholarship at University of New Hampshire Scholars' Repository. It has been accepted for inclusion in Doctoral Dissertations by an authorized administrator of University of New Hampshire Scholars' Repository. For more information, please contact nicole.hentz@unh.edu.

DEMOGRAPHY OF A RECOVERY: TRACKING THE REBOUND OF LITTLE BROWN
BAT (*MYOTIS LUCIFUGUS*) POPULATIONS

BY

Katherine M. Ineson

Baccalaureate degree (BA), Boston University, 2012

DISSERTATION

Submitted to the University of New Hampshire

in Partial Fulfillment of

the Requirements for the Degree of

Doctor of Philosophy

in

Natural Resources & Earth Systems Science

September, 2020

ALL RIGHTS RESERVED
© 2020
Katherine M. Ineson

This dissertation has been examined and approved in partial fulfillment of the requirements for the degree of Doctor of Philosophy in Natural Resources & Earth Systems Science by:

Dissertation Co-Director, Rebecca J. Rowe
Associate Professor of Natural Resources & the Environment
University of New Hampshire

Dissertation Co-Director, Jeffrey T. Foster
Associate Professor of Biological Sciences
Northern Arizona University

Adrienne Kovach
Associate Professor of Natural Resources & the Environment
University of New Hampshire

Erik Blomberg
Associate Professor of Wildlife Ecology
University of Maine

Jonathan Reichard
Assistant National White-nose syndrome Coordinator
United States Fish & Wildlife Service

On July 28, 2020

Approval signatures are on file with the University of New Hampshire Graduate School.

DEDICATION

To Dr. Thomas Kunz,
for introducing me to the world of bats,
inspiring me to pursue research,
and being a role model in his dedication to conservation.

ACKNOWLEDGEMENTS

I first have to thank my committee, especially my original advisor, Jeff Foster, who took me on as a graduate student and helped me cobble together funding to support my research ideas. Becca Rowe generously adopted me into her lab and became my co-advisor halfway through graduate school. With both Jeff and Becca as advisors, I feel I've had the best of both worlds in advising styles as well as endless encouragement. Jon Reichard has been a constant supporter since before graduate school and suggested I apply to the University of New Hampshire (UNH) to work with Jeff in the first place. Jon, along with Erik Blomberg and Adrienne Kovach, have provided important guidance in population ecology, bat biology, and fieldwork. Together, my committee has allowed me room to explore different avenues while also keeping me focused on the key questions.

I am grateful for my two lab groups, the Foster and Rowe labs, from whom I learned about many other aspects of biology, from genetics to community ecology. They provided important feedback on grant proposals, manuscripts, and presentations over the years. A big thank you goes to Katy Parise for testing hundreds of samples for me and being a key sounding board for my lab work. Matt MacManes gave me some time and space to work in his lab, allowing me to finish my telomere study. My fieldwork would not have been possible without the help of several UNH undergraduates, including Kim Celona, Joe Poggi, Liv Fortuna, Veronica Bodge, and Alexa DeMember, who were hardworking, patient, and willing to stay up to all hours of the night to help me catch bats. Family, friends, volunteers, and my lab mate, Meghan Ange, were also critical in providing assistance in the field.

The extent and scope of my research would not have been possible without the fieldwork of numerous other graduate students from Dr. Thomas Kunz's lab at Boston University (BU) over the last nearly 30 years, including Scott Reynolds, Jon Reichard, Chris Richardson, Nate Fuller, Kate Langwig, and Marianne Moore. Several of them I have known since I was an undergraduate at BU and they have all become colleagues, collaborators, or mentors. In turn, our fieldwork would not have been possible without the support of the landowners. I thank them for access to their property, their hospitality, and their willingness to provide for and protect hundreds of bats roosting in their barns. I am also grateful to the Massachusetts Department of Conservation and Recreation for access to an important little brown bat colony in Moore State Park as well as their staff, particularly Amanda Melinchuk. State and federal wildlife agency personnel from Massachusetts, New Hampshire, and Vermont have also played an important role in locating, protecting, and studying bat colonies in the region, which helped jumpstart some of my research.

The community of the UNH Natural Resources and Earth Systems Science (NRESS) PhD Program has been amazing. While our research is diverse, we always cheer on and learn from each other. The sense of community has grown, even as students come and go. I'd especially like to thank Lynne Cooper, our program director, and Steve Frolking, the program chair, for their support academically, emotionally, and financially.

My family has been incredibly supportive over the last five years. My mom, Sue Gillman, has endured many nights of mosquitoes to help me conduct emergence counts and record data during bat captures. Lastly, I want to thank my husband, Drew Ineson, for sitting through multiple rounds of practice talks, making motivational playlists, and giving constant encouragement.

Funding to support my research was provided by the University of New Hampshire NRESS Student Support Fund, the American Society of Mammalogists: Grants-in-Aid of Research, the American Museum of Natural History Theodore Roosevelt Memorial Fund, the Roger Williams Park Zoo Sophie Danforth Conservation Biology Fund, and a United States Fish & Wildlife Service White-nose Syndrome grant (F17AP00588). Further support was provided by the New Hampshire Agricultural Experiment Station as part of the USDA National Institute of Food and Agriculture McIntire-Stennis Project (NH00080-M). The UNH Graduate School helped fund travel to several conferences, provided summer funding through several Summer Teaching Assistantship Fellowships, and supported my final academic year with a Dissertation Year Fellowship.

TABLE OF CONTENTS

DEDICATION	iii
ACKNOWLEDGEMENTS	iv
LIST OF TABLES	ix
LIST OF FIGURES	xi
ABSTRACT	xv

CHAPTER	PAGE
1. AMBIGUITIES IN USING TELOMERE LENGTH FOR AGE DETERMINATION IN TWO NORTH AMERICAN BAT SPECIES	1
Abstract	1
Introduction	2
Methods	6
Results	12
Discussion	15
2. WHITE-NOSE SYNDROME AND CLIMATE INFLUENCE LIFE HISTORY AND REPRODUCTIVE PHENOLOGY IN LITTLE BROWN BATS	29
Abstract	29
Introduction	30
Methods	35
Results	43
Discussion	48

3. RETURN OF THE LITTLE BROWN BAT: LONG-TERM SURVIVAL AND POPULATION RECOVERY IN A WHITE-NOSE SYNDROME-IMPACTED SPECIES	67
Abstract	67
Introduction	68
Methods	71
Results	82
Discussion	87
LITERATURE CITED	113
APPENDICES	136
APPENDIX A IACUC APPROVAL FOR USE OF ANIMALS IN RESEARCH	136
APPENDIX B SUPPLEMENTARY FIGURES FOR CHAPTER ONE	139

LIST OF TABLES

<p>Table 1.1. Summary of multiple linear regression models of relative telomere length and chronological age in big brown bats (<i>Eptesicus fuscus</i>) sampled in and near Fort Collins, Colorado, 2005–2015. Linear, quadratic, cubic, and null regression models were considered and ranked by AICc. Coefficient estimates are shown for each model. K = number of parameters; logLik = log likelihood; w_i = model weight.</p>	21
<p>Table 1.2. Summary of linear mixed models of relative telomere length and predictor variables in little brown bats (<i>Myotis lucifugus</i>) sampled in New England, 2016–2019. Linear and quadratic age terms were considered along with wing score (WS) and reproductive status (Rep) at the time of capture. Models were ranked by AICc. Coefficient estimates are shown for each model. K = number of parameters; logLik = log likelihood, w_i = model weight.</p>	22
<p>Table 1.3. Summary of linear mixed models of relative telomere length and predictor variables in little brown bats (<i>Myotis lucifugus</i>) sampled in New England, 2016–2019, and tested for <i>Pseudogymnoascus destructans</i> (Pd). Models were ranked by AICc. Coefficient estimates are shown for each model. Pd = Pd status (positive or negative) at time of capture; K = number of parameters; logLik = log likelihood, w_i = model weight.</p>	23
<p>Table 2.1. Top five multiple linear regression models of climate variables and reproductive timing. Mean lactation date was estimated from pooled adult reproductive status data and mean date of birth was estimated from little brown bat pup epiphyseal gap size. Coefficient estimates are shown for each model. Models are ranked by AICc. AM = Apr + May, Spr = Spring, P = total precipitation, T = temperature, WNS = pre-/post-WNS, K = number of parameters; logLik = log likelihood; w_i = model weight.</p>	56
<p>Table 2.2. Top five linear regression models of climate variables and reproductive synchrony (middle 50% of births). Coefficient estimates are shown for each model. Models are ranked by AICc. T = temperature, P = precipitation, WNS = pre/post-WNS, K = number of parameters; logLik = log likelihood; w_i = model weight.</p>	57
<p>Table 2.3. Top five linear mixed-effects models of estimated parturition timing with maternity colony and individual ID as random effects and mass, wing score, and year as fixed effects. Model sets were created with and without fungal load data from wing swabs tested for the causative agent of white-nose syndrome, <i>Pseudogymnoascus destructans</i> (Pd). Coefficient estimates are shown for each model. Models are ranked by AICc. K = number of parameters; logLik = log likelihood; w_i = model weight.</p>	58
<p>Table 3.1. Historic (pre-2016) and current (2016–2019) data types collected at eight little brown bat maternity colonies in New England. Counts are emergence counts conducted in the field. Banded bats represent the total number of unique banded females at each site. Superscript letters next to colony name indicate that data from that colony has been used in a published study.</p>	96

Table 3.2. Model selection for Cormack-Jolly-Seber mark-recapture models using banding data from eight little brown bat maternity colonies in New England. Models are ranked by AICc. ϕ = survival; p = recapture rate; K = number of model parameters; w = model weight; a = age; t = time; g = colony; ad = adult; j = juvenile; $.$ = constant; T = linear time trend. 97

Table 3.3. White-nose syndrome invasion timeline models for survival using banding data from eight little brown bat maternity colonies in New England. All models included the recapture model $p(t+a+g)$. Models are ranked by AICc. The first year for pre-invasion, invasion front, epidemic, and established is included for each timeline: $dis1 = 2006, 2008, 2009, 2012$; $dis2 = 2006, 2008, 2009, 2011$; $dis3 = 2006, 2008, NA, 2012$; $dis4 = 2006, 2008, 2010, 2012$. ϕ = survival; K = number of model parameters; w = model weight; a = age class; g = colony. 98

Table 3.4. Climate models for survival using banding data collected at eight little brown bat maternity colonies in New England. Site-specific weather variables were calculated using data from six weather stations (www.ncdc.noaa.gov). All models included the recapture model $p(t+a+g)$. Models are ranked by AICc. ϕ = survival; K = number of model parameters; w = model weight; a = age class; g = colony; t = time. 99

Table 3.5. Robust design model selection results for passive integrated transponder tagging data from the Lincoln and Charlestown little brown bat maternity colonies. All models included $p(t)=c(t)$ for time-dependent recapture rates and $\gamma'(0)=\gamma''(1)$, indicating a ‘no movement’ model. Models are ranked by AICc. S = survival; K = number of model parameters; w = model weight; a = age; g = colony; t = time; $.$ = constant. 100

LIST OF FIGURES

- Figure 1.1. The relationship between relative telomere length and age in A) PIT-tagged big brown bats (*Eptesicus fuscus*) sampled in and near Fort Collins, Colorado, 2005–2015 and B) banded little brown bats (*Myotis lucifugus*) sampled in New England, 2016–2019. Bats marked as juveniles (closed triangles; known-age) and adults (open circles; minimum known-age) were combined in the model analysis. The dashed black line indicates a best-fit regression through the data where significant. 24
- Figure 1.2. The relationship between little brown bat (*Myotis lucifugus*) relative telomere length and A) wing score, where 0 indicates no damage and 2 indicates moderate to high levels of wing damage, and B) Pd status for individuals that tested negative (N) or positive (P) for *Pseudogymnoascus destructans* (Pd), the fungus that causes white-nose syndrome in bats. Bats were captured in New England, 2016–2019. Points represent mean RTL and bars represent +/- standard error. Letters indicate significantly different means among groups. 25
- Figure 1.3. Changes in relative telomere length between years, with samples collected from individual little brown bats (*Myotis lucifugus*) connected by dashed lines. Bats shown here were sampled twice over intervals of one to three years in New England, 2016–2019. 26
- Figure 1.4. Correlation in relative telomere length (RTL) between wing (biopsy), mucosal epithelial (buccal), and gastrointestinal epithelial (guano) tissues collected from the same individual little brown bats (*Myotis lucifugus*) in New England, 2016–2019. All three tissue types were not collected from every individual. Note that scales differ between graphs. 27
- Figure 1.5. Boxplot showing relative telomere length variation within and among sample types. Wing (biopsy), mucosal epithelial (buccal), and gastrointestinal epithelial (guano) tissues were collected from the same individual little brown bats (*Myotis lucifugus*) in New England, 2016–2019. Letters indicate significantly different means among groups. 28
- Figure 2.1. Map of little brown bat (*Myotis lucifugus*) maternity colonies studied for 4–16 years between 1993–2019, pre-white-nose syndrome (WNS) arrival in orange and post-WNS arrival in green. Diamonds are weather station locations (www.ncdc.noaa.gov) used to create a regional climate summary. Stars represent known hibernacula for bats from these maternity colonies. ... 59
- Figure 2.2. Boxplots of annual reproductive rates for little brown bat (*Myotis lucifugus*) yearlings (banded as juveniles and recaptured the following year) and adults, captured pre- and post-WNS from 1993–2019. Lowercase letters show significant differences between groups based on Tukey’s multiple comparison of means. 60

Figure 2.3. Correlation between mean date of birth estimated from little brown bat pup epiphyseal gap size compared to mean lactation date estimated from pooled adult reproductive status data. Bats were captured at maternity colonies in New England from 1993–2019. Each dot shows a year when both sets of data were available. The light gray dashed line shows a 1:1 reference line. The solid line is a linear regression and the black dashed line has the same slope as the regression, but with a y-intercept seven days earlier. The gray ribbon is the 95% confidence interval. 61

Figure 2.4. Reproductive phenology of little brown bats at maternity colonies in New England based on the proportion of pregnant (open triangles, dashed lines) and lactating bats (open circles, solid lines) out of the total number of adult females captured on a given sampling night. Adult reproductive data from pre- and post-WNS were pooled. Curves are non-linear least squares fits to the data. The intersection between the pregnancy and lactation curves represents the median parturition date. 62

Figure 2.5. Relationships between reproductive timing and climate variables for little brown bats in maternity colonies in New England pre- and post-WNS. Mean lactation date (A & B) was estimated from pooled adult reproductive status data and mean date of birth (C & D) was estimated from little brown bat pup epiphyseal gap size. Total April and May precipitation (A & C) and mean May temperature (B & D) are regional means calculated from six weather stations in the study area. Regression lines are in color when pre-/post-WNS was a significant factor in the multiple linear regression model and in black when not significant. 63

Figure 2.6. Reproductive synchrony of the middle 50% of births in little brown bats pre- and post-WNS related to A) mean June precipitation and B) mean May temperature. Date of birth was estimated from pup epiphyseal gap size. Mean June precipitation and May temperature are regional means calculated from six weather stations in the study area. Regression lines are in color when pre-/post-WNS was a significant factor in the multiple linear regression model and in black when not significant. 64

Figure 2.7. For two little brown bat colonies in New England, the relationship between timing of arrival A) for individuals between years and B) estimated parturition date based on gestation stage at time of capture. Arrival time is the earliest passive integrated transponder tag detection of the year. In A, the solid line is a linear regression and the dashed gray lines represent a 1:1 reference line. In B, bars show length of time for the estimated gestation stage (+/- 0.5 to 1.5 weeks) and the dashed gray lines are 40-, 50-, and 60-day gestation periods, assuming gestation is initiated upon arrival at the maternity colony. The open diamond is the estimated date of birth for the pup of the female first detected on April 28 (red point directly above). 65

Figure 2.8. Timing of parturition assessed by gestation stage at time of capture for little brown bats captured post-WNS (2016–2019) in New England maternity colonies in relation to A) wing damage due to WNS, assessed by wing score from 0 to 3; B) bat mass at time of capture; C) fungal load of the causative agent of white-nose syndrome, *Pseudogymnoascus destructans* (Pd); and D) sampling year. Lower case letters indicate significant differences between groups based on results from Tukey’s multiple comparison of means. Solid lines in B and C are linear regression best-fit lines by year. 66

Figure 3.1. Available mark-recapture and emergence count data (black boxes) by year from eight little brown bat maternity colonies. Dashed vertical lines separate the approximate pre-invasion (blue), invasion front (orange), epidemic (red), and established (dark red) phases of white-nose syndrome arrival and spread in New England. 101

Figure 3.2. Correlations between field and infrared (IR) video emergence counts of little brown bats at the Lincoln (2010–2019), Paxton (2010–2011), Newfane (2018–2019), and Charlestown (2018–2019) maternity colonies. Solid lines are linear regressions and gray ribbons are 95% confidence intervals. 102

Figure 3.3. A pre-breeding census, female-based, life cycle graph for little brown bats, consisting of two stages, yearling and adult. Survival of juveniles (s_j) is from birth (which occurs immediately after the census) through their first winter to the next pre-breeding census. Yearling bats then survive their second winter with the same probability (s_a) as older adults. Fecundity or the probability that a female will reproduce each year (f) is divided by two, assuming an equal offspring sex ratio, to represent only daughters returning to the maternity colony in subsequent years. On the right is the corresponding Lefkovich population matrix representing the change in yearling (N_1) and adult (N_a) population sizes from time t to $t + 1$ 103

Figure 3.4. Directed acyclic graph without the priors for an integrated population model in a Bayesian framework. Circles indicate model parameters: fecundity (f), colony size (N), juvenile survival (s_j), adult survival (s_a), and observation error (σ^2). The green circle indicates that recapture rate (p) is a nuisance parameter. Boxes indicate the data: number of reproductive females (B), number of captured adult females (J), emergence counts (y), and mark-recapture data (m). The large boxes indicate the three submodels within the integrated population model. Recreated from Kéry and Schaub (2012). 104

Figure 3.5. Adult colony census data from little brown bat maternity colonies, collected from early to mid-June between 2008 and 2020 via emergence counts in the field or from infrared video. 105

Figure 3.6. Prevalence and load (\log_{10}) of *Pseudogymnoascus destructans* (Pd) on little brown bats (A & C) and on roost surfaces (B & D) at summer maternity colonies sampled from 2016–2019. Lines are LOESS fits of the data. 106

Figure 3.7. Apparent survival estimates for adult and juvenile little brown bats using banding data from eight maternity colonies in New England. Model structure was $\phi(\text{time+age+colony})$ $p(\text{time+age+colony})$. Error bars represent 95% confidence intervals. The black dashed line represents the mean survival rate by year for all sites combined. The vertical dashed gray line represents the start of white-nose syndrome invasion in the region. 107

Figure 3.8. Apparent survival estimates for adults (A) and juveniles (J) by disease invasion phase using banding data collected at maternity colonies of little brown bats in New England. Model structure for survival included age and a disease invasion timeline (dis) of pre-invasion in 2006, invasion front in 2008, epidemic in 2009, and established in 2012: $\phi(\text{age}+\text{dis})$ $p(\text{time}+\text{age}+\text{colony})$. Error bars represent 95% confidence intervals. 108

Figure 3.9. Annual colony size (black line), age-dependent apparent survival, and colony growth rate estimates from integrated population models for three little brown bat maternity colonies. Error bars and gray ribbons are 95% credible intervals. Black triangles are early- to mid-June emergence counts collected in the field or from infrared video. 109

Figure 3.10. Comparison of annual apparent survival estimates for adults (A) and juveniles (J) at the Lincoln maternity colony (2016–2019) from three different models: a Cormack-Jolly-Seber (CJS) model using banding data, an integrated population model (IPM) using banding and emergence count data, and a robust design (RD) model using passive integrated transponder tag data. 110

Figure 3.11. Correlations between estimated annual demographic rates and colony growth rate for the Paxton little brown bat colony from 2008 to 2019. Error bars are 95% credible intervals for both the demographic and growth rate estimates. Correlation coefficients (r) are shown with 95% credible intervals. $P(r>0)$ is the probability of a positive correlation. 111

Figure 3.12. Colony size projections for 2020 to 2030 using a population viability analysis within an integrated population model under four different management scenarios for the A) Charlestown and B) Lincoln little brown bat maternity colonies. The black line shows colony size estimates and the dashed gray line indicates the start of the population projection. Management scenarios included “no action” (maintaining status quo), increasing juvenile (J) survival, increasing adult (A) survival, and increasing both juvenile and adult survival. Increases in survival were 10% on the log scale. The purple ribbon shows 95% credible intervals for the “no action” strategy with no additional human intervention beyond current measures. 112

ABSTRACT

DEMOGRAPHY OF A RECOVERY: TRACKING THE REBOUND OF LITTLE BROWN BAT (*MYOTIS LUCIFUGUS*) POPULATIONS

By

Katherine M. Ineson

University of New Hampshire, September, 2020

As the emergence of novel diseases in wildlife becomes more common, a better understanding of the impact of disease on populations and their demographic rates will be critical for their conservation. Populations naturally fluctuate over time as a function of the rates of birth, death, immigration, and emigration, while at the individual level the chances of mortality and reproduction may be influenced by age and physiological condition. Diseases, particularly emerging infectious diseases, can cause immediate and severe changes in demographic rates. While some populations and species may go extinct due to high mortality rates, others may persist in smaller, but stable numbers by evolving, adapting, or demographically responding. Diseases can also have sublethal impacts that may differentially effect individuals, sexes, or ages and may threaten the viability of a population. White-nose syndrome (WNS) is a recently emerged fungal disease that infects hibernating bats in North America. Little brown bat (*Myotis lucifugus*) populations have declined in some areas by more than 90%, but have stabilized in

remnant winter and summer colonies. In this study I investigated the long-term impacts of WNS and changes in demographic rates on little brown bat populations in New England.

Age-related demographic rates are often important to understand for conservation and management, but are hard to determine in long-lived species with no clear external indicators of age. In Chapter 1, I investigated whether relative telomere length could be used as a genetic marker of age for little brown and big brown bats (*Eptesicus fuscus*). I found that in big brown bats, there was a quadratic relationship with chronological age, where middle-aged individuals had the longest telomeres. For little brown bats, individuals with more wing damage due to WNS had shorter telomeres, suggesting an impact of disease on their physiological condition. Finding no relationship of telomere length to chronological age, little brown bats should, for now, continue to be grouped as either juveniles or adults, which may be appropriate as there is little evidence for senescence in *Myotis* bats.

In Chapter 2, I compared yearling (one-year-old) and adult reproductive rates using banding records from an extensive study at one summer maternity colony prior to WNS and from work at eight colonies since WNS emerged. I found that yearling reproductive rates have significantly increased and are now very similar to the observed adult reproductive rate of 0.95, suggesting a shift in life-history related to age of first reproduction. I also found that reproductive phenology has advanced by 6–10 days, most likely driven by warming spring temperatures, but also potentially as a response to WNS. Earlier reproduction could benefit offspring by giving them more time to accumulate fat stores before hibernation, thus increasing the chances of first-winter survival and reproduction as yearlings. Bats with more wing damage due to WNS had later parturition dates, suggesting that the energetic costs of infection delay reproduction for individuals, but are not delaying the overall timing of reproduction at the population level.

Long-term survival rates are also important to understand for population modeling. In Chapter 3, I used mark-recapture and colony count data to estimate survival in three different types of population models. I found that survival estimates were similar among models and showed that survival probabilities were lowest immediately after WNS invasion, but have since returned to or surpassed pre-WNS survival probabilities. Juvenile survival was lower than adult survival, but was generally higher than those reported from pre-WNS. I then used these survival estimates and the reproductive rates from Chapter 2 to conduct population viability analyses under different management strategies, which showed colony growth even without additional human intervention. These findings suggest that little brown bat populations in New England have responded to WNS and are beginning to rebound, but some management actions that boost survival could help ensure long-term recovery.

CHAPTER 1

AMBIGUITIES IN USING TELOMERE LENGTH FOR AGE DETERMINATION IN TWO NORTH AMERICAN BAT SPECIES¹

Abstract

The age of an animal, determined by time (chronological age) as well as genetic and environmental factors (biological age), influences the likelihood of mortality and reproduction and thus the animal's contribution to population growth. For many long-lived species, such as bats, a lack of external and morphological indicators has made determining age a challenge, leading researchers to examine genetic markers of age for application to demographic studies. One widely studied biomarker of age is telomere length, which has been related both to chronological and biological age across taxa, but only recently has begun to be studied in bats. We assessed telomere length from the DNA of known-age and minimum known-age individuals of two bat species using a quantitative PCR assay. We determined that telomere length was quadratically related to chronological age in big brown bats (*Eptesicus fuscus*), although it had little predictive power for accurate age determination of unknown-age individuals. The relationship was different in little brown bats (*Myotis lucifugus*), where telomere length instead was correlated with biological age, apparently due to infection and wing damage associated with white-nose syndrome. Furthermore, we showed that wing biopsies currently are a better tissue source for studying telomere length in bats than guano and buccal swabs; the results from the latter group were more variable and potentially influenced by storage time. Refinement of

¹K. M. Ineson, T. J. O'Shea, C. W. Kilpatrick, K. L. Parise, J. T. Foster. *In press*. Journal of Mammalogy.

collection and assessment methods for different non-lethally collected tissues will be important for longitudinal sampling to better understand telomere dynamics in these long-lived species. Although further work is needed to develop a biomarker capable of determining chronological age in bats, our results suggest that biological age, as reflected in telomere length, may be influenced by extrinsic stressors such as disease.

Introduction

Determining the age of individuals is critical to understanding mammalian demography, population ecology, and conservation or management needs. Chronological age, or time elapsed since birth, can influence the likelihood of reproduction or mortality, which in turn influences population growth rate (Stearns 1992, Brunet-Rossinni and Austad 2004, Roach and Carey 2014). Ecological factors interact with chronological age to determine physiological state, or biological age, which can lead to differences in development, reproduction, and longevity among individuals in a population (Stearns 1992, Dunshea et al. 2011, Jarman et al. 2015). Both chronological and biological age are needed to fully understand the ecology (Stearns 1992) and conservation (Roach and Carey 2014) of a species. Bats are a particularly interesting taxon for studying age because they are long-lived for their body size, generally have low extrinsic mortality, and in some lineages have evolved behavioral or genetic mechanisms to resist viruses and suppress cancer (Wilkinson and Adams 2019). Bats are, however, susceptible to some diseases. The arrival and spread of white-nose syndrome, a fungal disease, has led to the collapse of bat populations throughout eastern North America (Frick et al. 2010b), bringing new urgency to the need to better understand the demographics of remnant populations.

Bats pose a unique challenge to demographic studies because while they are long-lived, they do not have reliable external indicators of age (Brunet-Rossinni and Wilkinson 2009). Two

well-studied vespertilionid species in North America, the little brown bat (*Myotis lucifugus*) and the big brown bat (*Eptesicus fuscus*) have recorded lifespans of 34 years (Davis and Hitchcock 1995) and 19 years (Hitchcock 1965), respectively. These species may regularly live at least 10 years without signs of senescence in reproductive activity (Hall et al. 1957, Paradiso and Greenhall 1967) and there are multiple records of little brown bats living over 20 years (Keen and Hitchcock 1980, White et al. 2019). Although these species can be identified as juveniles during their first summer (Kunz and Anthony 1982), there is no reliable way to determine age after their first year. For example, tooth wear is not a dependable predictor of age in little brown bats (Hall et al. 1957) and has never been successfully calibrated against samples of known-age individuals for *Eptesicus* spp. (Christian 1956, Hood et al. 2002, Gol'din et al. 2018).

Incremental lines of cementum and dentin in teeth or bones likewise have not been well calibrated (Phillips et al. 1982) and also are impractical for studies of live animals. Without external indicators of age, long-term banding or passive integrated transponder (PIT) tagging efforts currently are the only options for determining the chronological age of individuals and studying age-related changes in survival and reproduction.

Whereas external markers have been unsuccessful for determining age in little and big brown bats, genetic markers such as telomere length offer a potential solution. Telomeres have been widely studied as genetic markers of both chronological (Jarman et al. 2015) and biological age in a variety of taxa (Monaghan 2010), but only recently in bats (Foley et al. 2018).

Telomeres are made up of the tandemly repeated nucleotide sequence TTAGGG and a suite of protein complexes, forming the protective endcaps on chromosomes that shorten each time a cell divides (Blackburn 1991). Studies across vertebrate taxa have shown that while telomeres tend to shorten in relation to chronological age in a population, there can be considerable variation in

telomere length between individuals of the same age (Dunsha et al. 2011). This variation, reflecting biological age, is thought to be mediated by a range of factors including inherited telomere length (Dugdale and Richardson 2018), environmental conditions during early life (McLennan et al. 2016, Dugdale and Richardson 2018), and extrinsic pressures throughout life, such as habitat (Ibáñez-Álamo et al. 2018), stress (Hausmann and Marchetto 2010), and disease (Beirne et al. 2014, Hammers et al. 2015). Declines in telomere length can be countered by telomere repair mechanisms, such as telomerase. Other telomere maintenance genes are still being discovered and seem to vary among tissues, individuals, and species (Dunsha et al. 2011, Foley et al. 2018).

Telomeres are present in all eukaryotic cells (Blackburn 1991), but the choice of tissue and the method of collection for the objective of age determination depend upon the study organism. In light of the impacts of white-nose syndrome on bat populations, non-lethal tissue sampling is preferred. This limits the types of tissue that can be collected, but permits the release of an organism after processing, with the potential for recapture and carrying out longitudinal studies. A small biopsy of wing tissue, which heals in 2–3 weeks (Weaver et al. 2009, Greville et al. 2018), has been the standard for non-lethally obtaining DNA from bats, but other sources increasingly are being used. Mucosal epithelial cells, collected with buccal swabs, and gastrointestinal epithelial cells, found in guano, yield lower amounts of DNA than do wing biopsies (Corthals et al. 2015), but have successfully been used for genotyping (Puechmaille et al. 2007, Ramón-Laca et al. 2015, Oyler-McCance et al. 2018) and species identification (Walker et al. 2016) in bats. Whereas buccal swabs have previously been used to study telomere length in edible dormice (*Glis glis*; Hoelzl et al. 2016b) and humans (e.g., Thomas et al. 2008, Finnicum et al. 2017), to our knowledge, guano or feces have not yet been used in any telomere studies.

The type of tissue used in studies of telomere dynamics may be important because telomeres may be shortened by different rates of cell division across tissue types, damaged by different levels of oxidative stress (von Zglinicki 2002), or repaired through differentially expressed mechanisms, such as telomerase (Gomes et al. 2011, Nussey et al. 2014, Foley et al. 2018). This results in disparities in telomere length and telomere attrition rate among tissue types. Numerous studies in humans have shown that telomere length and attrition rate are correlated between tissue types (Daniali et al. 2013, Schmidt et al. 2016, Finnicum et al. 2017), but results from other vertebrate species have been mixed (Reichert et al. 2013). Tissue samples collected non-lethally from bats, such as wing biopsies, buccal swabs, and guano, each contain epithelial cells, but experience different stressors and may therefore show differences in telomere length. Mucosal and gastrointestinal epithelial cells proliferate rapidly and experience high turnover rates due to their function as barriers from bacterial and mechanical damage during mastication and digestion (Squier and Kremer 2001), whereas skin epithelial cells typically divide slowly (Tian et al. 2018). For North American bats, however, the skin cells on their wings may be dividing at a faster rate than normal if they sustain wing damage (Cryan et al. 2010) due to *Pseudogymnoascus destructans* (Pd), the fungus that causes white-nose syndrome (Lorch et al. 2011).

The inability to age adult bats presents a challenge to describing age-related aspects of their biology, including demographic traits, with implications for the conservation of species impacted by white-nose syndrome. In this study, we investigated relative telomere length (RTL) as a possible marker of chronological age in two long-lived bat species, little and big brown bats. In addition, we explored RTL correlations and differences among tissue types collected from little brown bats and using longitudinal samples, we examined RTL as an indicator of

dynamically changing ecological events that may impact biological age. Furthermore, because disease is known to influence telomere length in other taxa, we investigated whether infection from white-nose syndrome was associated with shorter telomeres in little brown bats, a highly impacted species (Frick et al. 2010b).

Methods

Study area and sample collection

We sampled little brown bats at maternity colonies ($n = 6$) in Massachusetts, New Hampshire, and Vermont, from mid-May to mid-September of 2016–2019. Bats in all six colonies roosted in large wooden barns located within a 100 km radius centered in southwestern New Hampshire. Bats were banded beginning as early as 2006 at four sites and beginning in 2016 at two sites. We used harp traps (Bat Conservation & Management, Carlisle, Pennsylvania) to capture bats upon their return to the roost after their first foraging bout. All individuals were held in separate mesh bags before being identified to species, examined to determine sex and reproductive condition (Racey 2009), and measured for mass (g) and right forearm length (mm). We determined age (juvenile or adult) based on the presence of an epiphyseal gap in the fourth metacarpal joint (Kunz and Anthony 1982). For bats banded as adults and recaptured, we recorded their minimum age as years since initial capture plus one, such that if they were banded five years before recapture, they were at least six years old. Only bats banded as juveniles were considered to be known-age individuals. Wing damage associated with white-nose syndrome was assessed by transilluminating the wings over a light box and quantified using a modified version of a scoring system that ranks bats from zero (no damage) to three (heavy damage; Reichard and Kunz 2009). In addition, we collected wing swabs from a subset of bats to test for Pd and categorized them as positive or negative for the fungus based on assay results following

the qPCR methods of Muller et al. (2013) and the sampling and analysis of Langwig et al. (2015b). One wing biopsy was collected from a subset of bats captured on a given night using a sterile 2 mm (2016) or 3 mm (2017–2019) biopsy punch after cleaning the wing membrane with an isopropyl alcohol wipe. We also collected buccal cells from some bats by swabbing the inside of the mouth for one minute with a Whatman OmniSwab (GE Healthcare, Chicago, Illinois). Guano was collected opportunistically directly from the bats or from their holding bags. All samples were stored in separate tubes containing 0.5 ml RNAlater (Ambion, Austin, Texas) at -80°C until DNA could be isolated.

We collected big brown bats from maternity colonies ($n = 10$) roosting in buildings in and near Fort Collins, Colorado from 2005–2015. Study area descriptions in relation to use by big brown bats have been described in detail elsewhere (e.g. Neubaum et al. 2007, O'Shea et al. 2011). During 2001–2005, we used mist nets, harp traps, funnel traps, and handheld nets to capture bats as they emerged from roosts around dusk. At capture, bats were examined to determine sex and reproductive condition, classified as adults or juveniles based on the presence of an epiphyseal gap, and implanted with PIT tags (AVID, Norco, California). Beginning in 2005 and opportunistically through 2015, previously tagged bats were removed from the population and euthanized in the course of other studies (Cryan et al. 2012, Castle et al. 2015). All whole bats were stored at -80°C. In 2010, we collected two wing biopsies (3 mm) each from a subset of frozen bats and stored them in lysis buffer at room temperature until DNA extraction in 2019. To further expand the age range of samples, wing biopsies were obtained in 2019 from the carcasses of six older bats that had been previously collected during 2010–2015; these tissues were briefly stored in RNAlater until DNA extraction. All big brown bats included in this study were unaffected by white-nose syndrome as Pd had not reached Colorado in 2015 (Neubaum 2018).

Handling and sampling protocols for little brown bats were approved by the University of New Hampshire's Institutional Animal Care and Use Committee and work was conducted under appropriate state permits from New Hampshire, Vermont, and Massachusetts. All capture, tagging, sampling, and euthanasia procedures for big brown bats were approved by the Institutional Animal Care and Use Committees of the U.S. Geological Survey and Colorado State University. Big brown bats were captured under authority of scientific collecting licenses issued by the Colorado Division of Wildlife. All procedures followed the guidelines of the American Society of Mammalogists for the use of wild mammals in research (Sikes et al. 2011, Sikes et al. 2016).

DNA isolation and estimation of relative telomere length

We extracted genomic DNA from wing biopsy and buccal swab samples using the DNeasy Blood & Tissue kit (Qiagen, Inc., Valencia, California) following the Animal Tissue Spin-Column protocol. For buccal samples, we replaced the RNAlater with 1X Tris-EDTA after centrifuging and soaked swabs for one hour prior to extraction to remove some of the RNAlater salts (Walker et al. 2016). Biopsy samples were lysed for at least four hours and buccal swabs for at least 12 hours. From guano samples, we extracted DNA using the DNeasy PowerSoil kit (Qiagen, Inc., Valencia, California) following the manufacturer's recommended protocols. We quantified DNA concentration of biopsy and guano samples using a Qubit 2.0 Fluorometer (Life Technologies, Carlsbad, California). All isolated DNA was used immediately or stored at -20°C or -80°C until further use.

We determined RTL following the method of Cawthon (2002), which estimates the ratio of telomere repeats to a single or non-variable copy number reference gene in a sample relative

to a calibrator. The tel1b (CGGTTTGGTTGGGTTTGGGTTTGGGTTTGGGTTTGGGTT) and tel2b (GGCTTGCCTTACCCTTACCCTTACCCTTACCCTTACCCT) primers were used for the telomere reactions (Callicott and Womack 2006). Following Smith et al. (2011), we selected the reference gene primers from a panel including rag2 (Corthals et al. 2015), 36B4 (Cawthon 2002), 36B4u (Callicott and Womack 2006), c-myc (Hoelzl et al. 2016a), and BDNF (Foley et al. 2018). We chose the primers developed based on chiropteran sequences (Corthals et al. 2015), rag2-q2-F1 (ACACCAAACAATGAGCTTTC) and rag2-q2-R1 (CCATATCTGGCTTCAGG), as they showed the most consistent amplification and cleanest melt curves. After selection of the primers, we ran a conventional PCR and gel electrophoresis to verify correct band size of amplicons for each sample type.

All qPCR reactions were carried out in 20 μ l final volumes consisting of 10 μ l 2X Quantifast SYBR Green Mastermix (Qiagen, Inc., Valencia, California), 4 μ l ultrapure water, 2 μ l of forward and reverse primers (1 μ M final concentration), and 2 μ l of template DNA, with the exception of buccal samples, for which 4 μ l of template DNA and 2 μ l of water were used to increase the final DNA concentration in each well. No-template controls and a calibrator sample were run in triplicate on each plate. The calibrator sample for little brown bats came from a single individual not included in the analysis. For big brown bats, we pooled equal volumes of DNA eluate from 64 samples to create a calibrator sample. Samples were run in triplicate for both primer sets on the same plate to minimize inter-plate variation. Assays were run on a 7500 Fast Real-Time PCR System (Applied Biosystems, Foster City, California) with the following thermocycling conditions: 95°C for 5 min, 40 cycles of 95°C for 10 s and 60°C for 30 s, followed by a melt curve at the end of each run. To assess inter-run repeatability, we repeated the analysis of a single plate of samples under the same conditions.

We analyzed raw, non-baseline corrected fluorescence data using LinRegPCR (Ruijter et al. 2009) with separate windows-of-linearity for each amplicon group (telomere and rag2). Minor adjustments were made to individual windows-of-linearity to improve correlations between points in the exponential phase of the amplification curves. We calculated coefficients of variation (CV) using the Cq values of sample replicates and where CV exceeded 5%, we excluded single replicates from further analysis when they were clear outliers (Ehrlenbach et al. 2009). The following equation was then used to calculate RTL:

$$RTL = \frac{E_T^{(Cq_T \text{ calibrator} - Cq_T \text{ sample})}}{E_S^{(Cq_S \text{ calibrator} - Cq_S \text{ sample})}}$$

where E_T and E_S are the mean primer efficiencies among all samples on a plate for the telomere (T) and rag2 (S) primers, respectively. Mean calibrator Cq values ($Cq_{T\text{calibrator}}$ and $Cq_{S\text{calibrator}}$) are used to standardize RTL values across plates compared to the mean Cq values ($Cq_{T\text{sample}}$ and $Cq_{S\text{sample}}$) for each sample (Pfaffl 2001).

Statistical analyses

We analyzed RTL from the two species separately using R v3.6.1 (R Core Team 2018) and the ‘lme4’ package (Bates et al. 2015). For big brown bats, we first considered linear mixed models with RTL as the response variable and age as the fixed effect. Reproductive status was excluded from the analysis because incomplete data would have biased the results. We did not include plate or year as random effects because bats were not randomly distributed among qPCR plates by age and year was highly correlated with age due to our sampling method. Including colony as a random effect did not improve model fit based on a likelihood ratio test (LRT; $P = 0.999$), multiple linear regression therefore was used for further analyses. We created a set of models to assess whether RTL was related to age, including linear, polynomial (quadratic and

cubic), and null age terms, then selected the best model using Akaike's Information Criterion corrected for small sample size (AICc). Residuals were plotted against fitted values and examined for homogeneity and normality to assess model fit.

All models for little brown bats used RTL from the wing biopsy samples as the response variable and included individual ID and year as random effects. When tested as a random effect, we found that colony did not improve model fit ($P = 0.257$) and was subsequently excluded from the analysis. We did not include qPCR plate as a random effect because bats were not randomly distributed among plates by age. An a priori set of models was created with biologically relevant combinations of age (linear and quadratic), wing score, and reproductive status as fixed effects. Julian date was not included as it was highly correlated with reproductive status and wing score. Age also was partitioned into within- and between-subject effects using within-subject centering, which can be used to distinguish individual variation in RTL measurements from population-level variation in RTL (van de Pol and Wright 2009). For bats sampled more than once, mean age between sampling points (between-subject) and delta age or age at sample minus mean age (within-subject) were calculated. For bats sampled once, mean age is simply age at sampling and delta age is zero. The best model was selected based on AICc and model fit was evaluated by examining the residuals. Likelihood ratio tests were used to compare the fit of nested models. Pd status (positive or negative) was evaluated in a separate linear mixed model because not all bats were tested for Pd. The best model for each species was run again with only bats of known age (tagged or banded as juveniles) to evaluate the influence of including individuals of unknown age on the models.

To examine drivers of change in RTL over time for little brown bats, individuals sampled in consecutive years ($n = 16$) were included in a separate longitudinal analysis. Multiple linear

regression models were fit with delta RTL (change in RTL between years) as the response variable and initial reproductive status, wing score, and age included as fixed effects in separate models due to small sample size. Initial RTL was included as a fixed effect in each model to account for regression to the mean (Hoelzl et al. 2016a). Models were compared to a model with only initial RTL using likelihood ratio tests. To further explore within-subject changes in RTL, temporal autocorrelation was examined by fitting a linear mixed model of RTL_{T+1} with age and RTL_T as fixed effects and sample year as a random effect. The slope of the RTL_T term estimates the degree of temporal autocorrelation corrected for age effects (Fairlie et al. 2016).

Differences in RTL values among little brown bat tissues (biopsy, buccal, and guano) were examined using a linear mixed model with tissue type and age as fixed effects and individual ID as a random effect to control for multiple tissues coming from a single bat (although all three tissues were not collected from every individual). Differences in mean RTL among tissue types were determined post hoc with Tukey's contrasts using the 'multcomp' R package (Hothorn et al. 2008). Correlations in RTL among tissue types were determined using Pearson's correlation tests. The same calibrator sample was used for all tissue types to allow for comparison.

Results

We analyzed 153 wing biopsy samples from 122 female little brown bats ranging in age from 0 to ≥ 12 years old, 32 of which were banded as juveniles. Thirty-one little brown bats were sampled twice over the study period with time between sampling ranging from zero to three years. We also analyzed 34 buccal swabs and 32 guano samples collected from little brown bats. For big brown bats, we analyzed 73 wing biopsy samples from 71 females and 2 males ranging in age from 0 to ≥ 14 years old, 49 of which were PIT-tagged as juveniles.

The mean PCR efficiency for little brown bat samples was 1.93 ± 0.02 SD and 1.92 ± 0.02 for telomeres and rag2, respectively, while for big brown bats, PCR efficiency was 1.88 ± 0.02 for telomeres and 1.90 ± 0.01 for rag2. Mean inter-assay CV, based on the Cq values of the little brown bat calibrator samples, was 1.65% for both amplicons, while mean intra-assay CV was 1.88% for telomeres and 1.64% for rag2. For big brown bats, inter-assay CV was 2.54% for telomeres and 2.55% for rag2, while mean intra-assay CV was 2.44% for telomeres and 2.21% for rag2. RTL values from the samples analyzed twice were highly correlated ($R^2 = 0.89$, $P < 0.001$), supporting low among-run variation (Appendix B, Fig. B1).

RTL and predictor variables

The best model for big brown bats indicated a quadratic relationship between RTL and age, although it only explained a small amount of the variation in RTL (adj. $R^2 = 0.24$, $F_{2,70} = 12.62$, $P < 0.001$). There also was support for a model with cubic age ($\Delta\text{AICc} = 0.79$), but the quadratic model was selected as the more parsimonious of the two (Table 1.1). RTL in big brown bat samples appeared to increase with age until approximately 4–8 years of age, then decrease (Fig. 1.1A). Results were similar when the quadratic model was run again with only known-age bats tagged as juveniles (adj. $R^2 = 0.14$, $F_{2,46} = 4.99$, $P < 0.05$).

Delta age and mean age were not significant in explaining variation in RTL in little brown bats (see below); we therefore used age and age² in the final models. The best model indicated a relationship between RTL and wing score (LRT, $\chi^2 = 4.720$, $P < 0.05$; Table 1.2), followed by models with age² ($\Delta\text{AICc} = 2.12$) and wing score and age ($\Delta\text{AICc} = 2.12$). Age by itself was not related to RTL ($\chi^2 = 0.109$, $P = 0.74$; Fig. 1.1B). We found similar results when the best model was run again with only known-age bats, but as a linear model due to small

sample size (adj. $R^2 = 0.12$, $F_{1,33} = 5.56$, $P < 0.05$). Upon closer inspection of our data, we determined that, by chance, individuals with higher wing scores were all 1- or 2-year-old bats, which was not representative of our sampling population. To test whether the uneven distribution of wing scores by age influenced our results, we reran the model with only the 1- and 2-year-old bats and observed the same effect of wing score on RTL, while the inclusion of age had less support (Appendix B, Table B1). Tukey's post hoc tests showed that bats with more wing damage ($WS = 2$) had significantly shorter telomeres than those with a wing score of zero ($P < 0.05$), but not than those with intermediate wing damage ($P = 0.12$, Fig. 1.2A). Bats with a wing score of zero or one had similar telomere lengths ($P = 0.32$). We also found significant support for Pd status influencing telomere length compared to a null model ($\chi^2 = 5.245$, $P < 0.05$; Table 1.3), where Pd-positive individuals ($n = 45$) had significantly shorter telomeres than Pd-negative ($n = 50$) individuals (Tukey, $P < 0.05$; Fig. 1.2B), independent of age ($\chi^2 = 0.206$, $P = 0.65$).

Longitudinal samples and tissue comparisons

We detected a significant, but weak between-individual effect of age within little brown bats sampled twice (LRT, $\chi^2 = 4.388$, $P < 0.05$); however, when all bats were included in the analysis, we found no significant within- ($\chi^2 = 0.067$, $P = 0.79$) or between-individual ($\chi^2 = 0.637$, $P = 0.43$) effects of age on RTL. It is possible that RTL of bats sampled once may have masked any within- or between-subject effects in the dataset because there were nearly three times more bats sampled once than twice. Initial reproductive status ($t = 0.739$, $P = 0.48$), wing damage ($t = -0.983$, $P = 0.34$), and age ($t = -0.181$, $P = 0.86$) were not significant in explaining changes in RTL across ages in bats sampled in consecutive years ($n = 16$) when accounting for regression to the mean. In addition, there was no significant temporal autocorrelation in RTL

measurements of individuals between years ($\chi^2 = 1.134, P = 0.29$). Changes in telomere length within individuals appeared to be complex (Fig. 1.3) and were not explained by any covariates that we collected on little brown bats.

We found no correlation in RTL between wing tissue and buccal cells within individual little brown bats ($R = 0.01, P = 0.98, n = 32$). Similarly, guano RTL was not correlated with RTL in wing tissue ($R = -0.05, P = 0.79, n = 29$) or buccal cells ($R = 0.11, P = 0.60, n = 25$; Fig. 1.4). Mean wing tissue and buccal cell RTL measurements were not significantly different (Tukey; $P = 0.99$), but RTL was significantly longer in guano than in wing tissue ($P < 0.001$) and buccal cells ($P < 0.001$; Fig. 1.5), independent of age (LRT, $\chi^2 = 0.746, P = 0.39$). Guano samples had higher variation in RTL (mean \pm SD: 2.57 ± 1.92) than wing tissue (1.14 ± 0.31) and buccal swabs (1.13 ± 0.62).

Discussion

Our results demonstrate that telomere length is not a reliable predictor of chronological age in little or big brown bats and that age-related declines in telomere length vary between the two bat species we studied. While we did not find a correlation between age and RTL in little brown bats (Fig. 1.2B), we detected a quadratic relationship between age and RTL in big brown bats (Fig. 1.2A), albeit one with little predictive power to age individuals of unknown ages. Our results are similar to those of Foley et al. (2018), who did not find a correlation between RTL and age in *M. myotis* and *M. bechsteinii*, but found linear relationships in *Rhinolophus ferrumequinum* and *Miniopterus schreibersii*. This suggests that there may be something unique about age effects on telomeres of *Myotis* spp. Differences among species, particularly *Myotis* spp. compared to other genera, are potentially due to differences in telomere maintenance strategies. Some species of bats suppress or limit expression of telomerase (Gomes et al. 2011,

Foley et al. 2018), similar to large-bodied mammals (Tian et al. 2018), and instead rely on other mechanisms for DNA maintenance. Several recent studies have suggested a relationship between longevity and the unique set of genes under positive selection in *Myotis* spp., including those involved in repairing DNA, resisting tumors, and reducing oxidative damage (Ma et al. 2016, Tian et al. 2017, Foley et al. 2018). In *M. lucifugus*, the telomere maintenance genes DKC1 and TERT are under positive selection (Morgan et al. 2013). In addition, certain telomere maintenance genes appear to be differentially expressed in *Myotis* spp. compared to other mammals (Foley et al. 2018). This may explain the lack of telomere attrition observed in little brown bats, but further work is needed in non-*Myotis* species to see if there are phylogenetic patterns in telomere length maintenance. There also is room for more study within the genus, as the three *Myotis* species studied thus far all fall into lineages that have high maximum longevity according to current lifespan data (Wilkinson and Adams 2019).

The quadratic relationship between age and RTL in big brown bats previously has been observed in several vertebrate taxa, including mammals, reptiles, and fish (Anchelin et al. 2011, Fairlie et al. 2016, Rollings et al. 2017). Increases in RTL for middle-age individuals have been explained in part by selective disappearance, or mortality of young individuals with shorter telomeres (Fairlie et al. 2016), and partly by within-individual increases in telomere length, which could be due to increased telomerase expression (Ujvari et al. 2017). Similar to little brown bats, big brown bats appear to suppress telomerase (Gomes et al. 2011) and may instead have evolved alternate mechanisms for telomere maintenance. Both species are hibernators with high maximum longevity (Wilkinson and Adams 2019) and appear to be able to reduce oxidative damage compared to other groups of mammals of similar size or with similar metabolic rates (Brunet-Rossinni 2004, Brown et al. 2009). Because our study did not allow for a longitudinal

study of big brown bats, we cannot distinguish between selective disappearance and within-individual changes in telomere length as potential explanations for the observed quadratic trend.

Although our cross-sectional data show no significant changes in RTL for little brown bats with age, the longitudinal data suggest a more complex pattern of individual increases and decreases in RTL between years. Similar longitudinal patterns can be seen in Soay sheep (*Ovis aries*; Fairlie et al. 2016); European badgers (*Meles meles*; van Lieshout et al. 2019); Seychelles warblers (*Acrocephalus sechellensis*; Spurgin et al. 2017); great tits (*Parus major*; Salmón et al. 2017); and frillneck lizards (*Chlamydosaurus kingii*; Ujvari et al. 2017). Despite concerns of measurement error (Steenstrup et al. 2013), a recent study (Bateson and Nettle 2017) as well as our low inter- and intra-plate CVs and high inter-plate repeatability (Appendix B, Fig. B1) suggest that many of the observed changes in RTL were real. The lack of temporal autocorrelation between RTL measurements among years as well as the lack of support for within-subject age-related declines in RTL also support the complex patterns in telomere length we observed in little brown bats (Fig. 1.3).

While we were unable to explain inter-annual changes in RTL with reproductive status and age, there was evidence that white-nose syndrome was associated with shorter telomeres in little brown bats. Infections have been associated with shorter telomere length and poor biological state in several species (Monaghan 2010), including malaria in birds (Asghar et al. 2015, Hammers et al. 2015) and humans (Asghar et al. 2018); bovine tuberculosis in European badgers (Beirne et al. 2014); and *Salmonella enterica* in experimentally-infected house mice (*Mus musculus musculus*; Ilmonen et al. 2008). Hibernating bats in North America can be repeatedly infected with Pd each winter when they pick up the fungus from the substrate of hibernacula and from other bats (Lindner et al. 2011, Lorch et al. 2013). Pd infection loads

gradually increase over the winter (Langwig et al. 2015b) and cause changes in hibernation patterns. Colonies undergoing the early stages of WNS invasion show increased arousal frequency (Reeder et al. 2012), while remnant colonies that have been exposed to Pd for a decade or more appear to have similar arousal rates to pre-WNS bats, but arouse for longer periods and from lower skin temperatures (Lilley et al. 2016). Both increased arousal frequency and time spent euthermic have been associated with higher levels of telomere damage in edible dormice (Hoelzl et al. 2016a). Although bats naturally arouse periodically during the winter, it appears that Pd infection may contribute to telomere damage as a result of altered hibernation patterns, leading to bats having shorter telomeres when they emerge from hibernation.

For individuals that survive the winter, Pd infection results in a flare-up of wing damage within a few weeks after emergence from hibernation (Fuller et al. 2011, Meteyer et al. 2011, Fuller 2016). In the spring, females are recovering from hibernation, migrating to summer sites, and initiating fetal development, all energetically costly activities that compound the added costs of fighting Pd infection and recovering from WNS (Moore et al. 2013, Fuller 2016). Given these added costs, it is unsurprising that infected bats have shorter telomeres; however, it is also possible that bats can recover and restore telomere length over the course of the summer (Fig. 1.3). Djungarian hamsters (*Phodopus sungorus*) that use spontaneous daily torpor are able to elongate their telomeres and recover from telomere losses sustained during hibernation (Turbill et al. 2012). Bats also use torpor during the active season, particularly as an energy-saving strategy in the spring and summer, to compensate for cold temperatures and low food availability (Racey 1973, Besler and Broders 2019), but potentially also for telomere maintenance. Torpor may allow bats to repair their telomeres and even compensate for increased cell turnover in portions of their wings that repeatedly are damaged by white-nose syndrome. In a study of forced

tissue regeneration via fin-clipping, telomere length remained stable in zebrafish (*Danio rerio*) over their lifetime (Lund et al. 2009), suggesting that some animals may have cellular mechanisms, such as those discussed above, capable of maintaining telomere length in individuals over time.

Our results suggest that wing biopsies currently are the best source of tissue for studying telomere dynamics in bats. Buccal RTL was not significantly correlated with wing biopsy RTL, unlike the results of Hoelzl et al. (2016b). We cannot, however, rule out the use of buccal swabs as an alternative to wing biopsies for studying telomere dynamics in bats when the qPCR method is used, which requires a small amount of DNA compared to other telomere measurement techniques (Nakagawa et al. 2004). Our data suggest that storage time may have affected RTL measurements for the buccal swabs, where swabs stored for longer periods of time had more variable RTL. Although we were able to amplify telomere sequences from guano samples, there was much higher variation in RTL among individuals and there was no correlation in guano RTL with either buccal or wing biopsy RTL (Figs. 1.4 & 1.5). Boston et al. (2012) successfully used wing tissue and guano samples for genotyping purposes, but it is possible that telomere length assessment is more susceptible to PCR inhibitors present in guano samples (Taberlet et al. 1999) or that telomeres are more degraded in shed gastrointestinal epithelial cells. There also is much less endogenous DNA in guano relative to bacterial and insect DNA (Ramón-Laca et al. 2015), however, the telomere primers used in this study only should have amplified vertebrate telomeres (Hinnebusch et al. 1990, Vitková et al. 2005). Further refinement of sampling and assessment procedures may help reduce the variability in buccal swab and guano RTL measurements, making it easier to use these types of non-invasive samples in future telomere studies.

We found no significant difference between buccal and wing biopsy mean RTL, which was unexpected given the different turnover rates in these epithelial cells (Squier and Kremer 2001, Tian et al. 2018). Results from two human studies showed similar RTL between these tissue types, but were inconclusive (Gadalla et al. 2010, Dlouha et al. 2014). The variety of cell types found in each tissue may be partially obscuring differences in RTL. The wing membranes of bats are composed of epidermal epithelial, lymphatic, blood, nerve, and muscle cells (Cryan et al. 2010) whereas buccal samples can contain low levels of leukocytes (Finnicum et al. 2017, Theda et al. 2018). Multiple cell types in a sample may decrease observed differences in RTL between tissues even if RTL differs between cell types. Other studies that have compared tissue types suggest that telomere length differences are established during early life (Daniali et al. 2013, Reichert et al. 2013, Schmidt et al. 2016) and are not related to cell replication rates (Thomas et al. 2008). It also is possible that the mechanisms by which these tissues arrived at their current telomere lengths are drastically different, resulting in observed similarities that mask underlying tissue-specific telomere dynamics.

Our findings demonstrate that RTL in little brown bats is more a reflection of biological age than chronological age. In this species, telomere length was influenced by infection and wing damage associated with white-nose syndrome, but not chronological age. In big brown bats, RTL was quadratically associated with age, but our model explained little of the variation in RTL. Reasons for differences in the patterns between the two species are as yet unclear. Although telomere length will most likely not be useful in determining chronological age of unknown age bats, other molecular biomarkers such as DNA methylation patterns (De Paoli-Iseppi et al. 2017, Wright et al. 2018) may be more successful.

Table 1.1. Summary of multiple linear regression models of relative telomere length and chronological age in big brown bats (*Eptesicus fuscus*) sampled in and near Fort Collins, Colorado, 2005–2015. Linear, quadratic, cubic, and null regression models were considered and ranked by AICc. Coefficient estimates are shown for each model. K = number of parameters; logLik = log likelihood; w_i = model weight.

Model	Intercept	Age	Age ²	Age ³	K	logLik	AICc	Δ AICc	w_i
Age ²	0.926	0.136	-0.012		3	-17.47	43.52	0.00	0.60
Age ³	0.989	0.053	0.007	-0.001	4	-16.71	44.31	0.79	0.40
Null	1.165				1	-28.71	61.58	18.06	0.00
Age	1.203	-0.008			2	-28.47	63.29	19.76	0.00

Table 1.2. Summary of linear mixed models of relative telomere length and predictor variables in little brown bats (*Myotis lucifugus*) sampled in New England, 2016–2019. Linear and quadratic age terms were considered along with wing score (WS) and reproductive status (Rep) at the time of capture. Models were ranked by AICc. Coefficient estimates are shown for each model. K = number of parameters; logLik = log likelihood, w_i = model weight.

Model	Intercept	Age	Age ²	WS	Rep	K	logLik	AICc	Δ AICc	w_i
WS	1.243			-0.103		4	-58.23	126.88	0.00	0.42
Age ²	1.140	0.083	-0.008			5	-58.21	129.00	2.12	0.14
Age + WS	1.069	-0.002		-0.106		5	-58.21	129.00	2.12	0.14
Null	1.191					3	-60.59	129.46	2.58	0.12
Rep	1.234				+	7	-56.65	130.30	3.42	0.08
Age	1.198	0.004				4	-60.54	131.49	4.61	0.04
Rep + WS	1.240			-0.037	+	8	-56.45	132.16	5.28	0.03
Age + Rep	1.234	-0.001			+	8	-56.65	132.55	5.68	0.02
Age + Rep + WS	1.288	-0.001		-0.038	+	9	-56.45	134.44	7.57	0.01

Table 1.3. Summary of linear mixed models of relative telomere length and predictor variables in little brown bats (*Myotis lucifugus*) sampled in New England, 2016–2019, and tested for *Pseudogymnoascus destructans* (Pd). Models were ranked by AICc. Coefficient estimates are shown for each model. Pd = Pd status (positive or negative) at time of capture; K = number of parameters; logLik = log likelihood, w_i = model weight.

Model	Intercept	Pd	Age	K	logLik	AICc	Δ AICc	w_i
Pd	1.180	+		3	-29.13	68.93	0.00	0.61
Pd + Age	1.202	+	-0.006	4	-29.03	71.00	2.07	0.22
Null	1.103			2	-31.75	71.95	3.02	0.13
Age	1.115		-0.003	3	-31.72	74.12	5.19	0.05

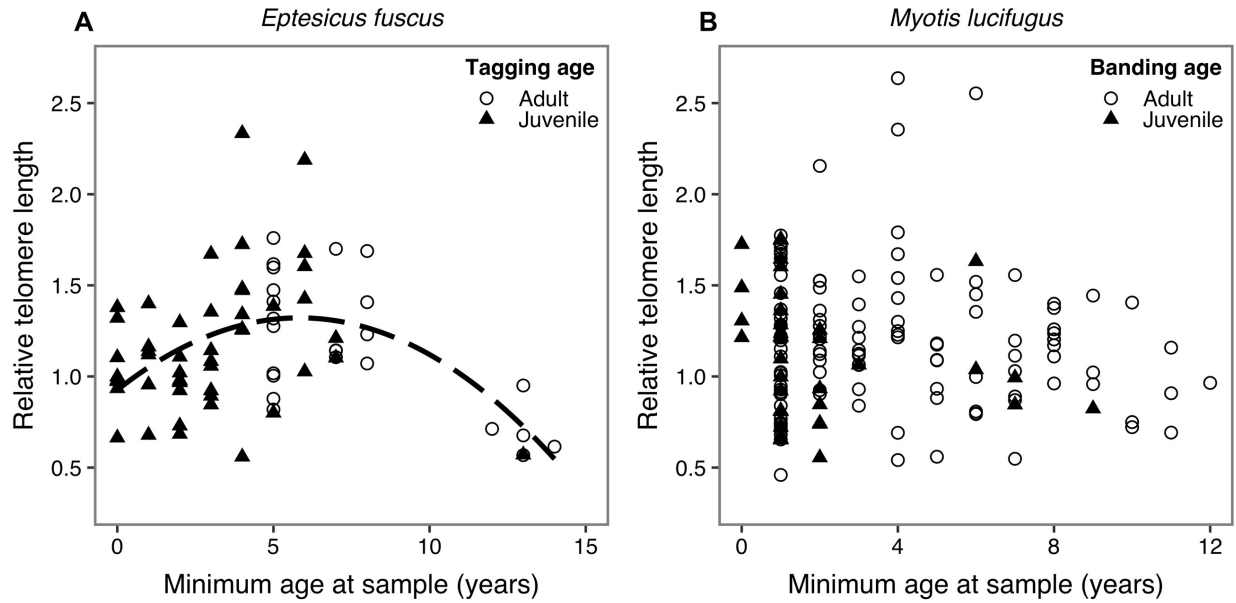


Figure 1.1. The relationship between relative telomere length and age in A) PIT-tagged big brown bats (*Eptesicus fuscus*) sampled in and near Fort Collins, Colorado, 2005–2015 and B) banded little brown bats (*Myotis lucifugus*) sampled in New England, 2016–2019. Bats marked as juveniles (closed triangles; known-age) and adults (open circles; minimum known-age) were combined in the model analysis. The dashed black line indicates a best-fit regression through the data where significant.

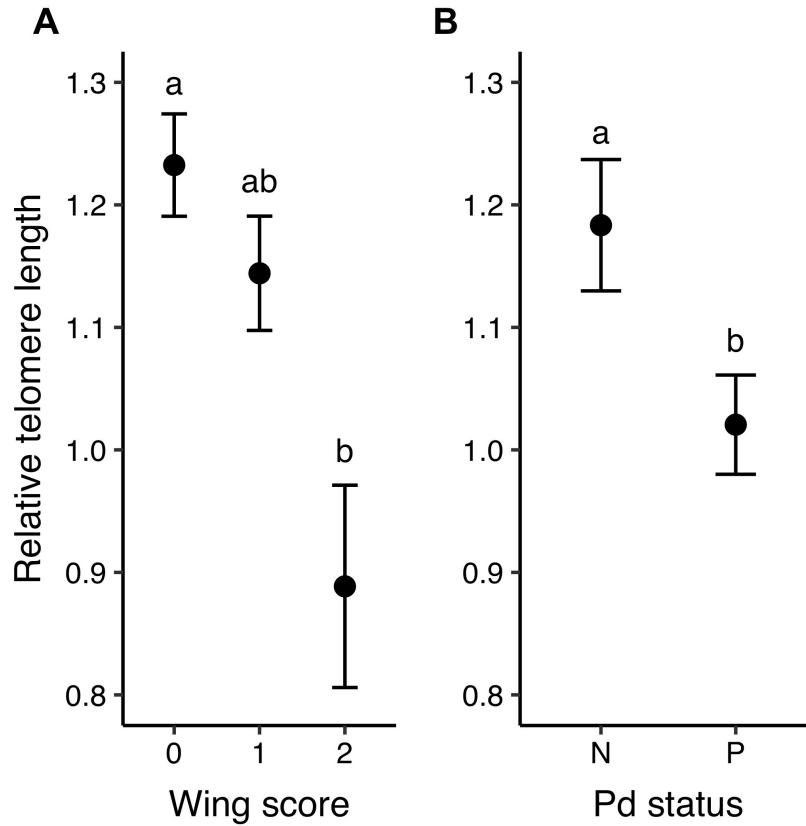


Figure 1.2. The relationship between little brown bat (*Myotis lucifugus*) relative telomere length and A) wing score, where 0 indicates no damage and 2 indicates moderate to high levels of wing damage, and B) Pd status for individuals that tested negative (N) or positive (P) for *Pseudogymnoascus destructans* (Pd), the fungus that causes white-nose syndrome in bats. Bats were captured in New England, 2016–2019. Points represent mean RTL and bars represent \pm standard error. Letters indicate significantly different means among groups.

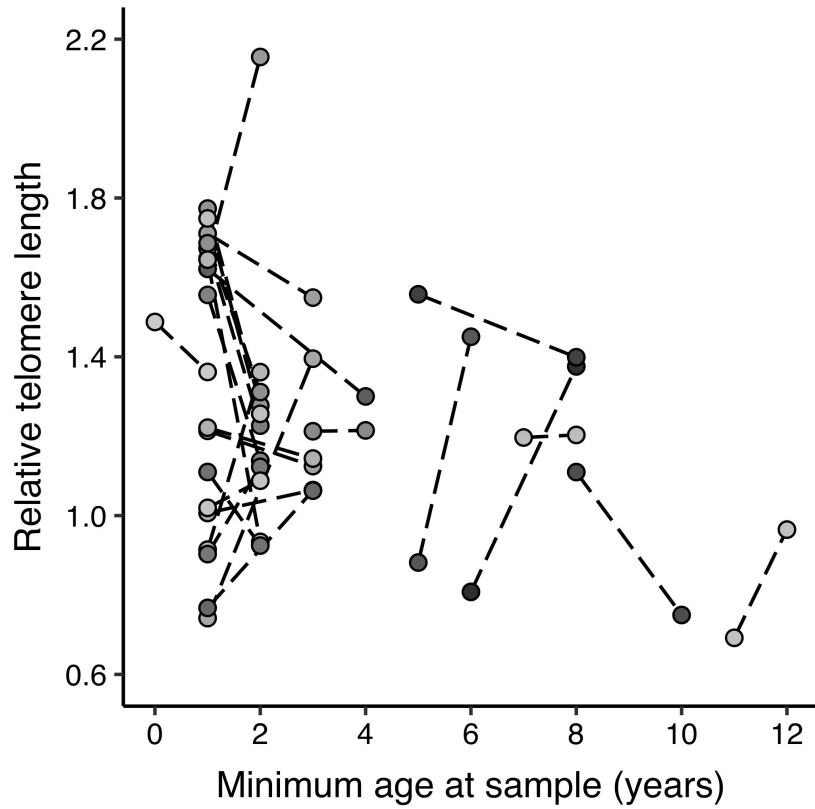


Figure 1.3. Changes in relative telomere length between years, with samples collected from individual little brown bats (*Myotis lucifugus*) connected by dashed lines. Bats shown here were sampled twice over intervals of one to three years in New England, 2016–2019.

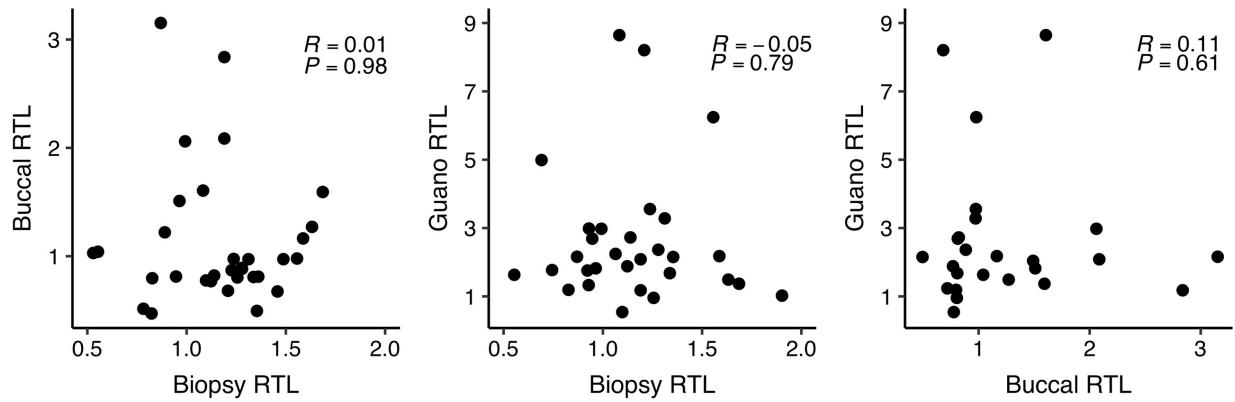


Figure 1.4. Correlation in relative telomere length (RTL) between wing (biopsy), mucosal epithelial (buccal), and gastrointestinal epithelial (guano) tissues collected from the same individual little brown bats (*Myotis lucifugus*) in New England, 2016–2019. All three tissue types were not collected from every individual. Note that scales differ between graphs.

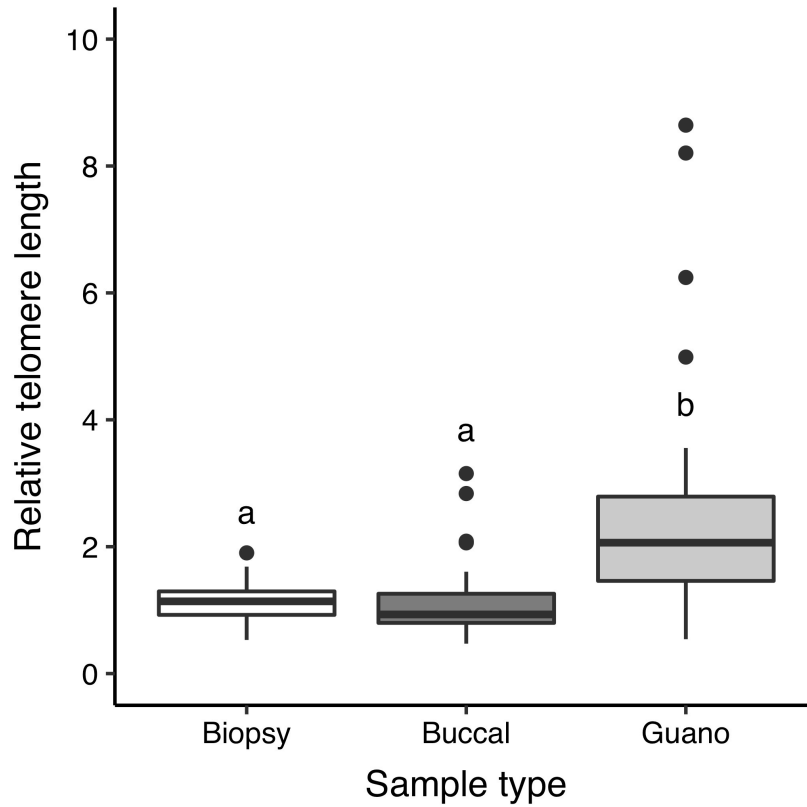


Figure 1.5. Boxplot showing relative telomere length variation within and among sample types. Wing (biopsy), mucosal epithelial (buccal), and gastrointestinal epithelial (guano) tissues were collected from the same individual little brown bats (*Myotis lucifugus*) in New England, 2016–2019. Letters indicate significantly different means among groups.

CHAPTER 2

WHITE-NOSE SYNDROME AND CLIMATE INFLUENCE LIFE HISTORY AND REPRODUCTIVE PHENOLOGY IN LITTLE BROWN BATS

Abstract

The rate and timing of reproduction, which can have important implications for the survival of individuals and growth of a population, are known to be influenced by extrinsic factors, such as climate and disease. Since 2006, the fungal disease white-nose syndrome (WNS) has resulted in catastrophic declines in the little brown bat (*Myotis lucifugus*) population in New England. Bats are annually re-infected during hibernation and female survivors recover from wing damage caused by WNS in the spring just as gestation begins. The goals of the study were to determine whether reproductive rates have changed since the onset of WNS and to assess the impacts of climate and disease on reproductive timing. We used a 27-year dataset spanning pre- and post-WNS arrival to compare reproductive rates in adults and yearlings and determine the drivers of inter-annual variation in reproductive timing. From 2016–2019, we assessed gestation stage and tested bats for the WNS pathogen, *Pseudogymnoascus destructans* (Pd), to further evaluate the impact of disease on the timing of parturition. We found that mean yearling reproductive rate increased from 0.49 (+/- 0.40) pre-WNS to 0.85 (+/- 0.13) post-WNS arrival and that more individuals were returning to their natal colonies as yearlings, suggesting a life-history shift in age of first breeding. Adult reproductive rate (0.95 +/- 0.03) did not change over time. Mean parturition date varied by as much as two weeks among years and was earlier when springs were warmer and drier. There was also some evidence for earlier reproductive timing post-WNS independent of climate, but not for a decrease in reproductive synchrony. At the

individual level, females with more wing damage had later parturition dates than those with less damage. Infection appears to impose high energy costs in the early spring, delaying or slowing gestation, but not preventing reproduction altogether in most individuals. Little brown bats may be benefiting from warming spring temperatures, which could reduce energy trade-offs and lead to advanced reproductive phenology at the population level that could offset delays associated with Pd infection at the individual level. Understanding both the demographic response to WNS and the impacts of climate on reproduction will be important for the conservation of little brown bats.

Introduction

Emerging infectious diseases are increasingly recognized as threats to wildlife populations and global biodiversity (Daszak et al. 2000, Fisher et al. 2012). Fungal pathogens alone are responsible for population declines in multiple taxa, including trees, amphibians, snakes, and North American bats (Fisher et al. 2012, Yap et al. 2015). Most diseases, however, do not end in extinction (Voyles et al. 2018). Disease-induced mortality can diminish over time as a disease shifts from epidemic to established (Langwig et al. 2015a), resulting in smaller, but stable, populations (Lampo et al. 2011, Maslo et al. 2015, Langwig et al. 2017, Scheele et al. 2017). These remnant populations are more vulnerable to extinction (De Castro and Bolker 2005, McKnight et al. 2017), but may persist for a variety of reasons, including reduced pathogen virulence (Newell et al. 2013), changes in host behavior or environmental conditions, immigration of individuals from other populations (rescue effect; Scheele et al. 2017), or genetic selection for resistance (evolutionary rescue; Gonzalez et al. 2013).

Populations can also respond to changes in abundance or density by altering particular life-history traits such as decreasing mean age of first reproduction, increasing reproductive rate, or increasing survival rate of some or all age classes (Eberhardt 2002, Coulson et al. 2004).

Shifts in life history related to changes in abundance and density have been documented in species that have become endangered due to non-disease factors (Grenier et al. 2007) or been over-harvested (Coulson et al. 2004, Olsen et al. 2004), but less commonly in species impacted by disease. A few long-term studies that preceded and continued after disease arrival have documented compensatory responses to disease-induced population declines in multiple amphibian species impacted by chytridiomycosis (Muths et al. 2011, Lampo et al. 2011) as well as in Tasmanian devils (*Sarcophilus harrisii*) impacted by Devil facial tumor disease (Jones et al. 2008, Lachish et al. 2009).

For disease-impacted populations, shifts in life history may be hindered by infection, which can impact reproduction directly (e.g., by damaging reproductive tissues) or indirectly by decreasing the nutritional status or physiological condition of individuals (Scott 1988). When resources are limited, individuals recovering from infection or healing from wounds may face a trade-off between immune response and maintenance or reproduction (Bernardo and Agosta 2005, Archie 2013). Females, for example, may be unable to allocate sufficient resources towards reproduction (Racey and Entwistle 2000, Reichard and Kunz 2009), meaning pregnancy may not be initiated or may be terminated; this is especially critical if infection reduces foraging efficiency, thereby limiting food intake and available resources (Reichard and Kunz 2009). For long-lived species under such unfavorable conditions, life-history theory predicts that females should forgo reproduction that breeding season (Barclay et al. 2004).

When reproduction does occur, energetically costly immune responses to infection and elevated maintenance costs may terminate, delay, or slow reproduction (Scott 1988, Archie 2013). Blood parasites and ectoparasites, for example, can delay reproduction or reduce reproductive rate in birds (Allander and Bennett 1995, Møller et al. 2006) and mammals (Lin et

al. 2014), although there are exceptions where parasites have either shown no impact (Murray et al. 2006) or even accelerated reproductive timing (Mulvey et al. 1994). In many species that breed seasonally, the timing of reproduction is critical to the survival and recruitment of offspring (Price et al. 1988, Ransome 1989, Frick et al. 2010a) and is already influenced by climate and food availability (Arlettaz et al. 2001). The impacts of disease on life history and reproductive phenology are, therefore, important for understanding population dynamics.

In North America, white-nose syndrome (WNS) first appeared in 2006 (Blehert et al. 2009) and has since spread throughout much of the continent, causing local declines of >90% in several hibernating bat species (Turner et al. 2011). The fungus that causes WNS, *Pseudogymnoascus destructans* (Pd), persists in environmental reservoirs (Lorch et al. 2013, Hoyt et al. 2015a), re-infecting bats during fall swarming and hibernation. Survivors of these annual infections and their subsequent offspring now make up remnant bat populations. Little brown bats (*Myotis lucifugus*) are one of the hardest hit species, but have persisted in hibernating winter colonies (Langwig et al. 2017, Frick et al. 2017) and summer maternity colonies (Dobony et al. 2011, Reichard et al. 2014, Dobony and Johnson 2018).

The period of recovery from infection may be crucial for conservation in terms of reproduction (Fuller 2016). In the spring, survivors emerging from hibernation continue to suffer from infection as an immune response to Pd causes severe inflammation and damage to the wing membrane (Fuller et al. 2011, Meteyer et al. 2011, 2012, Fuller et al. 2020). Bats with more extensive wing damage have a lower body-mass index (Reichard and Kunz 2009, Fuller et al. 2011) and shorter telomeres (Ineson et al. *In press*), suggesting poorer physiological condition. Most bats are able to heal from wing damage completely within a few weeks following peak

effects (Fuller et al. 2011, Pollock et al. 2015), however, survivors of infection have elevated cortisol levels, a sign of chronic stress (Davy et al. 2016).

Female little brown bats initiate pregnancy upon emergence from hibernation, when they may have to cope with suboptimal climate conditions or low food availability (Anthony and Kunz 1977). Adverse conditions in early spring have been shown to decrease reproductive rate and delay parturition in numerous bat species (Ransome and McOwat 1994, Burles et al. 2009, Lučan et al. 2013, Linton and MacDonald 2018). Temperate insectivorous bats may compensate by increasing torpor use (Geiser 2004, Wojciechowski et al. 2007, Dzal and Brigham 2013), particularly when they first arrive at their maternity colonies (Solick and Barclay 2007, Besler and Broders 2019). As the reproductive season progresses, however, the trade-off between the energy and water conservation of daily torpor conflicts with the delayed reproductive timing caused by reduced fetal and post-natal growth rates (Racey 1973, Racey et al. 1987, Audet and Fenton 1988, Grinevitch et al. 1995, Dzal and Brigham 2013). Bats impacted by WNS face additional energy costs from immune responses to Pd infection and wing damage repair. Infected bats in captivity only use shallow torpor, possibly as a fever response or trade-off between energy savings and immune function (Fuller et al. 2020).

Inter-individual variation in torpor use (Besler and Broders 2019) and wing healing rates (Fuller et al. 2011, 2020) could have further energy implications by reducing reproductive synchrony. For temperate mammals, reproductive synchrony optimizes the timing of seasonal food resources with the peak energetic demands of reproduction and has potential energetic and thermoregulatory benefits for species that aggregate (Webb et al. 1996). Although some studies have suggested reproduction in little brown bats is highly synchronous both within and between colonies (Schowalter et al. 1979), most research has shown that this species already has

relatively low levels of synchrony (O'Farrell and Studier 1973), or levels of synchrony that are influenced by intrinsic and extrinsic factors (Reynolds 1999). Decreased reproductive synchrony may exacerbate energy tradeoffs for adults and slow post-natal development of pups by reducing the thermal benefits of clustering while their mothers are foraging during the night (O'Farrell and Studier 1973).

Little brown bats present a unique opportunity for studying the impacts of WNS on life-history strategies and population-level demographic rates. Here we present the results of a demographic study conducted at nine maternity colonies in New England. One colony was extensively studied for 16 years beginning in 1993 and ending in 2009 when the colony was almost completely extirpated by WNS (Reynolds 1999, Frick et al. 2010a). Nearby colonies have been studied since the arrival of WNS (Reichard and Kunz 2009, Fuller et al. 2011, Reichard et al. 2014, Langwig et al. 2015b), providing a 27-year dataset that we used to compare aspects of reproduction and distinguish disease impacts from climate-related stochasticity. Previous research on mammal populations that have undergone dramatic population declines suggest an accelerated reproductive maturation or earlier age of first reproduction (Houston and Stevens 1998, Jones et al. 2008, Lachish et al. 2009). We therefore predicted 1) that a higher proportion of yearling females would reproduce post-WNS, which we would see through an increase in reproductive rate. As infection has been shown to delay reproduction in other animals, we also predicted that 2) bats with higher levels of wing damage would give birth later in the summer than bats with less damage, resulting in 3) a decrease in reproductive synchrony and 4) an overall shift in the timing of reproduction to later in the summer compared to pre-WNS.

Methods

Bat capture and data collection

We captured little brown bats at maternity colonies in New England roosting in wooden barns from early May to mid-September. Our pre-WNS analysis comes from data collected between 1993–2007 at a single colony in Peterborough, New Hampshire. Here, we captured bats by hand on 5–26 days per summer between 5 and 7am. Our post-WNS arrival dataset was collected from 2008–2019, where we captured bats at emergence or upon return to the roost at eight colonies in New Hampshire, Vermont, and Massachusetts (Fig. 2.1) using harp traps (Bat Conservation & Management, Carlisle, PA, USA). Not all colonies were trapped every year and the number of capture events varied widely among sites. The bats in these colonies are considered to be part of a single population (Wilder et al. 2015), so for the purposes of this study we pooled sites, resulting in 5–29 capture events per summer.

Bats were identified to species, sexed, and aged as juveniles or adults based on the presence of an epiphyseal gap in the fourth metacarpal joint (Kunz and Anthony 1982), the shape of the epiphyses, and darker fur coloration in juveniles (Davis and Hitchcock 1965). We assessed reproductive condition of adult females as pregnant (based on palpation of the abdomen), lactating (based on expression of milk from the mammary glands), post-lactating (based on nipple morphology), or non-reproductive (Racey 2009). From 1993–2007 and 2016–2019, we measured epiphyseal gap size of juveniles to the nearest 0.1 mm using a pre-calibrated ocular micrometer mounted in a portable dissecting microscope (Kunz and Anthony 1982, Kunz et al. 2009). For all bats, we measured mass to the nearest 0.1 g and forearm length to the nearest 0.1 mm. All bats were banded with lipped aluminum bands (Porzana Limited, East Sussex, UK) and released at the site of capture.

From 2016–2019, adult bats were assessed for wing damage using a modified version of the wing damage index scoring system (Reichard and Kunz 2009). We also swabbed the forearms of a subset of adult bats to test for Pd (Muller et al. 2013) and quantify fungal load (Langwig et al. 2015b). At two sites, Lincoln (2017–2019) and Charlestown (2017), we subcutaneously implanted a passive integrated transponder (PIT) tag (HPT9, Biomark, Boise, Idaho, USA) between the scapula in a subset of bats and sealed the insertion site with adhesive glue. A PIT tag reader (HPR Plus, Biomark, Boise, Idaho, USA) and antenna were deployed at each site before bats arrived in the spring and left to record until early October. The antenna was placed at the main opening used by bats to exit and enter the barn, but there were a few other small openings available to bats at each site that we did not attempt to close off.

All handling and sampling procedures were conducted under state scientific collecting permits and followed the guidelines of the American Society of Mammalogists for the study of wild mammals (Sikes et al. 2011, Sikes et al. 2016). Bat handling from 2016–2019 followed appropriate decontamination protocols and was approved by the University of New Hampshire’s Institutional Animal Care and Use Committee (#160105 and 181209).

Reproductive rate

For each year of the study, we calculated the reproductive rate as the proportion of captured adult females that showed signs of reproduction (pregnant, lactating, or post-lactating). Reproductive rate was calculated separately for yearling bats, which were banded as juveniles and recaptured the following summer. In the late spring to early summer, bats may be in early gestation and pregnancy can be difficult to determine by palpation (Kunz et al. 1999), potentially resulting in an underestimation of reproductive rate. Bats assigned as ‘non-reproductive’ before the first lactating female of the year were therefore excluded from our analyses (Dobony and Johnson

2018) while those captured after were considered non-reproductive (Barclay et al. 2004). For bats captured more than once in a summer, we only used their final reproductive status in the calculation of reproductive rate. Yearling females emerge from hibernation later (Norquay and Willis 2014) and reproduce later than adult females (Cagle and Cockrum 1943, Davis and Hitchcock 1965, Reynolds 1999), therefore for the calculation of yearling reproductive rate we added four days to the capture date of the first adult lactating female, which represents the difference between the mean lactation date for adults and yearlings. This four-day difference was consistent between pre- and post-WNS data sets. In this study, reproductive rate refers only to those bats roosting in maternity colonies. Non-reproductive females may simply not return to their summer colony in a given year, which means we may be overestimating the population-wide reproductive rate, but if so, we are consistent between comparison groups.

Reproductive phenology

We calculated an annual mean lactation date using the lactating females captured throughout the summer. We used lactation instead of pregnancy to determine reproductive timing because 1) the period of lactation (~3–4 weeks (Anthony and Kunz 1977)) is less variable and shorter in duration than gestation (Racey 1973), 2) lactation is more readily observed, whereas the early stages of gestation are harder to detect (Kunz et al. 1999) and 3) generally the entire lactation period was sampled in this study whereas sampling did not always cover the total gestation period. Due to coarse sampling, we used a generalization of Sheppard's method to calculate a corrected mean lactation date to represent reproductive timing (Johnson et al. 2004), which generally agreed with the logistic regression method of Arlettaz et al. (2001). Both methods had issues when there were few sampling nights or large gaps between sample nights. For one year post-WNS (2011), mean lactation date was adjusted using the day of year corresponding to the

peak of a LOESS smoothing curve fitted to the proportion of lactating females captured throughout the summer. Seven years with inadequate sampling periods were removed from further analysis, which also improved the match in sampling periods between years (Heideman and Utzurrum 2003). To compare overall reproductive timing between pre- and post-WNS arrival, we fit non-linear least-squares curves to the pooled pregnancy and lactation data. The intersection between the pregnancy and lactation curves indicates median parturition date (Kunz 1973, Reichard et al. 2009).

Date of birth timing

We used longitudinally-derived linear equations to estimate age (± 1 day) of juveniles captured before and soon after the onset of volancy (Kunz and Anthony 1982, Baptista et al. 2000). We were then able to estimate date of birth (DOB) by subtracting age (number of days old) from the Julian date of capture. Forearm length is a more accurate predictor of age for juveniles 0–11 days old whereas total epiphyseal gap length is more accurate for juveniles 12–32 days old. After approximately 32 days, the epiphyseal gap is nearly closed and becomes less accurate for age determination (Baptista et al. 2000). Juveniles in this latter group were excluded from DOB analyses. Pre-WNS, we handled both non-volant and volant pups, while nearly all of the pups captured after the onset of WNS were already volant. This meant that DOB for more bats pre-WNS was calculated with forearm length while we primarily used epiphyseal gap size post-WNS. To determine whether this difference in methodology influenced mean DOB, we removed all of the pre-WNS pups for which DOB was calculated using forearm length, then re-calculated mean DOB. Mean DOB with and without these pups included was highly correlated (Pearson correlation; $R = 0.88$, $P < 0.001$) and the average difference in mean DOB was 0.58 ± 1.87 SD

days. Since there was no bias in the estimates to an earlier or later mean DOB, we used all of the available pup data.

Due to different timing and level of sampling effort between years, we subset the capture nights in our dataset so that our sampling periods matched and differences in reproductive timing between years could be accurately assessed (Heideman and Utzurrum 2003). Looking across the entire study, we determined the maximum earliest and minimum latest sampling nights when juveniles were captured, then subset each year of data to fall within those dates. While this reduced our sample size in some years, mean DOB shifted by only 0.69 ± 2.14 SD days and was no longer significantly correlated with mean sample night ($R = -0.06$, $P = 0.912$). We used a Shapiro-Wilks test to determine whether DOB followed a normal distribution for each year. Although only a few years actually followed a normal distribution, mean and median values were generally within a few days of each other with no evidence of kurtosis. We therefore used mean DOB in further analyses.

Reproductive synchrony

As a measure of reproductive synchrony, we calculated the number of days over which the middle 50% of bats were born in a given year (interquartile range). By matching our sampling periods as described above, we effectively removed the beginning and end of the sampling periods as well as any outliers. We could not, therefore, accurately compare the entire parturition period between years and chose to look at the middle 50% of births to avoid the tails of the birth distributions.

Individual Parturition Date

For bats captured from 2016–2019, we further assessed gestation by assigning each bat to one of five stages based on palpation of the abdomen (Racey 1969, Kunz et al. 1999, Richardson et al. 2009, Mason et al. 2010). In the first few weeks of gestation the fetus is not detectable by palpation and females are either not pregnant or in early pregnancy (Kunz et al. 1999). After a few weeks, the embryo may be palpable (Racey 2009) as a small or medium embryo. The end of gestation was split into large embryo and bony embryo when the uterus is rapidly growing (Buchanan and Younglai 1986), fetus weight and length are increasing exponentially (Kunz 1973, Adams 1992), and the fetal skeleton can be easily palpated (Kunz et al. 1999). The little brown bat gestation period is estimated to be 50–60 days (Wimsatt 1945, O'Farrell and Studier 1973). We used 56 days (8 weeks) as the average gestation period, which was split among our five gestation stages to account for exponential fetal growth, where the later stages had shorter time periods. We assigned each gestation stage a period of time from 1–3 weeks and used the midpoint of these ranges to forecast the parturition date for each female. For the purposes of this study, we assumed that bats captured as “no embryo” were in the first few weeks of gestation, but excluded these individuals if they were captured after the first lactating bat of the year. When we examined the records for bats captured twice during pregnancy in the same summer ($n = 8$), the number of days and the change in gestation stage between captures roughly matched our timeline, which was more accurate when bats were first captured as medium embryo or later.

Bats that have recently fed, as is the case for bats captured from 2016–2019, may be more difficult to palpate and assess pregnancy (Racey 2009), but our data suggest that very few bats that were classified as reproductive and recaptured later in the summer were no longer classified as reproductive. A change from reproductive to non-reproductive could be due to misclassification during capture, resorption of the embryo, or postnatal pup mortality (Racey and

Entwistle 2000). Over 80% of bats classified as small or medium embryo and recaptured in the same summer ($n = 21$) were reproductive, suggesting that we were able to accurately assess early gestation most of the time. In addition, as part of another study, a subset of bats was held for several hours to measure basal metabolic rate, at which point they would have emptied their digestive tracks (Buchler 1975), and palpated again before release. For fewer than 2.5% of these bats (6 of 258) was gestation stage different by more than one stage as that assigned in the field.

Timing of arrival at maternity colonies

We used the PIT tag data from 2017–2019 to look at the timing of arrival at maternity colonies. To account for a truncated sampling period immediately after tagging, only data from years following the initial tagging year were used to determine date of arrival. The first detection was used as an indication of arrival at the colony, although bats could have used alternate openings and avoided detection. For bats tagged in 2017 and detected in both 2018 and 2019, we used a Pearson correlation to determine whether there were patterns in individual arrival timing. Bats tagged in one year and physically captured in subsequent years were used to look at the relationship between timing of arrival and parturition date, based on gestation stage.

Climate data

We combined daily temperature and precipitation data from six weather stations (www.ncdc.noaa.gov) located throughout the study area (Fig. 2.1) to represent the regional climate. Daily regional mean temperatures were highly correlated with daily mean temperatures calculated from temperature logger data (Thermochron iButton, Maxim Integrated Products, San Jose, CA, USA) collected hourly during the summer at the Lincoln colony from 2017–2019 ($R = 0.96$, $P < 0.001$) and the Charlestown colony from 2018–2019 ($R = 0.95$, $P < 0.001$). Since

iButton data were not available for all years and sites and they were correlated with the regional means, we used the regional means to calculate our monthly weather variables. For each month from April to June, we calculated mean average temperature, total precipitation (mm), and total days with precipitation over 1.3 mm. We also calculated cumulative precipitation for the periods April–May, May–June, and Apr–June. Lastly, we calculated monthly and seasonal severity indices by summing the number of days where average temperature was $<10^{\circ}\text{C}$, a threshold below which insect activity and bat foraging is reduced (Anthony et al. 1981, Rydell 1989). Severity was also a proxy for mean minimum temperature (Pearson correlation for May: $R = -0.75$, $P < 0.001$). Total number of days with precipitation over 1.3 mm was correlated with total monthly precipitation (Pearson correlation for June: $R = 0.81$, $P < 0.001$) and was excluded from model sets.

Statistical analyses

All analyses were conducted in R v3.6.1 (R Core Team 2018). We used Tukey’s multiple comparison of means to test whether annual reproductive rates were significantly different between pre- and post-WNS arrival for adults and yearlings as well as whether adult and yearling rates were different for each time period. We used linear models to test whether any of our monthly or seasonal weather variables were correlated with annual adult reproductive rate.

Reproductive timing data from pups and adults were analyzed separately. To determine which weather variables best predicted the timing of reproduction, we constructed a set of linear models with annual mean lactation date or annual mean DOB as the response variable and weather variables as the predictors. We limited models to a maximum of two predictor variables due to small sample size: models either had one weather variable or a weather variable and a categorical variable for pre-/post-WNS arrival. Models with an interaction between the weather

variable and pre-/post-WNS were also considered. Additive and interactive models with pre-/post-WNS were used to separate the influence of WNS on the timing of reproduction from changes in climate over time. We tested whether an additive model or an interactive model provided a better fit to the data. If the slopes for the pre- and post-WNS years were parallel, but offset, as in the additive model, this indicated an effect of WNS on the timing of reproduction independent of climate change, but only if the fit was also significantly better than a model with just the weather variable. We used similar methods to look at reproductive synchrony related to climate and WNS.

We then looked at the timing of reproduction in individuals by first examining whether arrival date corresponded to parturition date, then by testing the effect of WNS. We used the ‘lme4’ package (Bates et al. 2015) to construct a set of linear mixed-effects models with parturition date, as determined by gestation stage, as the response variable. Wing score, Pd load, mass, and year were included as fixed effects in all possible additive combinations with colony and individual as random effects. Year was included as a fixed effect to account for inter-annual variation in spring weather conditions.

All model sets were ranked using Akaike’s Information Criteria corrected for small sample size (AICc) with the MuMIn package (Bartón 2020). Model residuals were evaluated for normality and homogeneity. Nested models were compared using F-tests or likelihood ratio tests to determine the significance of predictor variables.

Results

We captured 3265 adult female little brown bats pre-WNS and 3149 post-WNS arrival over 179 and 186 trapping nights, respectively. Pre-WNS, we captured 2369 pups and from 2016–2019 we captured 457 pups for which we could determine date of birth.

Reproductive rate

Mean annual reproductive rates for adult females were 0.95 ± 0.03 pre-WNS and 0.95 ± 0.04 post-WNS arrival (Fig. 2.2), and were not significantly different (Tukey's test; $t = 0.033$, $P = 0.99$). Captures of yearling females ranged from 2–9 per summer pre-WNS and 2–16 per summer post-WNS. A total of 27 out of 63 and 13 out of 74 yearlings captured pre- and post-WNS, respectively, were excluded because they were captured before the first date of lactation. Mean annual reproductive rates for yearling females were significantly higher post-WNS (0.89 ± 0.13) than pre-WNS (0.49 ± 0.40 ; Tukey's test; $t = -3.455$, $P < 0.01$). Post-WNS, yearling and adult reproductive rates were not significantly different (Tukey's test; $t = -0.610$, $P = 0.93$). To reduce the influence of years with few captured bats, we pooled yearlings into pre- and post-WNS, resulting in slightly different reproductive rates of 0.55 (20/36) pre-WNS and 0.85 (52/61) post-WNS. We found no significant relationship between either yearling or adult reproductive rate and any of the monthly or seasonal weather variables.

Nearly all of the bats originally identified as 'non-reproductive' were found to be reproductive if recaptured later in the same summer. Of 639 pre-WNS and 182 post-WNS bats captured more than once in a summer, only 7 and 9, respectively, went from reproductive to non-reproductive, suggesting that fewer than 5% were misclassified or had terminated pregnancies.

Mean lactation date & pup date of birth

After excluding seven years without adequate sampling, we ended up with 12 years pre-WNS and 8 years post-WNS arrival where we were able to determine mean lactation date, which occurred between June 23 and July 7. For the pup data, we had 14 years pre-WNS and 4 years post-WNS, with mean DOB occurring between June 15 and June 30. Mean lactation date and

mean DOB were correlated (linear regression: $R^2 = 0.55$, $P < 0.001$) and the difference between them was 5.29 ± 3.08 days (Fig. 2.3).

Reproductive phenology & climate

The reproductive data, pooled for pre- and post-WNS arrival, suggested that reproduction occurred earlier in the summer post-WNS by approximately 10 days (Fig. 2.4). This comparison, however, did not account for potential climate effects, so we analyzed annual reproductive timing based on adult reproductive stage and pup DOB. To evaluate whether climate change has shifted the reproductive phenology of this population, we analyzed for a shift in reproductive timing in the context of our weather variables. We detected no significant trend in the timing of reproduction (linear regression: $R^2 = 0.03$, $P = 0.24$) from 1993 to 2019. There was also no significant trend in mean May precipitation ($R^2 = -0.02$, $P = 0.46$) or mean April temperature ($R^2 = 0.02$, $P = 0.23$), however, there was a marginally significant increase in May temperature ($0.07 \pm 0.03^\circ\text{C}/\text{year}$, $R^2 = 0.11$, $P < 0.05$) over the 27-year sampling period.

Inter-annual variation in spring weather had a significant impact on reproductive timing. The highest ranking models using mean lactation date included April–May precipitation, mean May temperature, May precipitation, total spring precipitation, and the categorical variable for pre- and post-WNS arrival (Table 2.1). Overall, parturition occurred earlier in years when May was warmer, and April and May were drier (Fig. 2.5). The top model indicated a significant interaction between April–May precipitation and pre-/post-WNS ($F_{1,16} = 14.03$, $P < 0.01$) and explained 62.1% of the variation in reproductive timing ($F_{3,16} = 11.36$, $P < 0.001$). Parturition was later in wetter years pre-WNS, but precipitation did not seem to explain reproductive timing post-WNS (Fig. 2.5A). Mean May temperature explained 28.7% of the variation in parturition

timing ($P < 0.01$) and including a pre-/post-WNS factor did not improve model fit ($F_{1,17} = 0.97$, $P = 0.34$; Fig. 2.5B).

Using the pup DOB data, the highest ranking models included May precipitation, April–May precipitation, mean May temperature, total spring precipitation, and the categorical variable for pre-/post-WNS arrival (Table 2.1). The top model with May precipitation explained 71.4% of the variation in reproductive timing ($F_{2,15} = 22.23$, $P < 0.001$), while May temperature and pre-/post-WNS explained 66.1% ($F_{2,15} = 17.57$, $P < 0.001$; Fig. 2.5D). There was no significant interaction between pre-/post-WNS and either May precipitation ($F_{1,14} = 0.65$, $P = 0.74$) or May temperature ($F_{1,14} = 0.08$, $P = 0.78$). The additive models indicated that the relationships between parturition date and May climate were the same pre- and post-WNS, but were 6.3 days earlier post-WNS. The second highest ranking model, April–May precipitation and pre-/post-WNS, explained 68.6% of the variation ($F_{2,15} = 19.57$, $P < 0.001$; Fig. 2.5C).

Reproductive synchrony

The middle 50% of births occurred within a 4–10 day period. The highest ranking models for reproductive synchrony included June precipitation, mean May temperature, and the categorical variable for pre-/post-WNS arrival (Table 2.2). Overall, synchrony increased with higher levels of precipitation in June and warmer mean temperatures in May (Fig. 2.6). The top model with June precipitation explained 39.7% of the variation in synchrony ($F_{1,16} = 12.19$, $P < 0.01$). Including pre-/post-WNS with June precipitation did not improve model fit as an additive ($F_{1,15} = 0.76$, $P = 0.40$) or interactive effect ($F_{1,14} = 1.14$, $P = 0.30$). May temperature only explained 17.4% of the variation in synchrony by itself, but had a nearly identical model weight with a model including pre-/post-WNS ($F_{1,15} = 3.01$, $P = 0.10$) that improved the adjusted R^2 to 26.7%.

This model indicated that parturition was slightly less synchronous post-WNS than pre-WNS and the middle 50% of births took an additional 1.72 days, independent of May temperature.

Effects of arrival time and white-nose syndrome on parturition

Bats PIT-tagged in 2017 and detected in both 2018 and 2019 ($n = 39$) showed that individuals arrive at approximately the same time each year (Fig. 2.7A), with a difference in arrival time ranging from 1–21 days (72% arrived within 10 days of previous year's arrival date). Timing of arrival at the maternity colony was not significantly correlated with parturition date ($F_{1,14} = 3.23$, $P = 0.10$, $R^2 = 0.13$), but there was a general trend of bats that arrived earlier giving birth earlier than those that arrived later (Fig. 2.7B). Parturition date tended to fall within a 40–60 day expected gestation period, assuming that bats initiated gestation immediately before or upon arrival at the maternity colony.

Linear mixed models indicated a significant effect of wing score, year, and mass on the timing of parturition ($n = 582$; Table 2.3). In a separate analysis of 340 bats with positive Pd swabs, including Pd load did not significantly improve model fit (LRT, $\chi^2 = 1.889$, $P = 0.17$, coefficient estimate 0.954, SE = 0.692), however, the top two models had nearly equal model weights (Table 2.3). Tukey's test indicated that bats with more wing damage, at or above an Early 1, had significantly later parturition dates than those with less damage, at or below Late 1 (Fig. 2.8A). Bats with higher mass (Fig. 2.8B) and lower Pd loads (Fig. 2.8C) at time of capture had earlier parturition dates. In addition, mean parturition dates were significantly different between years, except between 2016 and 2017, and were significantly later in 2019 (Fig. 2.8D). Linear models of PIT-tagged bats that were physically recaptured while pregnant ($n = 18$) also showed that bats with higher wing scores had later parturition dates than bats with lower wing

scores. Wing score explained 72.1% of the variation in parturition date, while arrival time ($F_{1,13} = 0.25$, $P = 0.63$) and mass ($F_{1,13} = 2.35$, $P = 0.15$) were not significant predictors.

Discussion

Reproductive rate

For iteroparous species, such as the little brown bat, age at first reproduction is likely the result of both life history and physiological constraint (Stearns 1989). We found age at first reproduction to be a flexible strategy with yearling little brown bats reproducing at higher rates than immediately before WNS (Frick et al. 2010a) and higher than what has been previously reported in the literature (Davis and Hitchcock 1965, Humphrey and Cope 1976), while adult females continue to reproduce at high rates of approximately 95% (Fig. 2.2). These results are similar to data from the same species in upstate New York (Dobony and Johnson 2018) and the greater horseshoe bat *Rhinolophus ferrumequinum*, where the youngest age class increased their reproductive rate following a population collapse (Ransome 1995). We did not detect a relationship between reproductive rate and any of the weather variables included in our study, unlike in two European *Myotis* spp. (Lučan et al. 2013, Linton and MacDonald 2018).

Our results also suggest a higher recruitment rate than pre-WNS, which is a function of the rate at which yearling females survive their first winter and return to their natal maternity colony to reproduce the following summer. Previous studies on known-aged individuals found that yearlings returned at much lower rates than adults (Brenner 1968, Tuttle 1976) and that yearlings were more likely to return and breed if born earlier in the summer (Frick et al. 2010a). In this study, we captured more yearling females at maternity colonies post-WNS than were captured in this population pre-WNS, suggesting that yearling females are returning to their natal colonies at a higher rate since the population collapse created by WNS.

As in many other studies of reproductive rates in bats at maternity colonies, our study similarly faces the challenges of accurately determining reproductive status and population level reproductive rate. Temperate hibernating bats, such as the little brown bat, have delayed fertilization (Wimsatt 1945, Oxberry 1979, Racey and Entwistle 2000), which allows females to begin reproduction immediately upon emergence from hibernation without the temporal or energetic costs of mating. However, under adverse conditions, temperate bats can control reproduction by resorbing embryos (Pearson et al. 1952). Resorption is most likely to occur during the early stages of pregnancy (Wasser and Barash 1983), therefore it is possible that some females initiate pregnancy, but convert to non-reproductive individuals soon after arrival to the maternity colony. The proportion of these females that remain in or abandon the maternity colony for the remainder of the season is poorly understood, but has important implications for the population-level reproductive rate. This may be especially important for yearling reproductive rate. If yearlings do not return to reproduce in their first year, then our estimates of yearling cohort size will be underestimated and reproductive rate will be biased high.

Our study attempted to control for changing reproductive condition by limiting our analysis to reproductive individuals that were palpably pregnant, lactating, or post-lactating, and excluding individuals that were undetermined or non-reproductive prior to this stage. Based on the low rate of re-classification of reproductive individuals to non-reproductive (<5%), our data suggest that there are low levels of pre-natal mortality and embryonic resorption once gestation has progressed to the point that it is physically detectable. There were also very few dead pups found within the maternity colony (Scott Reynolds, personal communication) suggesting that pre-weaning mortality is generally low in this species. While we lose some of the variation in life- history strategies that may be occurring early in the reproductive season, our methodology

produces a more repeatable estimate of reproductive rates for individuals that are roosting in maternity colonies. Better estimates of population level reproductive rates would require extensive trapping on the landscape, early spring trapping at hibernacula and maternity colonies with a reliable assay that could detect early pregnancy, or more intensive banding combined with the appropriate mark-recapture models to account for non-reproductive individuals that do not return to their maternity colonies or that abandon them after pregnancy termination.

Reproductive phenology

A possible mechanism for the increased recruitment of yearlings is an earlier reproductive phenology. We found that the mean reproductive timing since the onset of WNS has advanced by six to ten days (Figs. 2.4 & 2.5), similar to results from West Virginia (Francl et al. 2012). Young that are born earlier have a longer period to grow physiologically mature prior to hibernation (Ransome and McOwat 1994). Earlier reproductive timing would also create more opportunity for juveniles to accumulate body fat in anticipation of hibernation and would most significantly improve overwintering survivorship for juveniles, who are the most challenged to allocate adequate energy reserves prior to their first winter (Davis & Hitchcock 1965; Racey 1982, Lenihan and Van Vuren 1996). Increased fat stores may not only improve survival chances of juveniles, but also allow for reproduction as yearlings (Kunz et al. 1998), who are generally thought to be reproductively limited by their pre-hibernation fat stores (Kunz et al. 1998, McGuire et al. 2009). This energetic constraint is evidenced by the fact that yearling reproductive rates are dependent on the timing of birth (Frick et al. 2010a) and post-weaning foraging conditions (Holroyd 1993; Frick et al. 2010a). Earlier reproductive timing may also partly explain why little brown bats are now entering hibernation with higher levels of body fat

(Cheng et al. 2019). While we did not have the data to look at selection for larger offspring, larger and potentially fatter juveniles that survive may also reproduce earlier and their offspring may in turn inherit a larger body size, resulting in more higher quality individuals that could also potentially explain the observed higher recruitment rate.

There is also evidence to suggest that the shift towards earlier age at first reproduction could be partially explained by warming spring temperatures that allow females to emerge from hibernation earlier than they could prior to WNS. Spring emergence phenology is correlated with ambient temperature, hibernacula air flow (Meyer et al. 2016), and falling barometric pressure (Czenze and Willis 2015). Because successful emergence requires a positive energy balance, a shift in emergence timing created by warmer spring conditions likely results from either reduced thermoregulatory costs or improved foraging conditions (Czenze and Willis 2015). There also appears to be an individual quality component, as adult female bats with higher body condition index (BCI) emerged earlier in the spring than those with lower BCI and earlier than subadult (yearling) females (Norquay and Willis 2014). Although data from this study and others (e.g., Norquay and Willis 2014) do not show any detectable shift in seasonal arrival to the maternity sites compared to historical data (Davis and Hitchcock 1965), it is possible that improving early spring conditions are making emergence and initiation of reproduction more energetically favorable for all cohorts, including yearlings.

Although spring temperature and precipitation did not show a consistent temporal trend typical of climate change, variation in both weather variables contributed to inter-annual variation in reproductive phenology. Mean reproductive timing varied among years by up to two weeks over the course of the study (Fig. 2.5). Unlike other studies where spring temperature was more important (Rydell 1989, Ransome and McOwat 1994, Burles et al. 2009, Lučan et al. 2013,

but see Grindal et al. 1992, Linton and MacDonald 2018), we found that precipitation in April and May provided a better fit to the reproductive timing data (Fig. 2.5, Table 2.1). May temperature was also a significant predictor but carried less weight than precipitation. Variation in reproductive timing related to climate is expected for income breeders (Henry et al. 2002) who depend on constant food intake during reproduction rather than stored fat reserves. The timing of reproduction is thought to correspond with insect availability, such that insect abundance peaks during lactation, when energy demands are highest (Kurta et al. 1989, Racey and Entwistle 2000). The relationships between these weather variables and reproductive timing were the same pre- and post-WNS arrival when we used the pup DOB data (Fig. 2.5), but not when we used the adult lactation data, suggesting that there may be influences of both climate change and disease on annual reproductive timing. These disparate results are most likely a result of differences in sampling intensity and timing across our study, which we could not avoid, but attempted to minimize by matching the sampling periods.

Inter-annual variation in spring weather also influenced the synchrony of parturition, where years with higher precipitation in June had higher rates of synchrony (Fig. 2.6, Table 2.2). We predicted that reproductive timing would be less synchronous post-WNS due to individual variation in emergence BCI and wing damage. The higher reproductive rate of yearlings would also contribute to less reproductive synchrony, as yearlings typically reproduce later than other age cohorts. The data, however, did not support a significant decrease in reproductive synchrony following the onset of WNS. It is possible that bats returning late or with more extensive wing damage were able to compensate for the delay through faster pre-natal growth in May and June due to warmer temperatures, increasing insect abundance, and reducing the use of daily torpor (Racey and Swift 1981), however, our data did not allow for measurement of inter-annual or

inter-individual variation in pre- or post-natal growth rates. If there is compensatory growth, this would also partially explain why arrival time did not correlate well with estimated parturition date (Fig. 2.7B).

Effects of arrival time and white-nose syndrome on parturition

While reproductive timing was on average earlier post-WNS than pre-WNS arrival, contrary to what we predicted, there was considerable variation in the timing of parturition between individuals. We found that bats with higher levels of wing damage at the time of capture were in earlier stages of gestation than bats with less wing damage (Fig. 2.8A), independent of when they arrived at the colony. Individuals arrived at approximately the same time each year (Fig. 2.7A, which could mean it is an inherited trait, is dependent on individual quality, or is related to distance from hibernaculum to summer colony. The energy costs in the spring associated with immune responses to Pd and tissue repair (Archie 2013, Fuller et al. 2020) appear to be sufficiently high to delay the timing of reproduction at the individual level. However, even among bats with the same level of wing damage, there was variation in parturition date, which could be due to mis-classification of gestation stage, differences in capture date, or disparities in individual quality that would result in differences in arrival time (Fig. 2.7), wing healing rate (Fuller et al. 2011), or torpor use (Besler and Broders 2019). Energy costs from infection, however, do not appear to be high enough to force females at maternity colonies to forgo reproduction altogether nor to delay reproduction at the population level. Wing damage peaks and heals within three to four weeks of emerging from hibernation (Fuller et al. 2011, Meteyer et al. 2011, 2012, Fuller et al. 2020), which coincides with early gestation when energy demands related to reproduction are the lowest (Kurta et al. 1989). Warmer springs would create less need for torpor and potentially improve insect availability in early spring, reducing foraging costs that

might otherwise be higher with damaged wings (Fuller 2016). This may be allowing females to allocate sufficient resources to wing healing during this time without significantly delaying reproduction.

Although WNS inflicts high energy costs after emergence from hibernation and during early gestation, our observed rates of reproduction (Fig. 2.2) and survival (see Chapter 3) in both juveniles and adults suggest that there are no immediate, apparent tradeoffs between maintenance and reproduction or reproduction and survival. This may be contrary to studies of trade-offs and the costs of reproduction in wild mammals (Calow 1979). Recent evidence from European *Myotis* spp. suggests interspecific differences in reproductive costs on primiparous female survival as well as in the success of the first reproductive attempt. For most iteroparous species that can be flexible in their reproductive strategy, yearlings (or primiparous females in species that take multiple years to reach sexual maturity) that do reproduce generally have much lower reproductive success than other age cohorts (Green and Rothstein 1991, Derocher et al. 1992, O'Donnell 2002; Culina et al. 2019). For some species, early reproduction had a positive impact on lifetime reproductive success (Gustafsson and Pärt 1990, Cassinello and Alados 1996) and allowed individuals to reproduce before succumbing to disease (Jones et al. 2008). However, reducing the age of first reproduction may result in long-term trade-offs, such as shortened life expectancy (Reiter and Le Boeuf 1991, Ransome 1995, Wilkinson and South 2002, Desprez et al. 2014), and can impact offspring quality or the quality of parental care, leading to reduced offspring survival (Stearns 1989; Ransome and McOwat 1994; Ransome 1995). Further work is needed in this regional population to determine whether there are short-term or long-term trade-offs occurring, such as early reproduction and survivorship, which could shorten generation times, but would have important implications for population growth over time.

Our study shows that little brown bats have demographically responded to WNS by shifting their life history to decrease the mean age of first reproduction, while adult females are continuing to reproduce at high rates despite wing damage caused by WNS. The long-term nature of this study, combined with the use of known-age and marked individuals, suggests both inter-annual and inter-individual variation play a significant role in determining parturition date. Several factors may have contributed to the shift in reproductive phenology, including selection for higher quality individuals, phenotypic plasticity, and changing spring weather, ultimately leading to the population advancing the mean date of parturition. Warming spring temperatures could reduce energy trade-offs and lead to advanced reproductive phenology at the population level that could offset delays associated with Pd infection at the individual level.

Table 2.1. Top five multiple linear regression models of climate variables and reproductive timing. Mean lactation date was estimated from pooled adult reproductive status data and mean date of birth was estimated from little brown bat pup epiphyseal gap size. Coefficient estimates are shown for each model. Models are ranked by AICc. AM = Apr + May, Spr = Spring, P = total precipitation, T = temperature, WNS = pre-/post-WNS, K = number of parameters; logLik = log likelihood; w_i = model weight.

Intercept	AM P	Spr P	May T	May P	WNS	AM P* WNS	Spr P* WNS	May P* WNS	K	logLik	AICc	Δ AICc	w_i
Mean lactation date													
182.397	-0.019				+	+			4	-44.93	104.14	0.00	0.92
182.282		-0.012			+		+		4	-48.85	111.99	7.85	0.02
203.866			-1.719						2	-52.42	112.34	8.20	0.02
171.966	0.036				+				3	-51.22	113.11	8.98	0.01
172.343		0.022			+				3	-51.81	114.30	10.15	0.01
Mean date of birth													
172.745				0.046	+				3	-38.58	88.24	0.00	0.45
171.985	0.028				+				3	-39.43	89.93	1.69	0.20
193.572			-1.235		+				3	-40.12	91.32	3.07	0.10
172.276		0.017			+				3	-40.36	91.79	3.55	0.08
172.482				0.049	+			+	4	-38.51	92.01	3.77	0.07

Table 2.2. Top five linear regression models of climate variables and reproductive synchrony (middle 50% of births). Coefficient estimates are shown for each model. Models are ranked by AICc. T = temperature, P = precipitation, WNS = pre/post-WNS, K = number of parameters; logLik = log likelihood; w_i = model weight.

Intercept	May T	June P	WNS	June P * WNS	K	logLik	AICc	Δ AICc	w_i
9.355		-0.024			2	-32.26	72.23	0.00	0.61
9.116		-0.023	+		3	-31.81	74.70	2.47	0.18
9.272		-0.024		+	4	-31.11	77.22	4.98	0.05
15.820	-0.656				2	-35.10	77.91	5.67	0.04
17.000	-0.775		+		3	-33.45	77.98	5.75	0.03

Table 2.3. Top five linear mixed-effects models of estimated parturition timing with maternity colony and individual ID as random effects and mass, wing score, and year as fixed effects. Model sets were created with and without fungal load data from wing swabs tested for the causative agent of white-nose syndrome, *Pseudogymnoascus destructans* (Pd). Coefficient estimates are shown for each model. Models are ranked by AICc. K = number of parameters; logLik = log likelihood; w_i = model weight.

Intercept	Pd Load	Mass	Wing Score	Year	K	logLik	AICc	Δ AICc	w_i
Without Pd swab data									
185.438		-2.578	+	+	10	-1231.50	2490.12	0.00	1.00
177.244		-1.284	+		7	-1262.90	2546.47	56.34	0.00
164.244			+		6	-1266.58	2551.70	61.58	0.00
203.016		-3.374			2	-1295.73	2601.63	111.51	0.00
168.497				+	4	-1304.23	2622.80	132.68	0.00
With Pd swab data									
185.438		-2.578	+	+	10	-1231.50	2490.12	0.00	0.54
187.768	0.954	-2.342	+	+	11	-1230.56	2490.42	0.29	0.46
171.436	2.091		+	+	10	-1241.50	2510.12	20.00	0.00
187.865	3.222	-0.899	+		8	-1250.29	2523.38	33.25	0.00
179.670	3.422		+		7	-1252.20	2525.06	34.93	0.00

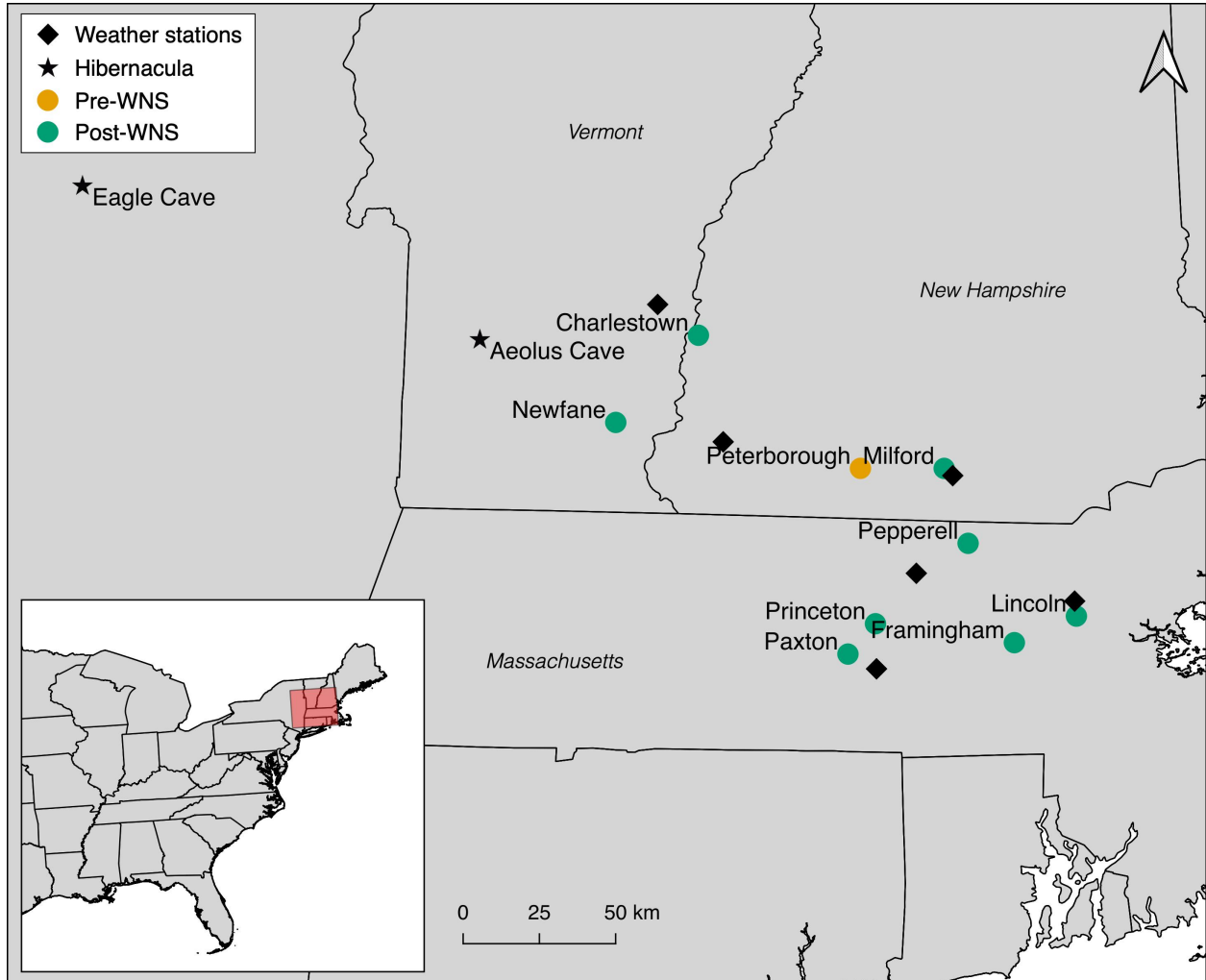


Figure 2.1. Map of little brown bat (*Myotis lucifugus*) maternity colonies studied for 4–16 years between 1993–2019, pre-white-nose syndrome (WNS) arrival in orange and post-WNS arrival in green. Diamonds are weather station locations (www.ncdc.noaa.gov) used to create a regional climate summary. Stars represent known hibernacula for bats from these maternity colonies.

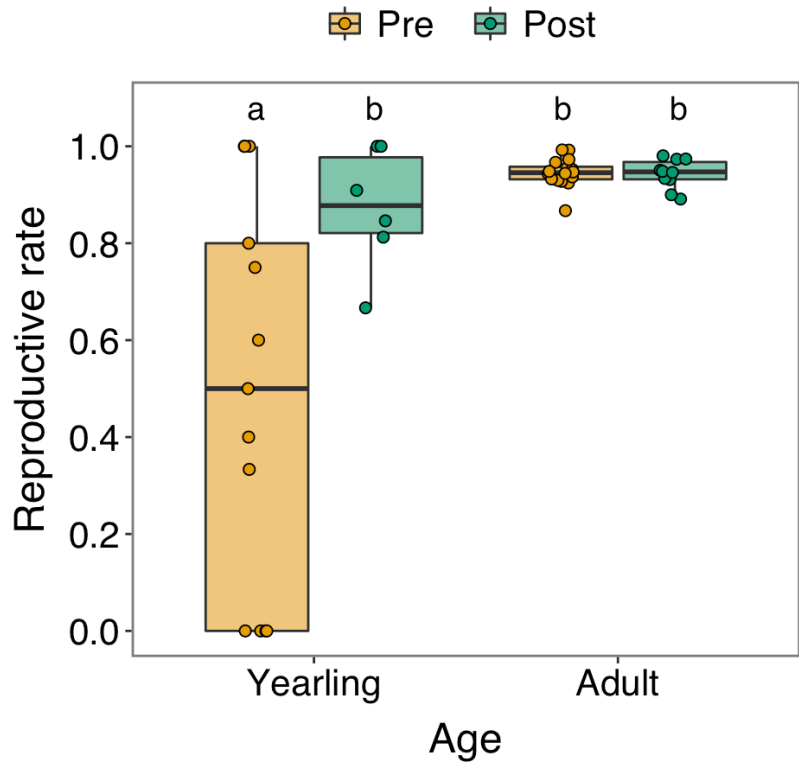


Figure 2.2. Boxplots of annual reproductive rates for little brown bat (*Myotis lucifugus*) yearlings (banded as juveniles and recaptured the following year) and adults, captured pre- and post-WNS from 1993–2019. Lowercase letters show significant differences between groups based on Tukey's multiple comparison of means.

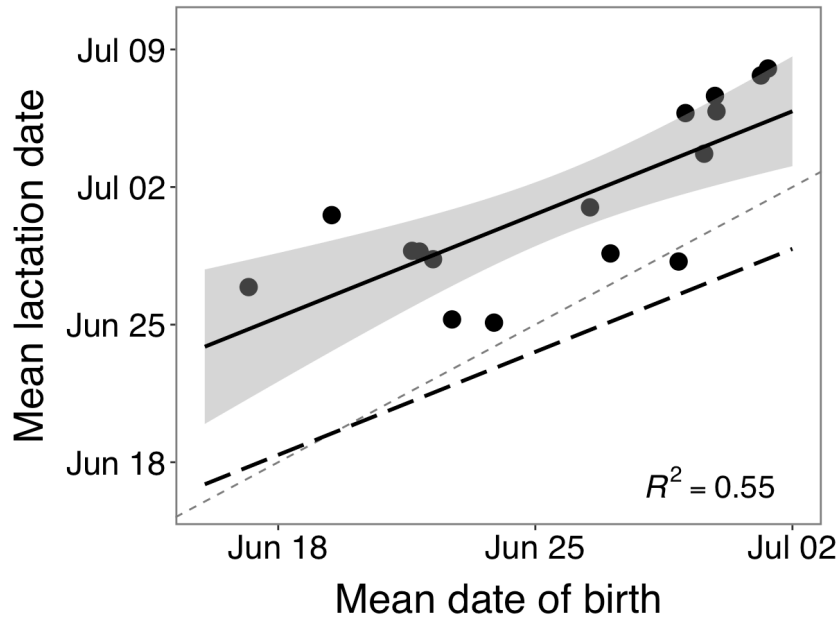


Figure 2.3. Correlation between mean date of birth estimated from little brown bat pup epiphyseal gap size compared to mean lactation date estimated from pooled adult reproductive status data. Bats were captured at maternity colonies in New England from 1993–2019. Each dot shows a year when both sets of data were available. The light gray dashed line shows a 1:1 reference line. The solid line is a linear regression and the black dashed line has the same slope as the regression, but with a y-intercept seven days earlier. The gray ribbon is the 95% confidence interval.

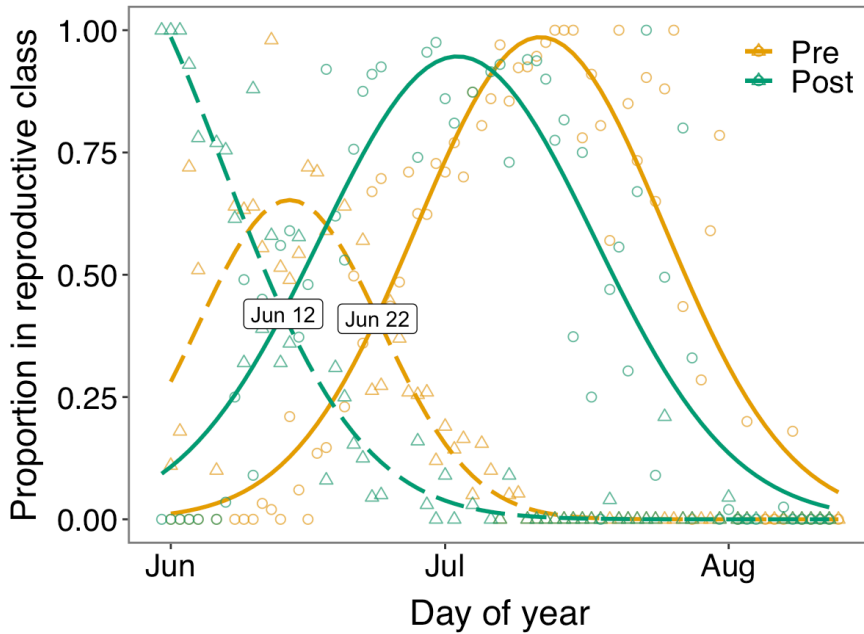


Figure 2.4. Reproductive phenology of little brown bats at maternity colonies in New England based on the proportion of pregnant (open triangles, dashed lines) and lactating bats (open circles, solid lines) out of the total number of adult females captured on a given sampling night. Adult reproductive data from pre- and post-WNS were pooled. Curves are non-linear least squares fits to the data. The intersection between the pregnancy and lactation curves represents the median parturition date.

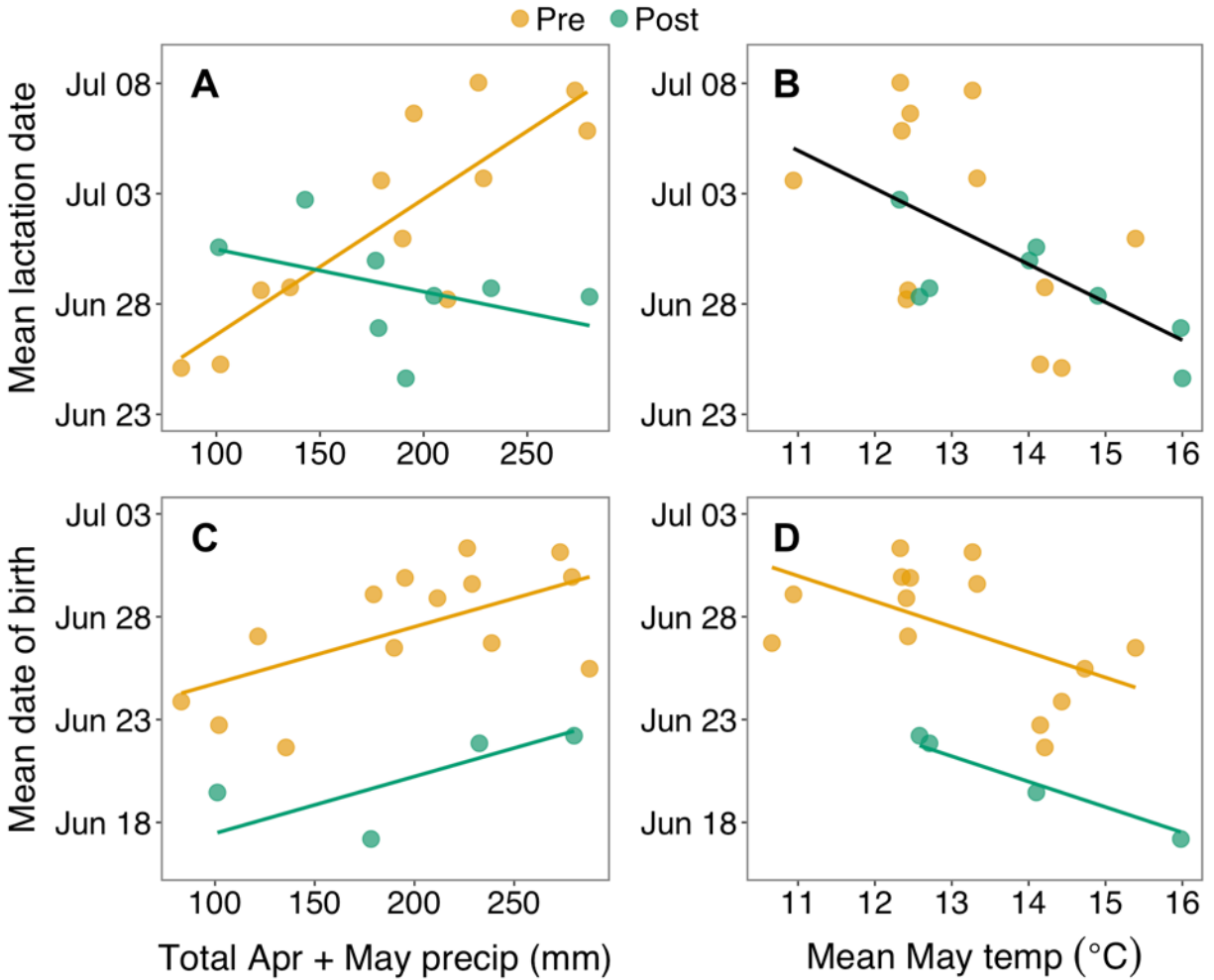


Figure 2.5. Relationships between reproductive timing and climate variables for little brown bats in maternity colonies in New England pre- and post-WNS. Mean lactation date (A & B) was estimated from pooled adult reproductive status data and mean date of birth (C & D) was estimated from little brown bat pup epiphyseal gap size. Total April and May precipitation (A & C) and mean May temperature (B & D) are regional means calculated from six weather stations in the study area. Regression lines are in color when pre-/post-WNS was a significant factor in the multiple linear regression model and in black when not significant.

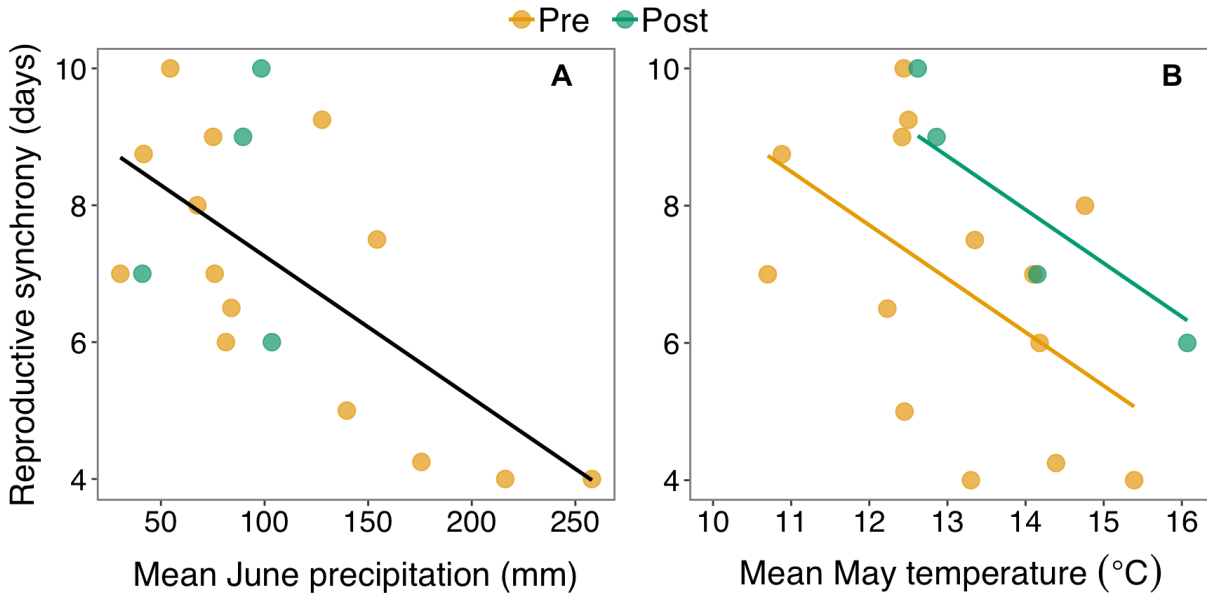


Figure 2.6. Reproductive synchrony of the middle 50% of births in little brown bats pre- and post-WNS related to A) mean June precipitation and B) mean May temperature. Date of birth was estimated from pup epiphyseal gap size. Mean June precipitation and May temperature are regional means calculated from six weather stations in the study area. Regression lines are in color when pre-/post-WNS was a significant factor in the multiple linear regression model and in black when not significant.

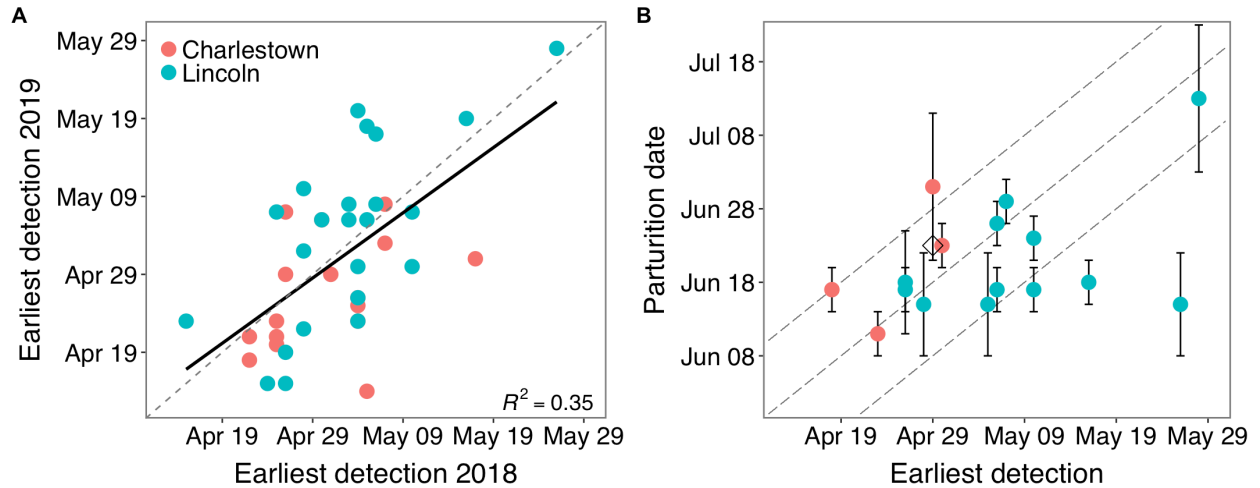


Figure 2.7. For two little brown bat colonies in New England, the relationship between timing of arrival A) for individuals between years and B) estimated parturition date based on gestation stage at time of capture. Arrival time is the earliest passive integrated transponder tag detection of the year. In A, the solid line is a linear regression and the dashed gray lines represent a 1:1 reference line. In B, bars show length of time for the estimated gestation stage (± 0.5 to 1.5 weeks) and the dashed gray lines are 40-, 50-, and 60-day gestation periods, assuming gestation is initiated upon arrival at the maternity colony. The open diamond is the estimated date of birth for the pup of the female first detected on April 28 (red point directly above).

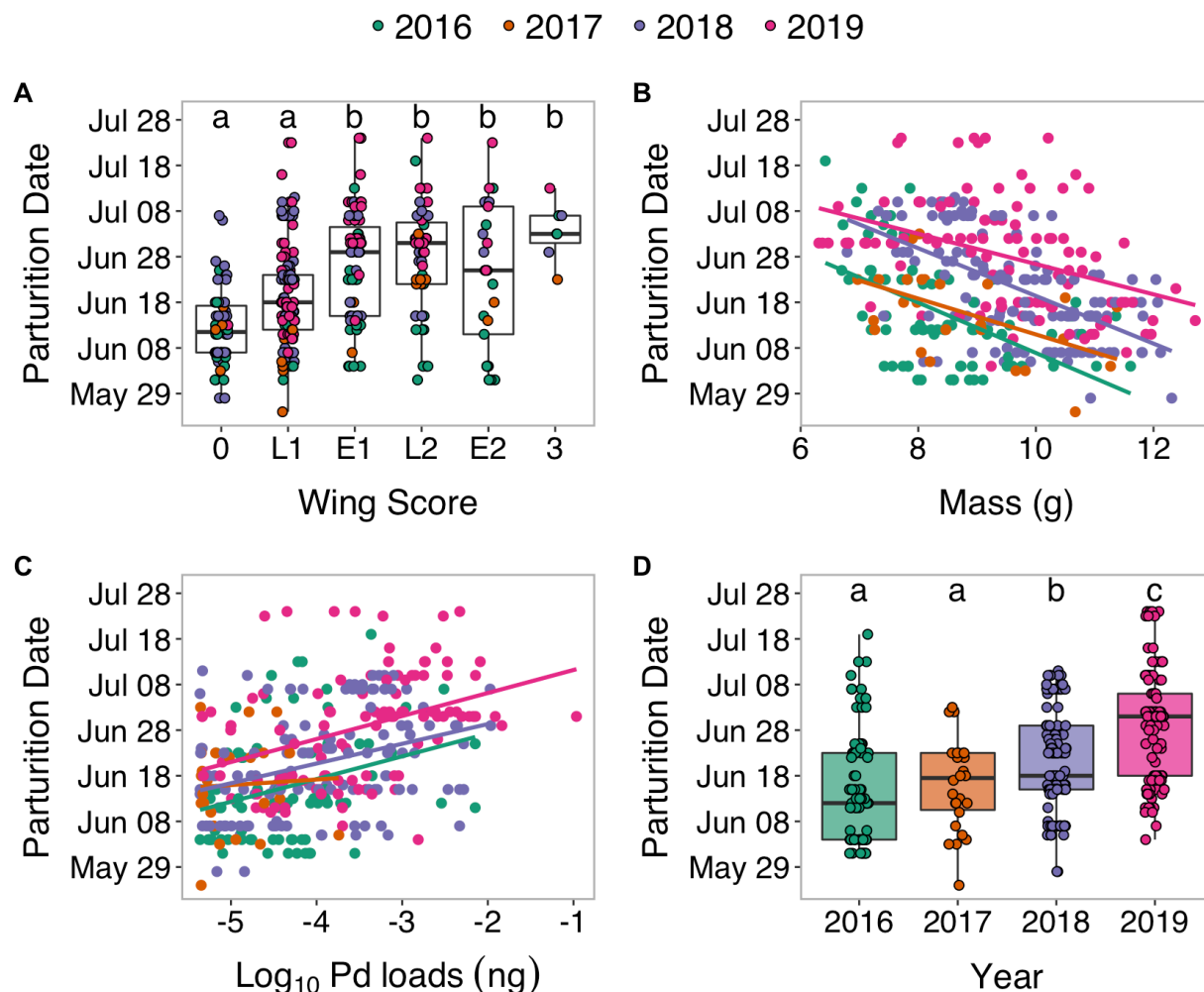


Figure 2.8. Timing of parturition assessed by gestation stage at time of capture for little brown bats captured post-WNS (2016–2019) in New England maternity colonies in relation to A) wing damage due to WNS, assessed by wing score from 0 to 3; B) bat mass at time of capture; C) fungal load of the causative agent of white-nose syndrome, *Pseudogymnoascus destructans* (Pd); and D) sampling year. Lower case letters indicate significant differences between groups based on results from Tukey's multiple comparison of means. Solid lines in B and C are linear regression best-fit lines by year.

CHAPTER 3

RETURN OF THE LITTLE BROWN BAT: LONG-TERM SURVIVAL AND POPULATION RECOVERY IN A WHITE-NOSE SYNDROME-IMPACTED SPECIES

Abstract

Effective conservation of disease-impacted wildlife populations depends on understanding both the immediate and long-term effects of disease on demographic rates. Little brown bat (*Myotis lucifugus*) populations in the Northeastern United States have declined by over 90% since the emergence of white-nose syndrome (WNS), leaving small, remnant populations. Despite repeated exposure to *Pseudogymnoascus destructans* (Pd), the fungal pathogen that causes WNS, individuals are surviving and some colonies are persisting and even growing. To understand how demographic rates have changed over time, we conducted a 14-year mark-recapture study at eight summer maternity colonies in New England, close to the WNS epicenter. Our banding study showed that survival rates crashed upon Pd invasion and have since increased and stabilized at rates similar to or higher than survival rates pre-WNS. In all years, adult survival rates were higher than those of juveniles, and survival rates varied between sites. We also documented long-term survival, with some individuals living for at least 10–12 years. Combining the mark-recapture data with up to 13 years of emergence count data, we created integrated population models for three colonies, and extrapolated them as population viability analyses under different management scenarios. Since WNS became established in the region, mean growth rates for all three colonies were above 1 and population projections suggested colony growth into the future, even without additional human intervention beyond current

management efforts. This study provides evidence of regional population growth and suggests that management efforts targeted at slower-growing colonies, such as summer roost or habitat enhancement, will further ensure recovery for the little brown bat.

Introduction

Wildlife populations naturally fluctuate over time due to environmental and demographic stochasticity (Seber 1982, Morris and Doak 2002, Mills 2013). Novel threats, such as emerging infectious diseases, can have immediate and catastrophic impacts on population size (Daszak et al. 2000, Fisher et al. 2012), sometimes leading directly to extinction or leaving small, remnant populations that are more vulnerable to extinction (De Castro and Bolker 2005, McKnight et al. 2017). Compensatory demographic responses (Coulson et al. 2004), behavioral adaptations (Langwig et al. 2012), or the evolution of resistance or tolerance to the pathogen (Gonzalez et al. 2013, McKnight et al. 2017) may allow populations to stabilize, even when pathogen prevalence remains high (Scheele et al. 2017, Frick et al. 2017). For these persisting populations, the long-term effects of disease on demographic rates and viability can be hard to disentangle from changes in pathogen virulence or host evolution (De Castro and Bolker 2005). Long-term monitoring may be required to see changes in demographic rates, life history (Scheele et al. 2017, Lazenby et al. 2018), or population growth (Newell et al. 2013).

White-nose syndrome (WNS) is a recently emerged infectious disease that is caused by the fungal pathogen *Pseudogymnoascus destructans* (Pd; Lorch et al. 2011, Warnecke et al. 2012). Since its discovery in upstate New York in the winter of 2006–2007 (Blehert et al. 2009), WNS has killed millions of bats and now threatens the extinction of several hibernating bat species in North America (Frick et al. 2017). Pd quickly spread throughout much of the Northeastern United States and has been present in some hibernacula there for over a decade

(whitenosesyndrome.org). Little brown bats (*Myotis lucifugus*) have been heavily impacted, with population declines of >75% observed in winter hibernacula (Frick et al. 2010b, Turner et al. 2011) and during the summer (Dzal et al. 2011, Brooks 2011, Dobony et al. 2011). Extensive studies of little brown bats in this region prior to and after the emergence of WNS makes them an ideal candidate to study the long-term impacts of disease on population dynamics and recovery.

Work at summer maternity colonies in the Northeast since WNS has shown that individuals are surviving Pd infection and reproducing (Fuller et al. 2011, Dobony et al. 2011, Reichard et al. 2014, Dobony and Johnson 2018, Chapter 2). Although some maternity colonies have disappeared, others have stabilized, resulting in fewer and smaller colonies. Some winter sites are also persisting (Maslo et al. 2015, Langwig et al. 2017) and even increasing (Frick et al. 2017), which suggests a regional transition into the established phase of disease invasion (Langwig et al. 2015a). Persistence may be the result of evolved resistance or tolerance to Pd (Langwig et al. 2017, Frick et al. 2017) with the potential for evolutionary rescue (Maslo et al. 2015), but there has been little work on the demography of these persisting colonies (Dobony et al. 2011, Dobony and Johnson 2018) and possible compensatory responses to WNS.

Compensatory demographic responses are important to understand for management and conservation, yet are not always taken into account in population models. Context-dependent management strategies, such as facilitating demographic rates (e.g., increasing survival), promoting the evolution of resistance, and reducing secondary stressors (Kilpatrick 2006, Langwig et al. 2015a) depend on a solid understanding of current demographic rates as well as the potential impacts of management strategies on those demographic rates. Significant differences in vital rates can exist between healthy and declining populations or between populations before and after disease emergence (Johnson et al. 2010), so relying on previous

demographic rates in population models could create misleading results. However, obtaining adequate, long-term data on small, disease-impacted populations, can be a challenge (Beissinger and Westphal 1998), which sometimes necessitates using old, short-term, or sparse data to try to inform management strategies. Several previous studies on little brown bat population dynamics related to WNS have relied on published or estimated vital rates from before or immediately after the emergence of WNS (Frick et al. 2010b, Erickson et al. 2014, Maslo et al. 2015, Russell et al. 2015, Fletcher et al. 2020) to estimate population viability and future population trajectories. Ours is the first study to incorporate long-term changes in demographic rates post-disease invasion in population models and future projections.

For little brown bats, WNS has not resulted in immediate extirpation, however, the population may still be vulnerable and the full impact of WNS on demographic rates remains unknown. In this study, we used mark-recapture data from summer maternity colonies monitored as early as 2006, just prior to WNS invasion, to the present to estimate survival rates in a Cormack-Jolly-Seber (CJS) framework. We also combined the mark-recapture data with emergence counts and annual reproductive rates in integrated population models (IPM) to estimate annual survival and colony growth rates (Besbeas et al. 2002, Schaub and Abadi 2010) at three different sites. IPMs allow the estimation of certain demographic parameters even when there are missing data or mis-matching timeframes. Combining these data in a Bayesian hierarchical framework enables improved precision of demographic rates and adequately incorporates process and observation error from all data sets into one model (Schaub and Abadi 2010, Zipkin and Saunders 2018). An IPM can also easily be modified into a population viability analysis (PVA) and used to evaluate potential management strategies (Schaub and Abadi 2010). To our knowledge, this is the first study to conduct a PVA on a bat species using an IPM. We

evaluated the effectiveness of a range of improvements in survival rates for adults, juveniles, or both on colony size projections, taking into account inter-colony differences. Our aim was to better inform future population models and help target conservation measures to best support the recovery of little brown bats in the region.

Methods

Study sites

We conducted fieldwork from 2006 to 2020 at eight little brown bat maternity colonies in New England. Seven of the colonies roosted in large wooden barns on private property while the eighth roosted in a specially built bat shed in a state park. A variable number of big brown bats (*Eptesicus fuscus*) also roosted in several of the barns and a few eastern small-footed bats (*Myotis leibii*) were captured at the Milford colony. Previous banding efforts (Griffin 1940, Davis and Hitchcock 1965) as well as genetic work (Burns and Broders 2014, Vonhof et al. 2015, Wilder et al. 2015) suggest that the little brown bats in this study are part of one large population. Bats have been tracked between a few hibernacula in Vermont and New York and summer colonies throughout a large part of New England (Griffin 1940, Davis and Hitchcock 1965, Reichard et al. 2014). Along with band recaptures during our study, the evidence suggests that a substantial number of bats from these summer colonies are hibernating in or near Mt. Aeolus in Vermont, which was first detected as positive for Pd in the winter of 2007–08, while some may be hibernating in alternate locations, such as Eagle Cave in New York (see Fig. 2.1).

Bat capture and Pd sampling

Bats were captured at maternity colonies between May and September. The first year of trapping, number of captures per year, and the number of capture years varied widely between sites (Fig.

3.1, Table 3.1). We used harp traps (Bat Conservation & Management, Carlisle, Pennsylvania) to capture bats either at emergence or upon return to the roost and held them in individual paper, mesh, or cloth bags before processing. All individuals were identified to species, sexed, and measured for mass and forearm length. An epiphyseal gap (Kunz & Anthony 1982), darker fur coloration, and epiphyseal gap shape (Davis & Hitchcock 1965) were used to distinguish juveniles from adults. For adults, we assessed bats for reproductive status as pregnant, lactating, post-lactating, or non-reproductive (Racey 2009). All individuals were banded with aluminum alloy lipped 2.9 mm bands (Porzana Limited, East Sussex, UK).

From 2016–2019, we assessed wing damage due to WNS using a modified version of the wing damage index (Reichard and Kunz 2009) and swabbed the right wing and muzzle of a subset of bats following Langwig et al. (2015b). From 2018–2019, we also swabbed roost surfaces before the bats returned in the spring, throughout the summer, and after the bats departed in the fall. We used sterile polyester swabs dipped in sterile deionized water and stored them in RNAlater. Swabs were tested for Pd presence and load following Muller et al. (2013). At two sites, Charlestown (2017) and Lincoln (2017–2019), a subset of bats were implanted subcutaneously with 9 mm passive integrated transponder (PIT) tags (HPT9, Biomark, Boise, Idaho). These two sites were monitored with PIT tag readers (HPR Plus, Biomark, Boise, Idaho) from early April to early October (Charlestown: 2017–2019 and Lincoln 2017–2020).

Emergence counts

Emergence counts can provide highly reliable estimates of maternity colony size on a given night, assuming all openings are being watched and there are fewer than 1000 individuals (Kunz and Reynolds 2003). From 2016–2019, emergence counts were conducted at seven sites in the

evening immediately before each capture event. Prior to 2016, the number of emergence counts varied widely between sites (Table 3.1, Fig. 3.1). We conducted emergence counts by sitting or lying beneath an exit point in order to silhouette bats against the sky (Kunz 2003, Kunz and Reynolds 2003) and counted bats entering and exiting the roost. The emergence was considered complete after no bats had emerged for approximately 10 minutes. When present, big brown bats were included in the total count as they could not always be reliably distinguished from little brown bats. Volunteers conducted emergence counts at Charlestown (2009–2016) and Newfane (2013–2015). These counts were shorter than our average count or only included bats emerging from one opening when there were two. We corrected their counts by approximating the percentage of missed bats using counts that we conducted from 2017–2019 at the same sites during the corresponding times of year.

Near infrared (IR) cameras (Lorex Technology, Inc., Markham, Canada or AXIS Communications, Lund, Sweden) were set up to record nightly from approximately 7–10 pm at four colonies: Charlestown (2017–2019), Lincoln (2010–2020), Newfane (2017–2019), and Paxton (2009–2011). Emergence counts were conducted from the IR videos and, when available, compared to field counts from the same night. Overall, field counts were higher by 6.8 ± 15.7 SD bats, but were highly correlated with video counts (Fig. 3.2). As field and video counts were similar and neither were consistently available throughout the study, we considered counts from the two methods interchangeable. Counts from early- to mid-June, a relatively stable period during which adult females are all present and juveniles are not yet volant (Kunz and Anthony 1996, Kunz 2003, Kunz and Reynolds 2003), were used to represent annual adult colony size. When both field and video counts were available for early- to mid-June in a given year, the highest count was used.

Climate data

We calculated seasonal weather variables for each colony using daily temperature and precipitation data from the closest available weather station (www.ncdc.noaa.gov; see Fig. 2.1). We considered the summer active season to be April to October and the winter hibernation season to be November to March (Frick et al. 2010a). From each weather station, we calculated total precipitation (mm) by season, mean daily minimum temperature in the winter, and mean daily average temperature during the summer. Lastly, we calculated seasonal severity indices by summing the number of days when average temperature was below 10°C, when insects are less active and bat foraging is reduced (Anthony et al. 1981).

Mark-recapture data

Band recaptures and PIT tag detections were used to construct individual capture histories, consisting of a 1 if captured/detected and a 0 if not captured/detected in a given time period. For the banding data, multiple capture sessions within a summer were condensed into one occasion for estimates of annual survival. Detections of PIT-tagged bats within each summer were divided into four sessions, two before and two after juveniles became volant. Separate sets of detection histories were created for each colony. Males disperse on the landscape and are rarely captured at maternity colonies (Davis & Hitchcock 1965; Humphrey & Cope 1976), so they were excluded from the mark-recapture data.

Goodness-of-fit (GOF) for the banding data was assessed using U-CARE v2.3.4 (Choquet et al. 2009). U-CARE does not accept age-based groups, so adults and juveniles were combined (Gimenez et al. 2018). The model we assessed included an interaction between colony

(g) and time (t) for both survival (ϕ) and recapture (p): $\phi(t^*g)p(t^*g)$. The global test indicated a good fit of this model to the data ($\chi^2 = 92.61$, $df = 112$, $P = 0.91$) and slight underdispersion ($\hat{c} = \chi^2/df = 0.827$), so we did not adjust the AICc values (Cooch and White 2019). There was evidence of trap-dependence in only one colony (Charlestown; standardized log-odds-ratio = 2.41, $P < 0.05$, signed statistic = 2.18 (>0 indicates trap-shyness)), however the overall test was not significant (Test2.CT: $\chi^2 = 8.84$, $df = 4$, $P = 0.07$). There was also evidence of transience in one colony (Milford; standardized log-odds-ratio = 3.03, $P < 0.01$), but the overall test was not significant (Test3.SR: $\chi^2 = 10.05$, $df = 8$, $P = 0.26$). We accounted for transience by structuring our model to include young transitioning to adults after one year (Pradel et al. 1997, Cooch and White 2019). There is currently no clear method for assessing GOF of robust design models; typically, secondary sessions are collapsed within primary sessions, resulting in a CJS-type model (Kendall 2018). For the PIT-tag data from Lincoln, we collapsed the capture histories into annual occasions and tested the fully time-dependent model in U-CARE. We found no evidence for lack of fit ($\chi^2 = 4.84$, $df = 2$, $P = 0.09$).

Mark-recapture models

All mark-recapture models were analyzed in R v3.6.1 (Team 2018) using the RMark package v2.2.7 (Laake 2013, Laake and Rexstad 2017), calling Program MARK (White and Burnham 1999). We estimated survival and recapture probabilities from the banding data using a CJS model (Cooch and White 2019). Our data were too sparse to estimate all of the parameters in the global model with full age- (a), time-, and colony-dependence, so we reduced model complexity in a stepwise fashion to the model $\phi(t^*a+g)p(t+a+g)$. We fixed p to zero when there was no trapping at a site in a given year, including years before trapping was initiated at each site. The

additive structure of the colony term in the model permitted estimation of survival for years before trapping was initiated at each site, however, we discarded these estimates from the results.

We first accounted for potential temporal differences in recapture rate by comparing models with time-dependence, site-specific capture effort (number of trapping nights per year), and a site-specific capture index (total bats captured divided by the number of trapping nights per year). The three models were ranked on the basis of the Akaike Information Criteria corrected for small sample size (AICc). Time-dependence had the most support ($\Delta\text{AICc} = 52.83$ between first and second models) and was used for all subsequent models. We then created an *a priori* set of additional models with age, colony, and time variables to explain variation in recapture rate, keeping the survival model the same. The recapture model with the lowest AICc value was then used to select the best model for survival. We again built an *a priori* set of candidate models with age, colony, and time variables to explain variation in survival. We also included models where adult survival was allowed to vary over time while juvenile survival was constant, and we considered a linear time trend. We ranked models by AICc and if the ΔAICc value was greater than two from the top model, we considered that model to have substantially less support (Burnham and Anderson 2002).

Influences of disease and climate on survival were explored in two separate sets of models. In the first set, we compared models with different timelines for Pd invasion in our study area, following the invasion phase designations from Langwig et al. (2015a): pre-arrival, invasion front, epidemic, and established. We used our colony count data and Pd spread data (whitenosesyndrome.org) to create four different timelines, all of which had 2006 as the pre-arrival phase and 2007 as the invasion front phase. We varied the start of the epidemic phase between 2009 and 2010 and the start of the established phase between 2011 and 2012. In one

timeline, we considered the invasion front and epidemic stages to be simultaneous. Survival was held constant during each invasion stage, but could potentially vary by additive effects of age and/or colony. In the second set of survival models, we tested a suite of weather covariates. Environmental conditions, such as rainfall, have been shown to be important predictors of bat survival (e.g., Frick et al. 2010a, O'Shea et al. 2011). Spring and fall severity, summer and winter precipitation, and mean winter and summer temperature were tested along with colony and age covariates. Models without weather covariates were also included in the model set.

Using the PIT tag detections, we estimated survival (S) using the Huggins robust design model (Huggins 1989), which uses a conditional-likelihood approach and does not include population size as a parameter within the model likelihood. The robust design (RD) combines open and closed population models by including multiple secondary capture sessions within primary capture sessions, between which the population is considered open. This allows the simultaneous estimation of temporary emigration, apparent survival, and recapture probabilities (Kendall and Nichols 1995, Kendall et al. 1997, Kendall 2018). We again employed a stepwise model selection procedure and first tested combinations of age, time, and colony variables for recapture and within-primary session recapture rate (c). Then we tested for parameters representing the probability of temporarily emigrating away from the colony (γ'') as well as the return rate of temporary emigrants ($1 - \gamma'$). Lastly, we tested models for survival and ranked models by AICc.

Integrated population models

Mark-recapture data were combined with annual emergence count (Fig. 3.1) and reproductive data to build separate IPMs for three of the eight colonies: Charlestown, Lincoln, and Paxton.

These three sites had the longest and most consistent count data available, had few to no big brown bats, and represented a range of colony size trends from stable, to moderately increasing, to rapidly growing. Though the count and mark-recapture datasets were obtained from the same colonies, different sampling protocols were used, which should minimize bias and adequately ensure independence (Abadi et al. 2010).

Emergence count data were used in a state-space model, which takes into account the state process (the true, but unknown population size at different times described by the demographic parameters) and the observation process (observation error; Schaub and Abadi 2010). Colony size in a given year (y_t) was modeled with a normal distribution,

$$y_t \sim \text{Normal}(N_{j,t} + N_{a,t}, \sigma^2)$$

where σ^2 is the observation error, N_j is the number of one-year-old (yearling) females, and N_a is the number of 2+ year-old females in the colony.

Capture-recapture data were used in a CJS model with time-dependent recapture and age-dependent survival (juvenile survival S_j and adult survival S_a) that was allowed to vary by Pd invasion phase, using the best supported timeline from the mark-recapture models described above. For the three colonies we chose, there were no pre-invasion mark-recapture data available. We used constant survival rates for the invasion front and epidemic phases as they had only 1–3 years of data. For the established phase, we allowed for random time effects, which also enabled future population projection. Without accounting for invasion phase, the mean survival rate used for population projection would have been lower and the variation larger due to the inclusion of the initial low survival rates and high colony declines. Capture histories were summarized into m-arrays, one for juveniles and one for adults, taking into account the transition

from juvenile to adult after one year (Kéry & Schaub 2012). We modeled survival and recapture following a multinomial distribution,

$$m \sim \text{Multinomial}(R, \Pi)$$

where R is the number of marked individuals released each year and Π is a function of survival and recapture probability (Kéry & Schaub 2012).

The number of reproductive adults was used as a measure of fecundity since little brown bats typically only have one pup per year (Fenton and Barclay 1980). Bats captured early in the season were excluded as their reproductive status could not always be reliably determined. We pooled reproductive data across sites as it was not available for each site in all years. Mean juvenile reproductive rate post-WNS arrival is not significantly different than adult reproductive rate (see Chapter 2), therefore we assumed the same fecundity for adults and juveniles in this analysis. Adult females show high fidelity to their maternity colonies, returning year after year to reproduce (Hall et al. 1957; Davis & Hitchcock 1965; Humphrey & Cope 1976; Norquay et al. 2013), with little evidence for temporary emigration (Frick et al. 2010a). Recent evidence suggests that yearling females are now returning to their natal colonies at higher rates than pre-WNS (see Chapter 2), so we assumed a breeding propensity of 1 for both age classes (Frick et al. 2010a). The number of reproductive females (J) in year t was modeled with a binomial distribution as a function of the total number of females examined (B) and fecundity (f):

$$J_t \sim \text{Binomial}(B_t, f_t)$$

Demographic rates were linked to the number of individuals of each age class within a colony with a female-based, pre-breeding, 2 x 2 stage population projection model (Fig. 3.3). Fecundity was divided by two, assuming an equal offspring sex ratio (Reynolds 1999), to include only female offspring. The contributions of yearlings (N_j) and adults (N_a) at time t to the size of

each colony segment in year $t + 1$ were modeled with Poisson and binomial distributions, respectively:

$$N_{j,t+1} \sim \text{Poisson}((N_{j,t} + N_{a,t}) * S_{j,t} * \frac{f_t}{2})$$

$$N_{a,t+1} \sim \text{Binomial}(N_{j,t} + N_{a,t}, S_{a,t})$$

Juvenile survival, as modeled here, encompasses the entire period from birth to the following summer. We assumed that all pups survived to volancy, which is supported by the low observed rate of pre-weaning mortality (Chapter 2). Total population size in year t was the sum of the number of adults and yearlings:

$$N_{tot,t} = N_{j,t} + N_{a,t}$$

We derived annual growth rate (λ_t) along with credible intervals within the IPM as:

$$\lambda_t = N_{tot,t+1}/N_{tot,t}$$

and calculated a geometric mean growth rate to compare among colonies.

The overlapping parameters among the three datasets represent the integration of the three sub-models (Fig. 3.4). The product of the component likelihoods is the joint likelihood of the model, which is informed by the priors and from which the posterior samples were generated (Kéry & Schaub 2012). We used vague uniform priors $U(0,1)$ for the survival, recapture, and productivity parameters, which ensures that the posterior distribution is driven by the data. For the hyperpriors for the random effects, representing standard deviation, we used uniform priors, $U(0,5)$ for the demographic parameters and $U(0.5,50)$ for the observation error. For initial population size, we used informative priors to improve model convergence (Schaub and Abadi 2010). For the starting population size of the yearling and adult age classes, we used normal priors truncated to positive values where adults were 60% and yearlings were 40% of the colony count in the first year (Fletcher et al. 2020).

Population viability analysis and management strategies

We incorporated a population viability analysis into two of the IPMs by extrapolating the model for an additional 10 years. We projected colony size for only 10 years, to 2030, as uncertainty rapidly increases when projecting farther into the future. The mean demographic rates from the established phase along with their temporal variability were used to project the population forward in time in a stochastic manner while accounting for all of the uncertainty in each parameter (Kéry & Schaub 2012). Within each PVA we incorporated three different management strategies: 1) increase juvenile survival, 2) increase adult survival, and 3) increase both juvenile and adult survival. Proportional increases of 5, 10, and 20% on the log scale were evaluated for each strategy. For each strategy and each proportional increase, we evaluated the effect on the final colony size after 10 years. Management strategies were compared to the “status quo”, or no additional action, to assess their relative effectiveness.

Statistical analysis

IPMs were fit in a Bayesian framework and implemented in JAGS (Plummer 2003) via R (R Core Team 2018) using the R2jags package (Su and Yajima 2020). We used Markov Chain Monte Carlo (MCMC) simulations to calculate the posterior distributions for the parameters of interest. Models were run for 30,000 iterations with a burn-in of 5,000 iterations and thinning to every 5 iterations. We visually examined traceplots and considered convergence achieved if all R-hat values were < 1.1 (Gelman and Rubin 1992). Parameter estimates are presented below along with 95% credible intervals (CRI), which represent the highest posterior density intervals (Kéry and Schaub 2012).

Results

Population monitoring

We conducted trapping on a total of 188 nights at eight maternity colonies between 2006 and 2019, with the number of trapping events ranging from 0–9 per colony in a given year. The number of years of trapping at each colony ranged from 4–10 (Fig. 3.1). We captured and banded 3,344 unique female little brown bats, 2608 as adults and 736 as juveniles. The number of unique females banded at each colony ranged from 210–606 (Table 3.1), with the number banded at a colony in a given year ranging from 9–282 individuals. We recaptured 557 individuals banded as adults and 117 individuals banded as juveniles a total of 867 times, 212 of which were same-summer recaptures (bats were captured twice or more in the same summer). Over the study, we captured 10 individuals that were banded as adults between 2006 and 2009 that were at least 10–12 years old at the time of recapture. We captured 54 adult and 479 juvenile male individuals, with only 12 total recaptures of male bats.

Emergence counts were conducted in the field or from infrared video 1–38 times per summer at seven of eight colonies beginning as early as 2008 (Table 3.1). From these, we had a total of 59 emergence counts that were conducted from early- to mid-June that were used as an estimate of annual adult colony size (Figs. 3.1 & 3.5). The colony count data showed declines in three colonies from 2008 to 2011, after which colony size appeared to stabilize for some colonies and increase at others (Fig. 3.5). Colony size in 2020 ranged from 170–735 adult female bats. The two smallest colonies, Pepperell and Milford, also contained the largest number of big brown bats, estimated to comprise 30–50% of the total number of bats.

We PIT-tagged 71 female little brown bats at the Lincoln colony between 2017 and 2019, 57 as adults and 14 as juveniles. From June 2017 to June 2020, we detected these individuals

over 17,000 times. All PIT-tagged bats that were physically recaptured had retained their tags, so we have no direct evidence of tag loss (all tagged bats were also banded), however, there is evidence that detection of PIT tags was not perfect. In 2019, we recaptured two bats tagged in 2017 that had no or very few detections in 2018 and 2019, but we were able to read their tags with a handheld PIT tag reader, suggesting that they may have consistently been using an alternate opening or were temporarily absent. At the Charlestown colony, we PIT-tagged 29 females in 2017, 25 as adults and four as juveniles. We detected these bats over 17,000 times from June 2017 to September 2019.

We swabbed 1414 bats from 2016–2019 to test for Pd and found that in most years, prevalence was nearly 100% in mid-May, when our sampling began, and declined to 25% or less by mid- to late-June (Fig. 3.6A). From 521 roost swabs collected in 2018–2019, over half contained detectable Pd throughout the year (Fig. 3.6B). For both wing and roost swabs, however, we may have been detecting remnant DNA and not viable fungal spores. Pd loads on bats and roost surfaces both declined over the course of the summer (Figs. 3.6C & D). Prevalence and load patterns were similar between years. Together with data from previous studies at summer maternity colonies and winter hibernacula (Langwig et al. 2015b, Frick et al. 2017), these results suggest that Pd is persisting in hibernacula and has not diminished over time. As in Langwig et al. (2015) and Dobony et al. (2018), we found that bats are not avoiding being re-infected each winter and are carrying Pd to their summer colonies. From these data, we therefore assumed that all the bats in our study were annually infected with Pd and did not attempt to model survival as a function of Pd status, fungal load, or wing damage.

CJS and robust design models

Our CJS model selection procedure resulted in an additive model for both survival and recapture with age, time, and colony covariates (Table 3.2). We could not reliably estimate survival in 2010 and 2014 from any model due to data sparseness, so these years were removed from the results. Survival estimates for adults in 2006 (Framingham: 0.53, 95% CI 0.11–0.91; Milford: 0.62, 95% CI 0.30–0.86) were similar to pre-WNS rates reported in Frick et al. (2010a). Between 2006 and 2008, survival rates sharply declined to 0.18 (95% CI 0.04–0.53) in Framingham and 0.23 (95% CI 0.12–0.40) in Milford. After 2008, survival rates gradually increased until 2012 then remained relatively stable until 2017 when they fell slightly (Fig. 3.5). Juvenile survival was lower than adult survival in all years and for all sites by an average of 0.19 \pm 0.06 SD (range 0.07–0.26).

The disease invasion models showed the most support for a Pd invasion timeline separated into four phases, pre-invasion in 2006, invasion front in 2007, epidemic from 2009 to 2011, and established from 2012 and on (Table 3.3). Survival rates for adults were 0.61 (95% CI = 0.29–0.85) pre-invasion, lowest during the invasion front (0.21, 95% CI = 0.12–0.33), significantly higher in the epidemic phase (0.64, 95% CI = 0.56–0.71), and significantly higher still in the established phase (0.88, 95% CI = 0.84–0.92; Fig. 3.8). Juvenile survival was lower than adult survival, increasing from 0.07 (95% CI = 0.03–0.16) during the invasion front to 0.35 (95% CI = 0.23–0.49) in the epidemic phase and to 0.70 (95% CI = 0.55–0.81) in the established phase (Fig. 3.8). No juveniles were banded in 2006, so we could not estimate juvenile survival rate pre-WNS.

The climate models suggest that the demographic response to WNS has overwhelmed any clear relationship between survival and inter-annual variation in spring weather. The model

with just time-dependence received 100% of the model weight, whereas models including a weather variable received 0% of the model weight and a ΔAICc of at least 33.93 (Table 3.4). Even when we examined the second ranked model with summer precipitation further, we found that while there was a negative correlation between summer precipitation and survival, summer precipitation was also negatively correlated with year. The time-dependent model shows that survival was increasing over this same time period, suggesting that summer precipitation was not the primary driver of survival patterns.

Using the PIT-tag detections from the Lincoln colony, the RD model with age-dependent survival had the most support (Table 3.5). Adult survival was 0.78 (95% CI = 0.70–0.85) and juvenile survival was 0.50 (95% CI = 0.26–0.74). For the Charlestown colony, all models had a ΔAICc value < 2.5 from that of the top model (Table 3.5). Interestingly, the age-dependent model survival estimates were very similar to those from the Lincoln colony, though with wider confidence intervals. Adult survival was 0.76 (95% CI = 0.62–0.86) and juvenile survival was 0.50 (95% CI = 0.12–0.88).

Integrated population models

The IPMs for the Lincoln, Charlestown, and Paxton colonies showed that the estimated colony sizes had high precision and largely matched our emergence counts (Fig. 3.9). Mean fecundity was approximately 0.95 for all three colonies, which was expected given that we used the same reproductive data for each IPM and the observed reproductive rates were consistently high (see Chapter 2). We found similar trends in apparent survival estimates between colonies over time (Fig. 3.9) and, for the Lincoln colony, similar survival estimates for 2016 to 2019 to those from the CJS and RD models (Fig. 3.10). The Paxton colony was the only one with a colony count in

2008 during the invasion front, but did not have corresponding banding data. We found that survival was low for both juveniles (0.31, 95% CRI = 0.01–0.62) and adults (0.13, 95% CRI = 0.01–0.28) in 2008 (Fig. 3.9). During the epidemic phase, we estimated survival as a constant for all colonies due to little or no available mark-recapture data. We found that survival for both age classes was greater than 25%, though the credible intervals for juveniles in Lincoln and Paxton were wide. During the established phase, adult survival was generally > 75%, while juvenile survival estimates were more variable and less precise (Fig. 3.9). The dip in juvenile survival for the Lincoln colony in 2017 may be due to few juveniles being banded in 2017 and none of them being recaptured in 2018 or 2019. The CJS and RD models suggest that juvenile survival was closer to 50% in 2017 (Fig. 3.10).

Colony growth rates likewise increased between the epidemic and established phases. Geometric mean growth rates ($\hat{\lambda}$) during the epidemic phase were 0.75 or less for Lincoln and Charlestown and close to 1 for Paxton. During the established phase, the credible intervals did not cross 1 in most years, indicating that the colonies were definitely growing (Fig. 3.9). Mean geometric growth rates calculated from the epidemic phase only indicated that, as expected, the Paxton colony had the highest mean growth rate ($\hat{\lambda} = 1.17 \pm 0.08$, range: 1.04–1.28), while Charlestown ($\hat{\lambda} = 1.14 \pm 0.09$, range: 1.01–1.27) and Lincoln ($\hat{\lambda} = 1.10 \pm 0.08$, range: 0.96–1.17) had lower mean growth rates. A retrospective analysis showed that for the Paxton colony, adult survival had the highest correlation with colony growth rate (Fig. 3.11) suggesting that variation in adult survival rate contributed more to variation in colony growth rates from 2008 to 2019 than variation in juvenile survival or fecundity.

Population viability analysis and management strategies

Our PVAs for both colonies suggest that increasing both juvenile and adult survival results in a larger colony than increasing adult or juvenile survival alone, which had about the same impact on colony size projections. Increasing adult and juvenile survival by 10% on the log scale resulted in colony sizes in 2030 that were 70 (Lincoln) and 134 (Charlestown) bats larger compared to colony sizes under a “status quo” strategy. However, none of the strategies that we evaluated resulted in significantly better outcomes than the “status quo” strategy (Fig. 3.12). Rate of colony growth varied, with the Charlestown colony projected to triple in size (Fig. 3.12A), compared to slower growth in Lincoln, with the colony barely surpassing its 2009 size by 2030 (Fig. 3.12B).

Discussion

Our results show that, despite repeated infection with Pd (Fig. 3.6), little brown bats are now surviving at high rates (Fig. 3.7) and can endure annual infections over multiple years, with some individuals surviving since early in the WNS epizootic. While the Framingham colony was apparently extirpated by WNS, the other colonies in our study persisted and, in some cases, increased in size (Fig. 3.5). Increasing survival rates (Maslo et al. 2015), population growth rates (Langwig et al. 2012), and colony sizes (Langwig et al. 2017, Frick et al. 2017, Frank et al. 2019) have been documented at some winter colonies within a few years after Pd arrival, but there have only been two quantitative studies of survival at summer colonies of little brown bats thus far (Dobony et al. 2011, Dobony and Johnson 2018). As in Dobony et al. (2018), we found increasing survival probabilities over time. Survival of both adult and juvenile females were severely impacted during the first few years of the arrival of Pd, but have since returned to or even exceeded pre-WNS survival (Frick et al. 2010a; Fig. 3.8). Our disease timeline model

(Table 3.3) and colony count data (Fig. 3.5) suggest that the little brown bat population in New England hit a low point and Pd became established or enzootic around 2012, just 4–5 years after initial arrival.

The survival rates ascribed to invasion phases here differ from those described by Langwig et al. (2015), who considered population size during the invasion front to be stable or to show initial declines. Our invasion front phase, with the lowest survival rates, more closely lines up with the epidemic phase described in Langwig et al. (2015a). We suggest that in New England, the invasion front was essentially simultaneous with the epidemic phase, as Pd quickly swept through the region and large declines were observed in both winter (Frick et al. 2010b) and summer (Fig. 3.3) within 1–2 years after Pd arrival. Aeolus Cave was first detected as having infected bats in the winter of 2007–2008, however, we have no emergence count or banding data from 2007 to track the very beginning of the invasion front in New England.

We used three types of models with different combinations of demographic and count data and found similar results. Overall, there was agreement in estimated survival between the CJS model, RD model, and IPMs (Fig. 3.10). Our CJS models had the most support for age- and colony-dependent survival, suggesting inter-colony differences and lower juvenile survival. Our IPMs also suggested that survival probabilities were different between colonies, resulting in some colonies that were stable or growing slowly while others were growing rapidly (Fig. 3.9). All model types showed that while juvenile survival was highly variable, it was not half of adult survival, as found in Frick et al. (2010a & b) pre-WNS, and was in some cases nearly the same as adult survival. Juvenile survival estimates from our RD model were not more precise than those from the CJS model, but this may be due to the low number of PIT-tagged juveniles.

Precision improved compared to the IPM and for adult survival (Fig. 3.10), similar to previous research on big brown bats (Ellison et al. 2007).

Immigration has been proposed as a potential explanation for the observed increases in winter and summer colonies post-WNS arrival. While female roost fidelity is thought to be high in little brown bats (Norquay et al. 2013), we cannot rule out the possibility of some dispersal by juvenile females (Dixon 2011), particularly from the colonies that are stable rather than increasing. We found no evidence of permanent movement of juvenile females, however one individual PIT-tagged in Lincoln was briefly detected at the Charlestown colony before returning to Lincoln. Documented instances of roost switching are rare (Davis and Hitchcock 1965, Dobony and Johnson 2018), but may be extremely difficult to detect. In the CJS models, dispersal is not distinguishable from mortality, which means our high apparent survival probabilities also support high fidelity. We also found no evidence of temporary emigration from our RD models, suggesting that bats are returning to their maternity colonies at high rates every year. This agrees with the results for adult females from Frick et al. (2010a), though they found that juvenile females had a much higher probability of temporary emigration than adults that depended on weather conditions in the summer of their birth. While it is possible that some colonies in our study could be acting as source populations, the observed survival and reproductive rates are sufficient to explain the increases in colony size without immigration. Other studies from the Northeast suggest that immigration, if occurring, is not a major factor in the observed increases in survival and colony size (Maslo et al. 2015, Dobony and Johnson 2018).

We found no relationship between weather and survival rates (Table 3.4), suggesting that changes in survival rates since WNS are due to some form of disease response rather than

climate. White-nose syndrome has placed a strong selective pressure on little brown bats and increasing survival rates may be a result of one or several factors, including genetic selection, adaptive immune responses, changes in little brown bat hibernation patterns or selection of microclimates, reduced pathogen virulence, or a demographic response. Early reports of bats flying outside hibernacula in the winter (Blehert et al. 2009) most likely represented individuals that succumbed to WNS, caused by a depletion of fat reserves due to increased arousal frequency (Warnecke et al. 2012). Within a few years after WNS emerged, bats were observed hibernating in different microclimates and exhibiting different clustering behavior (Langwig et al. 2012). Populations exposed to WNS for about a decade appear to shift back to “normal” torpor bout durations (Lilley et al. 2016, Frank et al. 2019) and are going into and emerging from hibernation with higher mass (Frank et al. 2019, Cheng et al. 2019). Genetic selection has also been documented in several populations of little brown bats post-WNS; genes associated with thermoregulation, brown fat production, and hibernation behavior have been identified as under selection (Gignoux-Wolfsohn et al. 2019, Auteri and Knowles 2020, Lilley et al. 2020), suggesting the potential for evolutionary rescue (Gonzalez et al. 2013, Maslo and Fefferman 2015). The observed changes in demographic rates also match theoretical expectations for a demographic response in long-lived species undergoing drastic change in population size. For long-lived vertebrates, demographic rates generally respond to changes in density in a specific order: juvenile survival, age at first reproduction, adult reproductive rate, and then adult survival (Eberhardt 2002). Age at first reproduction has decreased (see Chapter 2) and in this study we observed increases in adult and juvenile survival rates, though it is hard to say in what order this occurred. Variation in adult survival seems to have had the strongest effect on variation in growth rate since WNS (Fig. 3.11). Evidence of lower fungal loads on bats in persisting winter

colonies compared to bats in recently infected hibernacula is also occurring (Langwig et al. 2017). While nearly all of the bats sampled in our study were infected with Pd (Fig. 3.6) and had some level of wing damage related to WNS, it is possible that infection intensity has declined over time for this population. Most likely, there are multiple simultaneous responses to WNS (Dobony and Johnson 2018) that are all contributing to little brown bats' persistence.

While survival and growth rates at each of the colonies in our study followed similar trends, there were some differences among colonies according to the CJS models and IPMs (Fig. 3.9). The Paxton colony had the highest growth rate, which can be seen in the rapid change in colony size since 2011. For this reason, we did not conduct a PVA for Paxton and focused on two colonies with slow to moderate growth. Both of our PVAs predicted colony growth under the status quo, but there was higher uncertainty in the population trajectory for Lincoln than Charlestown (Fig. 3.12). Differences in survival and growth rate could reflect a variety of factors, including genetics, though these colonies are thought to be panmictic (Wilder et al. 2015), hibernation conditions, summer roost conditions, or habitat quality. Management strategies could therefore be undertaken to reduce uncertainty and promote population recovery by targeting the slower-growing summer colonies. Alternatively, management actions undertaken during the winter would potentially benefit many summer colonies at once, as bats from one hibernaculum disperse to several maternity colonies in the summer (Davis and Hitchcock 1965, Burns et al. 2014).

Management strategies for increasing survival or reproductive rates of one or both age classes can take on many forms. Ongoing studies of a variety of potential treatments, including biological, chemical, and immunological options are meant to prevent or slow the growth of Pd. Some of the treatments have to be applied directly to bats, such as probiotics (Cheng et al. 2016),

chitosan (Hoyt et al. 2019), bacteria (Hoyt et al. 2015b), or a vaccine (Rocke et al. 2019). Other treatments, such as UV light (Palmer et al. 2017) or volatile organic compounds (Padhi et al. 2018) would be applied to the environment, mainly cave or mine walls, to prevent Pd growth. Treatment effectiveness at the population level is generally higher when more of the population is treated (Fletcher et al. 2020), which may be challenging, particularly if portions of hibernacula are inaccessible or hibernation sites are unknown. Other options that could be implemented during the winter include manipulating the temperature and humidity in hibernacula to reduce Pd growth and providing dietary supplementation (McGuire et al. 2019). Habitat improvements in the vicinity of hibernacula could increase the abundance or diversity of insects available for bats to consume, potentially helping bats accumulate fat in the fall during swarming and thus increase the chances of overwinter survival (Cheng et al. 2019).

Enhancement of summer roosts and habitat are likely to be beneficial without the potential negative effects of disturbing hibernating bats (Thomas 1995). During the active season, providing heated bat boxes (Wilcox and Willis 2016) may help bats recover from WNS and benefit offspring by enhancing pre- and post-natal growth rates (Zahn 1999). Providing a stable, warm environment that minimizes heat loss during the night should increase post-natal growth, increasing the fitness of both mom and offspring (Studier and O'Farrell 1972, Kunz and Anthony 1982, Gilbert et al. 2009, Olson and Barclay 2013) by giving juveniles more time to forage before hibernation (Frick et al. 2010a, Cheng et al. 2019). Yearling females may then emerge from hibernation in better body condition and thus be more capable of successful reproduction. Although it may be more difficult to enhance roosts for adult males, as they tend to be dispersed on the landscape (Fenton and Barclay 1980), juvenile males would benefit from more favorable roost conditions at maternity colonies.

Roost enhancement should not, however, be limited to bat boxes. Little brown bats in New England, and possibly throughout much of their range, almost exclusively use anthropogenic roosts, such as attics, barns, and bridges in the summer months (Fenton and Barclay 1980, Johnson et al. 2019). These roosts provide relatively stable temperatures compared to ambient conditions (Burnett and August 1981, Burnett and Kunz 1982, Zahn 1999, Sedgeley 2001, Willis and Brigham 2007, Betts 2010), offer more places for bats to roost that mimic the cavities and crevices in tree roosts (Bergeson et al. 2015), and give bats the opportunity to optimize temperature and humidity, resulting in lower metabolic rates and reduced heat loss (Kurta 1985, Sedgeley 2001, Willis and Brigham 2007). Structural complexity was suggested to be the key factor in roost preference for brown long-eared bats (*Plecotus auritus*), which appear to prefer complex attic spaces with more roof compartments and a range of temperatures (Entwistle et al. 1997). Larger structures may also protect bats from extreme heat compared to bat boxes. Bats will move within structures to avoid extreme, dangerous temperatures (e.g., Humphrey 1971, Burnett and August 1981), but juveniles may be less mobile and less tolerant to heat, so the architecture of roosts may be important to consider in management plans. While climate change may promote healing and growth in the early spring, these benefits could be negated if warmer temperatures and rising prevalence of extreme heat waves increase pup mortality. All age classes may benefit from enhancing roosting locations, whether through supplying an artificial heat source, protecting known roosting sites, installing large bat houses, or providing roost modules within larger structures.

Our results suggest that at least some colonies in the Northeast are on track to recover to their pre-WNS levels. While we are encouraged by the observed trends, the response of one population to disturbance may not be a reliable indicator of another's response (Caro et al. 2005),

a potential problem when attempting to extrapolate the response of little brown bats in New England to populations across their entire range or to other species. Ideally, each population and species should be monitored to develop appropriate management actions (Johnson et al. 2010). A similar enzootic fungal disease, chytridiomycosis, shows how different responses can be among populations and species of amphibians. Chytridiomycosis has resulted in the extinction of dozens of species, but other species are stable or recovering due to compensatory recruitment, the evolution of resistance (Scheele et al. 2017), and reduced pathogen virulence (Newell, Goldingay & Brooks 2013). Even within species, such as the common mistfrog (*Litoria rheocola*), some populations are persisting while others have been extirpated (Sapsford et al. 2015), similar to what we observed at maternity colonies in New England.

In this study we showed that survival has increased over time since the initial phase of WNS invasion, resulting in stable to growing summer colonies. We also showed that emergence count and mark-recapture data are both important for monitoring, but do not have to overlap entirely to be able to generate demographic rate estimates, as we were able to do with the IPMs. Future work on the rates and role of dispersal and immigration in little brown bats would greatly contribute to understanding whether or not they are significantly contributing to the observed population recovery. This could potentially be accomplished using IPMs, which can estimate or account for unknown parameters, such as immigration (Besbeas et al. 2002), though there is concern about the reliability of indirectly estimated latent parameters (Riecke et al. 2019). If little brown bat colonies continue to grow, as predicted by our PVAs, this may also present a unique opportunity to monitor populations for signs of positive density-dependence, such as decreases in reproductive rates or increased dispersal. Questions also remain about the role of inter-specific competition in population recovery as well as if and where new colonies of little brown bats will

form in the future. Our system is well suited to monitor these dynamics with the loss of some colonies due to WNS leaving some sites vacant while other sites, such as Milford and Pepperell, have seen increases in their big brown bat colonies, a species much less affected by WNS. Most significantly, our findings have important implications for future population modeling efforts and show that long-term monitoring is important for tracking changes in demographic rates in persisting populations.

Table 3.1. Historic (pre-2016) and current (2016–2019) data types collected at eight little brown bat maternity colonies in New England. Counts are emergence counts conducted in the field. Banded bats represent the total number of unique banded females at each site. Superscript letters next to colony name indicate that data from that colony has been used in a published study.

State	Colony	Pre-2016			2016–2019			Banded bats	
		Banding	Counts	IR video	Banding	PIT-tagging	Counts		IR video
VT	Newfane		2013–15*		X		X	X	210
NH	Charlestown ^{d,e,f}	2009–13	2009–15*		X	X	X	X	546
	Milford ^{b,c,d,e,f}	2006–12			X		X		499
	Framingham ^{b,c,d,e}	2009–11							471
	Lincoln		2010–15	2009–15	X	X	X	X	268
MA	Princeton ^{d,e,f}	2010–15	2010		X		X		606
	Paxton ^a	2011–15	1979–15 [^]	2008–11	X		X	X	448
	Pepperell ^{d,f}	2011–15			X		X		296

*Counts pre-2016 were conducted by volunteers

[^]Counts were conducted in 1979, 1984, 1993–1996, and 2010–2015

^a Burnett and August (1981)

^b Reichard and Kunz (2009)

^c Fuller et al. (2011)

^d Reichard et al. (2014)

^e Langwig et al. (2015)

^f Fuller (2016)

Table 3.2. Model selection for Cormack-Jolly-Seber mark-recapture models using banding data from eight little brown bat maternity colonies in New England. Models are ranked by AICc. ϕ = survival; p = recapture rate; K = number of model parameters; w = model weight; a = age; t = time; g = colony; ad = adult; j = juvenile; $.$ = constant; T = linear time trend.

	ϕ	p	K	AICc	Δ AICc	w_i	Deviance
p models							
	$g + t + a$	$g + t + a$	40	4487.44	0.00	0.99	656.92
		$a + t$	33	4500.83	13.38	0.00	684.60
		$t + g$	39	4501.71	14.27	0.00	673.24
		$ad:t + j$	33	4512.11	24.67	0.00	695.89
		t	32	4515.85	28.41	0.00	701.67
		$a * g$	36	4554.62	67.17	0.00	732.27
		$a + g$	29	4554.64	67.19	0.00	746.56
		a	22	4562.33	74.88	0.00	768.46
		g	28	4570.28	82.84	0.00	764.24
		$.$	21	4573.71	86.26	0.00	781.86
ϕ models							
	$g + t + a$	$g + t + a$	40	4487.44	0.00	0.78	656.92
	$g * a + t$		47	4489.96	2.51	0.22	645.08
	$t + g$		39	4498.46	11.02	0.00	669.99
	$t * a + g$		51	4501.72	14.27	0.00	648.61
	$t + a$		33	4506.15	18.71	0.00	689.93
	t		32	4512.56	25.12	0.00	698.38
	$T + a$		23	4512.66	25.21	0.00	716.76
	$t * a$		44	4520.59	33.15	0.00	681.87
	T		22	4523.32	35.87	0.00	729.45
	$ad:t + j + g$		41	4525.16	37.71	0.00	692.59
	$T + g$		29	4535.19	47.74	0.00	727.11
	$ad:t + j$		33	4538.77	51.33	0.00	722.55
	$g * a$		36	4543.90	56.45	0.00	721.55
	$g + a$		29	4544.79	57.35	0.00	736.71
	g		28	4558.18	70.74	0.00	752.13
	a		22	4575.43	87.99	0.00	781.56
	$.$		21	4581.83	94.39	0.00	789.98

Table 3.3. White-nose syndrome invasion timeline models for survival using banding data from eight little brown bat maternity colonies in New England. All models included the recapture model $p(t+a+g)$. Models are ranked by AICc. The first year for pre-invasion, invasion front, epidemic, and established is included for each timeline: dis1 = 2006, 2008, 2009, 2012; dis2 = 2006, 2008, 2009, 2011; dis3 = 2006, 2008, NA, 2012; dis4 = 2006, 2008, 2010, 2012. ϕ = survival; K = number of model parameters; w_i = model weight; a = age class; g = colony.

ϕ model	K	AICc	Δ AICc	w_i	Deviance
a + dis1	25	4498.24	0.00	0.86	698.29
a + dis4	25	4502.91	4.67	0.08	702.96
g + dis4 + a	32	4505.53	7.29	0.02	691.35
g + dis1 + a	32	4505.83	7.59	0.02	691.64
a + dis2	25	4508.16	9.92	0.00	708.21
dis1	24	4508.89	10.65	0.00	710.97
a + dis3	24	4512.60	14.36	0.00	714.68
g + dis2 + a	32	4513.00	14.76	0.00	698.82
dis4	24	4514.94	16.69	0.00	717.01
g + dis3 + a	31	4515.59	17.35	0.00	703.44
g + dis1	31	4515.96	17.72	0.00	703.81
g + dis4	31	4519.25	21.00	0.00	707.10
dis3	23	4520.07	21.83	0.00	724.18
dis2	24	4520.70	22.45	0.00	722.77
g + dis3	30	4527.59	29.35	0.00	717.48
g + dis2	31	4527.86	29.62	0.00	715.71

Table 3.4. Climate models for survival using banding data collected at eight little brown bat maternity colonies in New England. Site-specific weather variables were calculated using data from six weather stations (www.ncdc.noaa.gov). All models included the recapture model $p(t+a+g)$. Models are ranked by AICc. ϕ = survival; K = number of model parameters; w = model weight; a = age class; g = colony; t = time.

ϕ model	K	AICc	Δ AICc	w _i	Deviance
t + g + a	40	4487.43	0.00	1.00	656.92
Summer precipitation + g + a	30	4521.35	33.93	0.00	711.23
Winter precipitation + g + a	30	4526.79	39.35	0.00	716.68
Summer mean temperature + g + a	30	4531.45	44.01	0.00	721.34
Winter mean temperature + g + a	30	4540.71	53.27	0.00	730.59
Fall severity + g + a	30	4541.65	54.20	0.00	731.53
Spring severity + g + a	30	4546.83	59.38	0.00	736.71

Table 3.5. Robust design model selection results for passive integrated transponder tagging data from the Lincoln and Charlestown little brown bat maternity colonies. All models included $p(t)=c(t)$ for time-dependent recapture rates and $\gamma'(0)=\gamma''(1)$, indicating a ‘no movement’ model. Models are ranked by AICc. S = survival; K = number of model parameters; w = model weight; a = age; g = colony; t = time; . = constant.

Colony	S	K	AICc	Δ AICc	w _i	Deviance
Lincoln						
	a	15	725.85	0.00	0.68	1174.42
	.	14	728.50	2.66	0.18	1179.21
	t + a	17	729.61	3.76	0.10	1173.88
	t	16	731.68	5.83	0.04	1178.11
Charlestown						
	.	12	239.75	0.00	0.45	337.12
	a	13	240.92	1.17	0.25	335.96
	t	13	241.64	1.89	0.17	336.68
	t + a	14	242.18	2.43	0.13	334.88

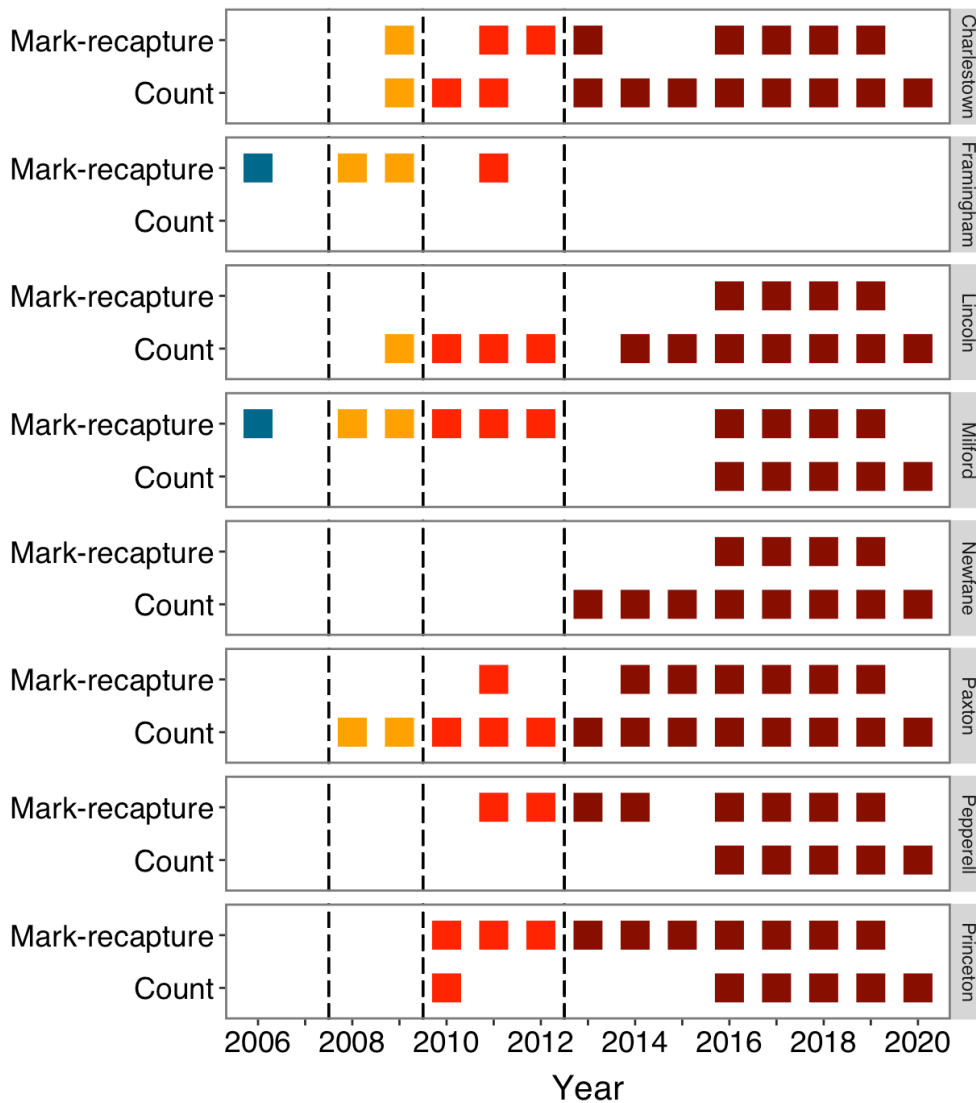


Figure 3.1. Available mark-recapture and emergence count data (black boxes) by year from eight little brown bat maternity colonies. Dashed vertical lines separate the approximate pre-invasion (blue), invasion front (orange), epidemic (red), and established (dark red) phases of white-nose syndrome arrival and spread in New England.

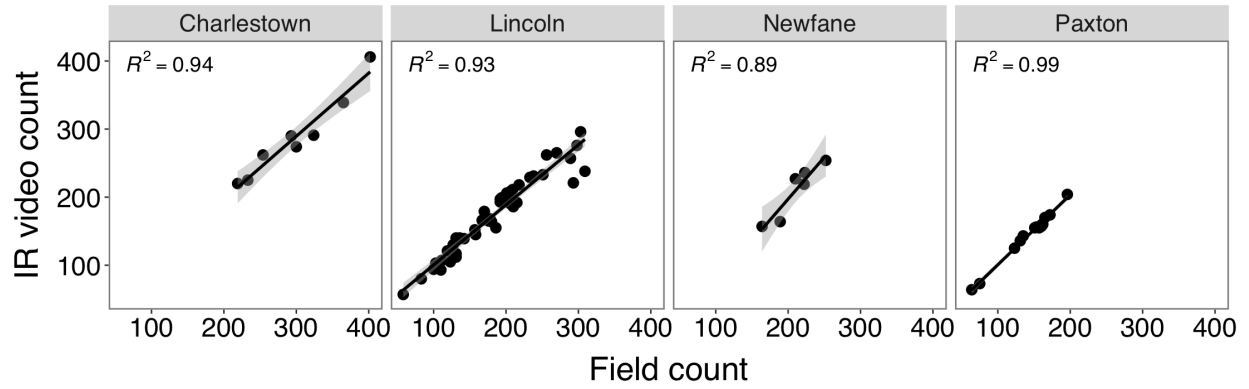


Figure 3.2. Correlations between field and infrared (IR) video emergence counts of little brown bats at the Lincoln (2010–2019), Paxton (2010–2011), Newfane (2018–2019), and Charlestown (2018–2019) maternity colonies. Solid lines are linear regressions and gray ribbons are 95% confidence intervals.

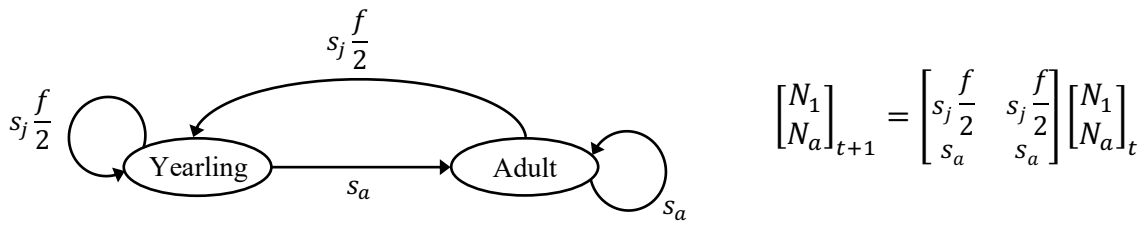


Figure 3.3. A pre-breeding census, female-based, life cycle graph for little brown bats, consisting of two stages, yearling and adult. Survival of juveniles (s_j) is from birth (which occurs immediately after the census) through their first winter to the next pre-breeding census. Yearling bats then survive their second winter with the same probability (s_a) as older adults. Fecundity or the probability that a female will reproduce each year (f) is divided by two, assuming an equal offspring sex ratio, to represent only daughters returning to the maternity colony in subsequent years. On the right is the corresponding Lefkovich population matrix representing the change in yearling (N_1) and adult (N_a) population sizes from time t to $t + 1$.

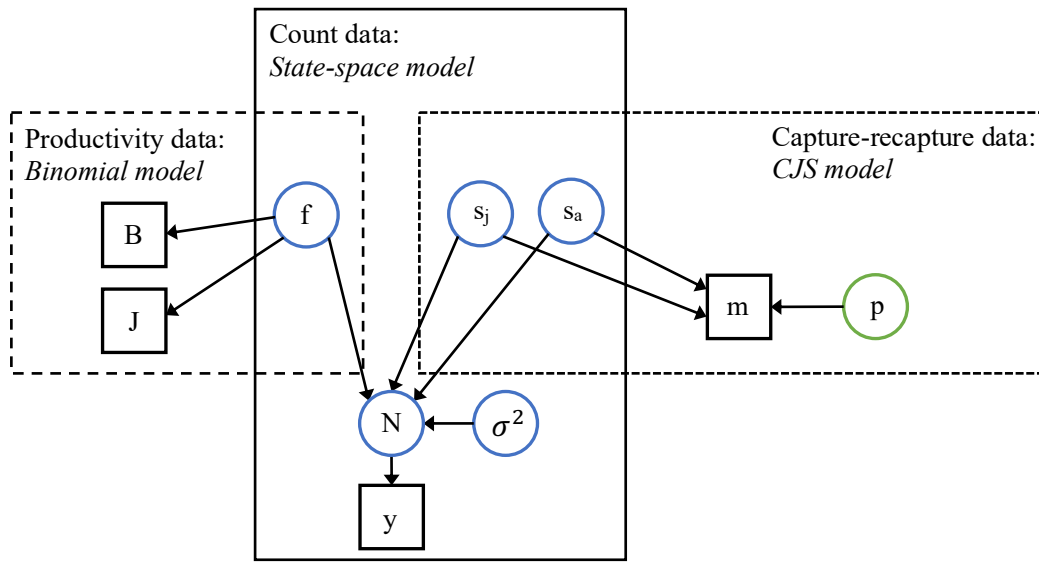


Figure 3.4. Directed acyclic graph without the priors for an integrated population model in a Bayesian framework. Circles indicate model parameters: fecundity (f), colony size (N), juvenile survival (s_j), adult survival (s_a), and observation error (σ^2). The green circle indicates that recapture rate (p) is a nuisance parameter. Boxes indicate the data: number of reproductive females (B), number of captured adult females (J), emergence counts (y), and mark-recapture data (m). The large boxes indicate the three submodels within the integrated population model. Recreated from Kéry and Schaub (2012).

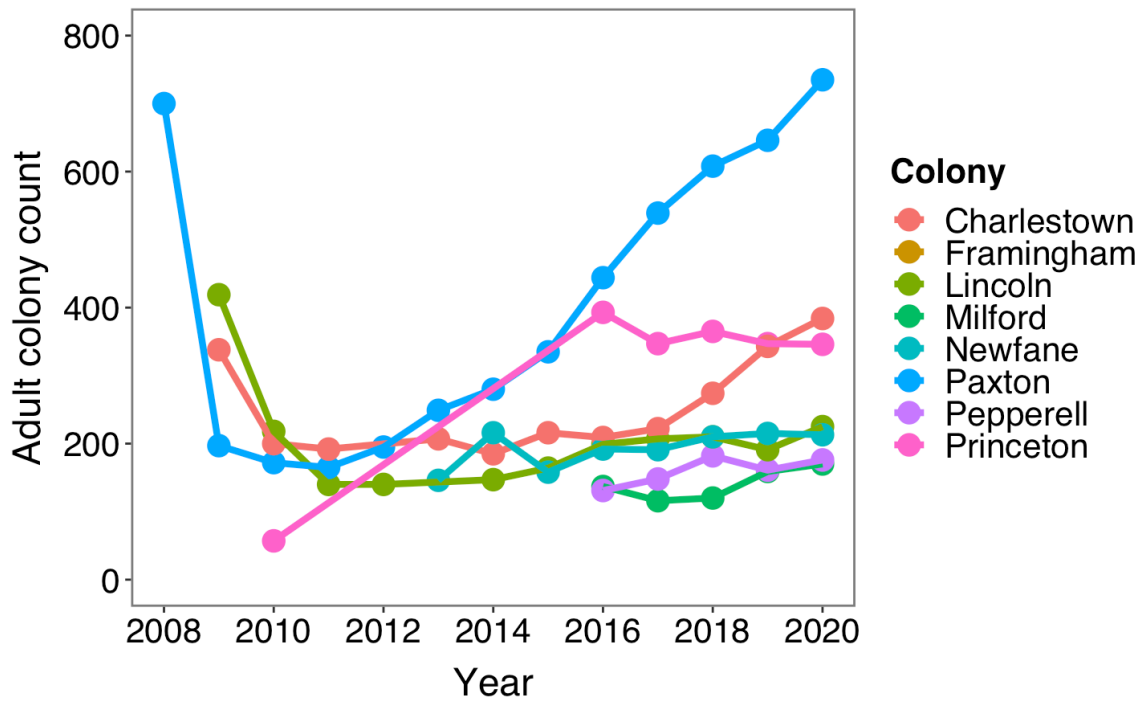


Figure 3.5. Adult colony count data from little brown bat maternity colonies, collected from early to mid-June between 2008 and 2020 via emergence counts in the field or from infrared video.

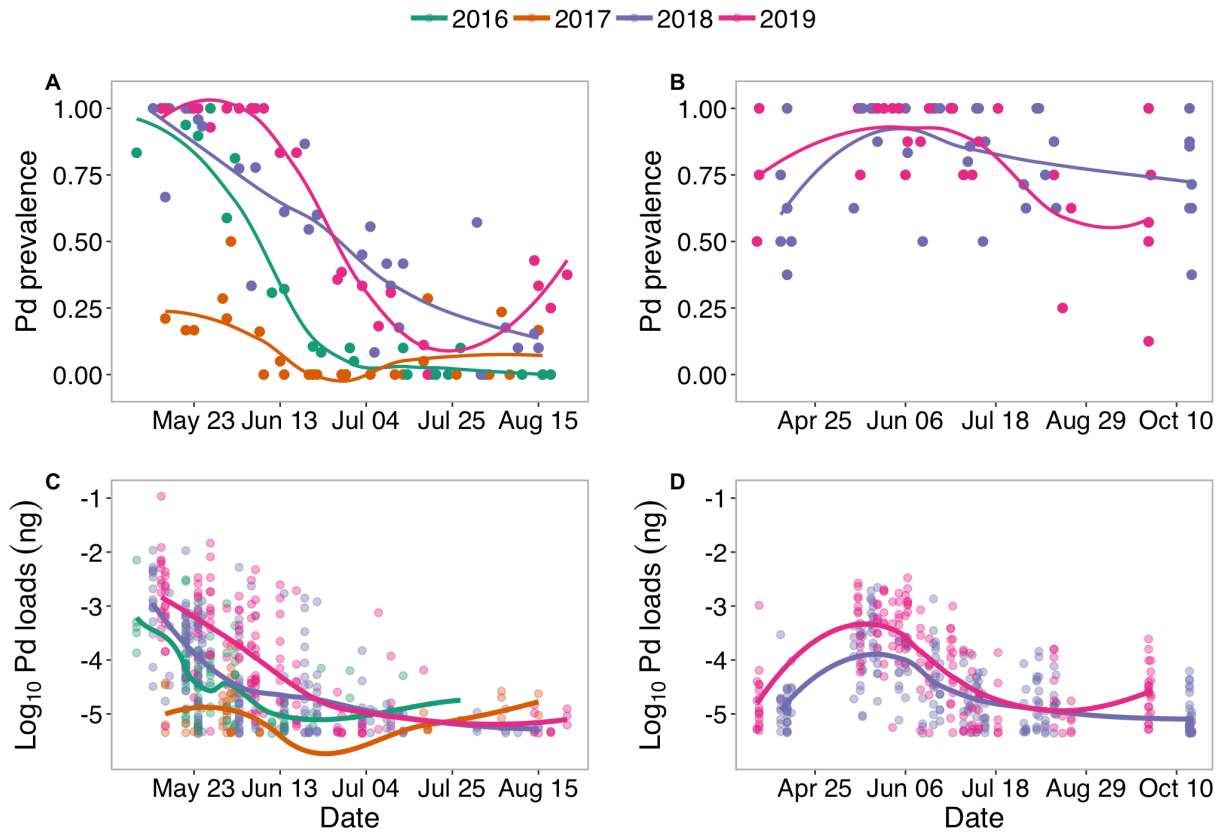


Figure 3.6. Prevalence and load (\log_{10}) of *Pseudogymnoascus destructans* (Pd) on little brown bats (A & C) and on roost surfaces (B & D) at summer maternity colonies sampled from 2016–2019. Lines are LOESS fits of the data.

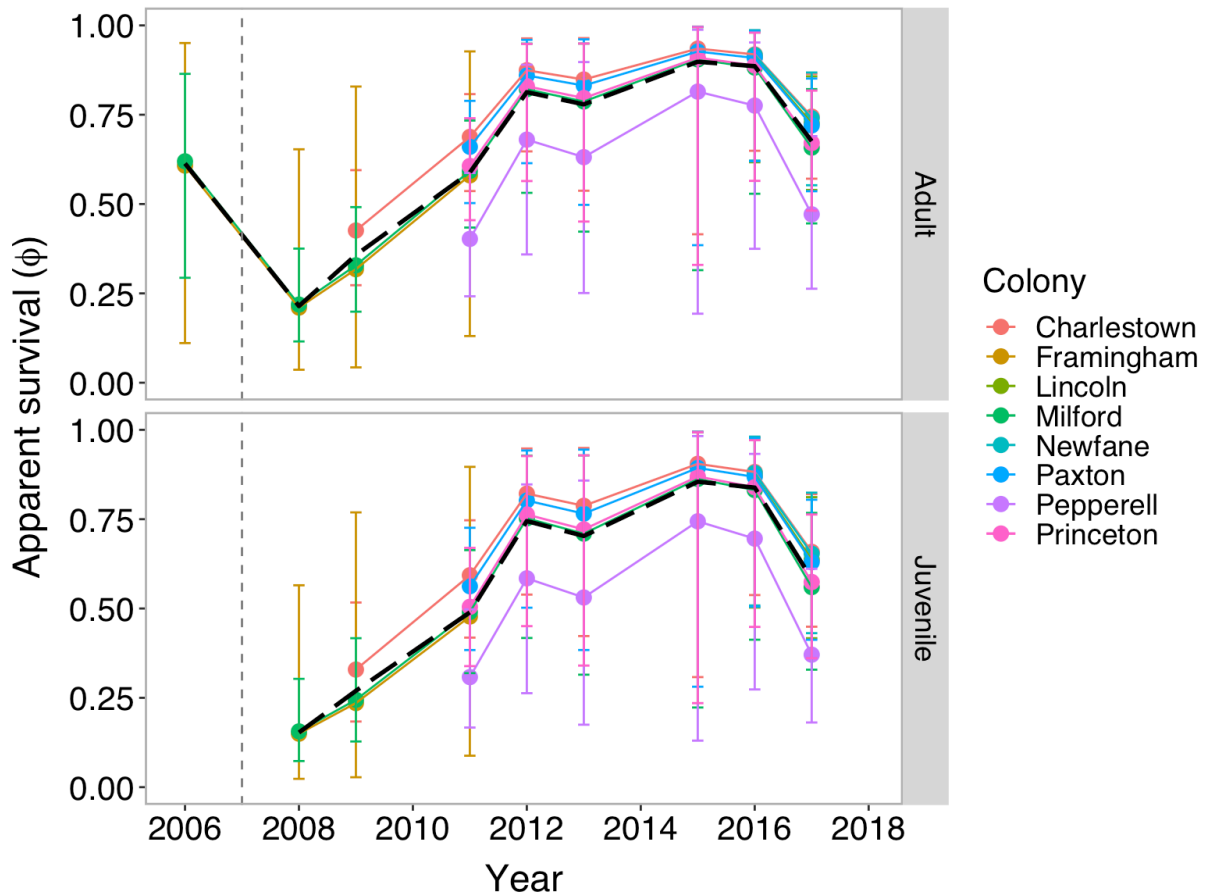


Figure 3.7. Apparent survival estimates for adult and juvenile little brown bats using banding data from eight maternity colonies in New England. Model structure was $\phi(\text{time}+\text{age}+\text{colony})$ $p(\text{time}+\text{age}+\text{colony})$. Error bars represent 95% confidence intervals. The black dashed line represents the mean survival rate by year for all sites combined. The vertical dashed gray line represents the start of white-nose syndrome invasion in the region.

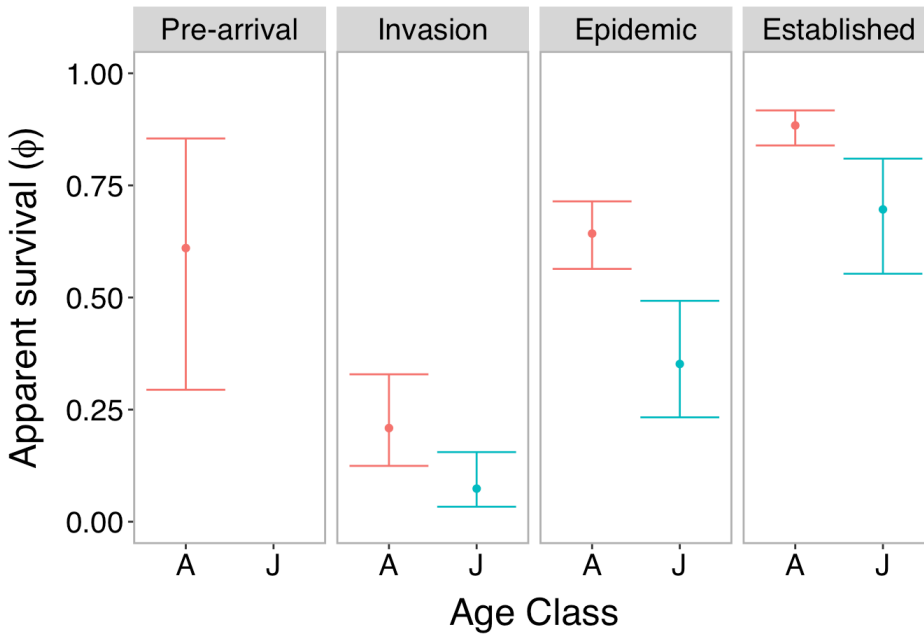


Figure 3.8. Apparent survival estimates for adults (A) and juveniles (J) by disease invasion phase using banding data collected at maternity colonies of little brown bats in New England. Model structure for survival included age and a disease invasion timeline (dis) of pre-invasion in 2006, invasion front in 2008, epidemic in 2009, and established in 2012: $\phi(\text{age}+\text{dis})$ $p(\text{time}+\text{age}+\text{colony})$. Error bars represent 95% confidence intervals.

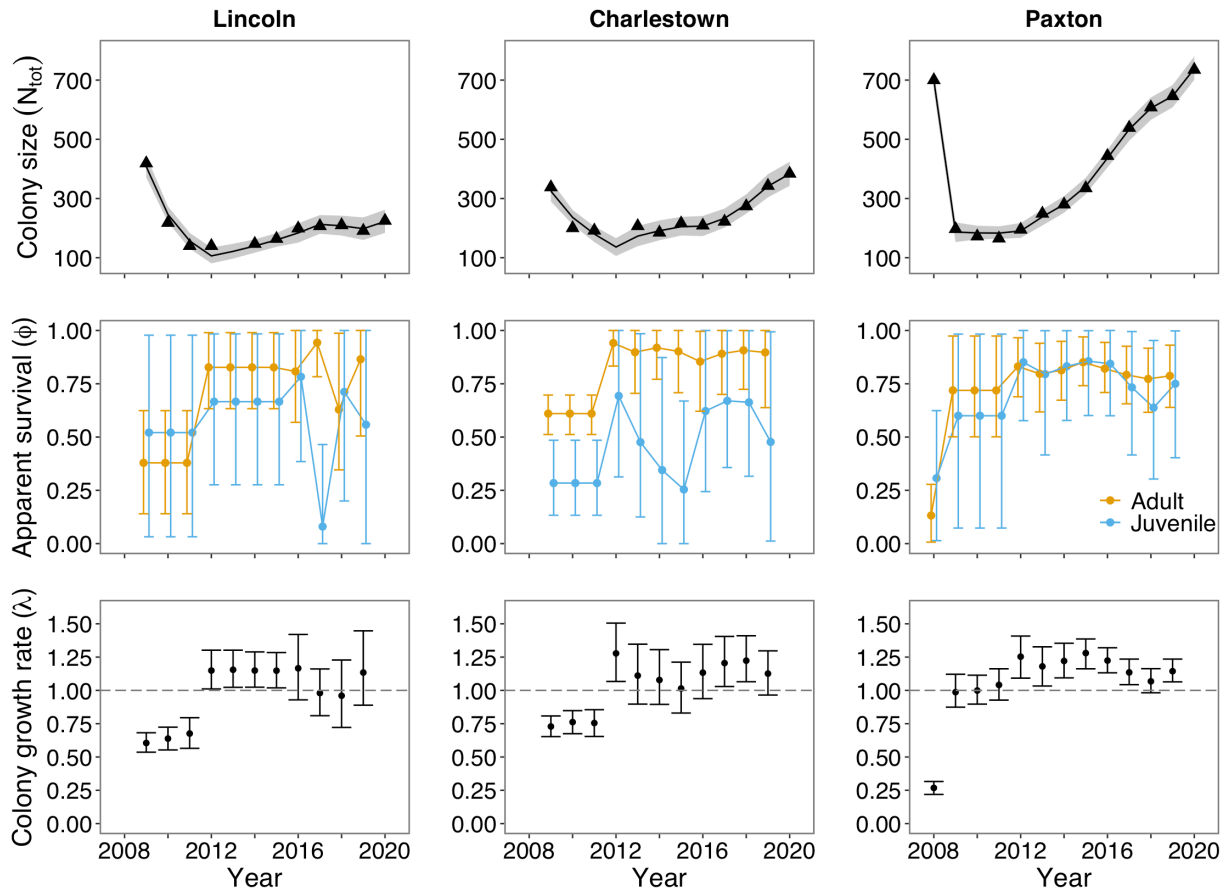


Figure 3.9. Annual colony size (black line), age-dependent apparent survival, and colony growth rate estimates from integrated population models for three little brown bat maternity colonies. Error bars and gray ribbons are 95% credible intervals. Black triangles are early- to mid-June emergence counts collected in the field or from infrared video.

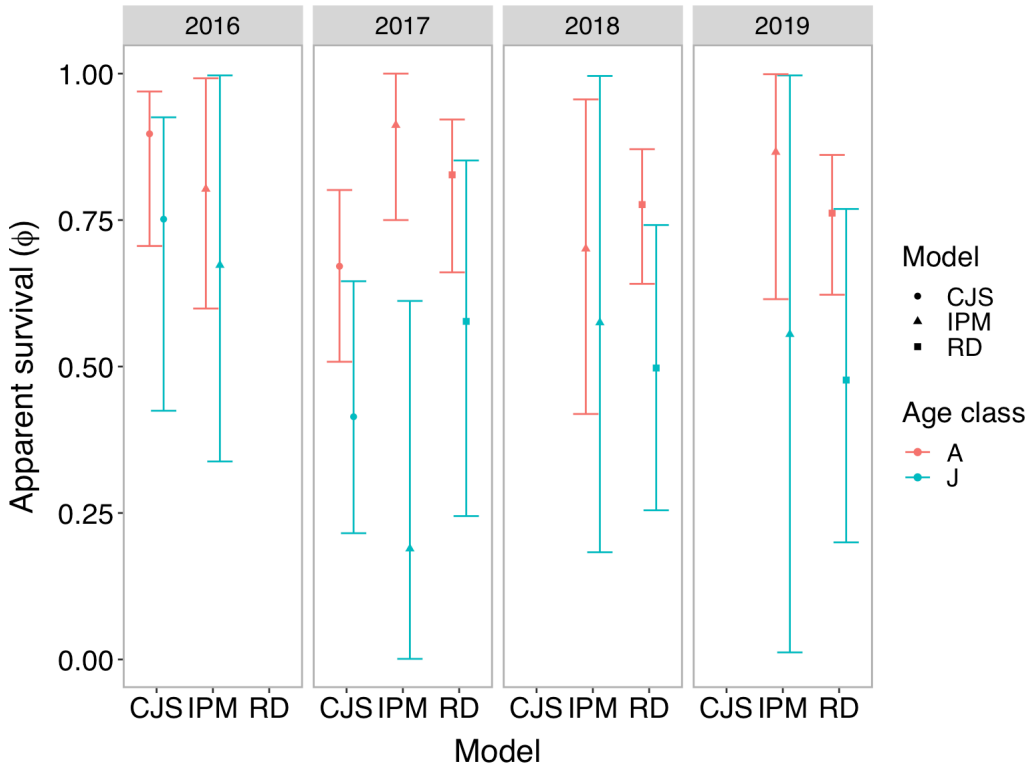


Figure 3.10. Comparison of annual apparent survival estimates for adults (A) and juveniles (J) at the Lincoln maternity colony (2016–2019) from three different models: a Cormack-Jolly-Seber (CJS) model using banding data, an integrated population model (IPM) using banding and emergence count data, and a robust design (RD) model using passive integrated transponder tag data.

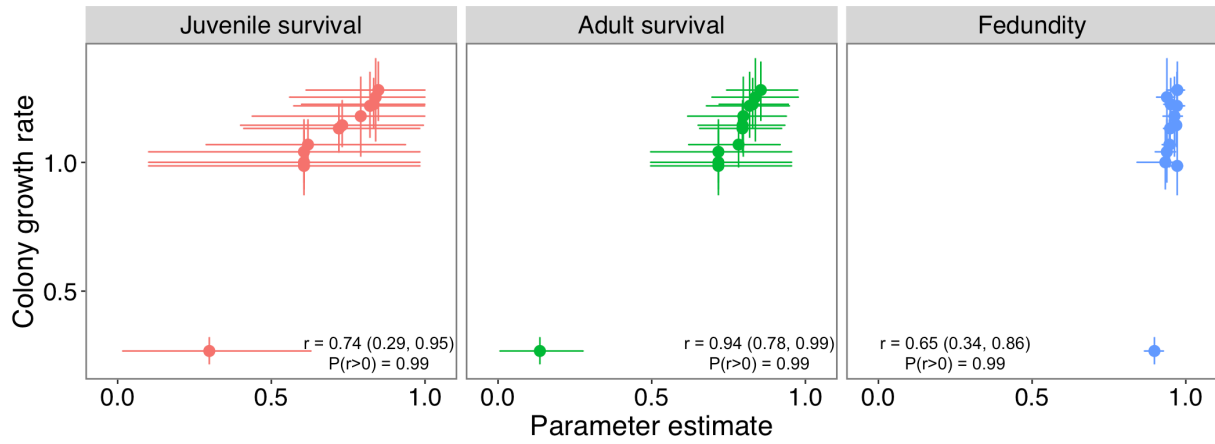


Figure 3.11. Correlations between estimated annual demographic rates and colony growth rate for the Paxton little brown bat colony from 2008 to 2019. Error bars are 95% credible intervals for both the demographic and growth rate estimates. Correlation coefficients (r) are shown with 95% credible intervals. $P(r>0)$ is the probability of a positive correlation.

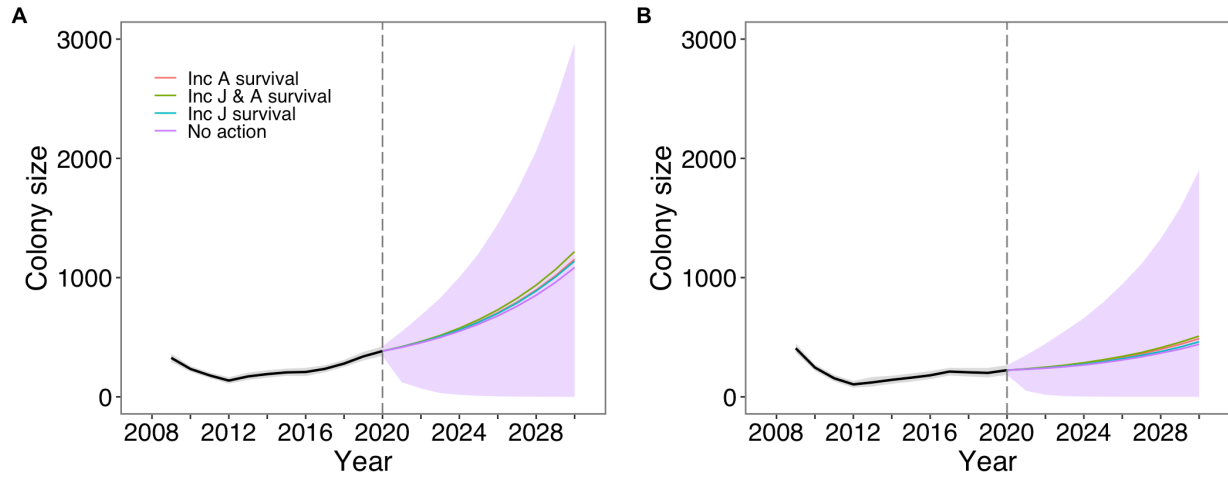


Figure 3.12. Colony size projections for 2020 to 2030 using a population viability analysis within an integrated population model under four different management scenarios for the A) Charlestown and B) Lincoln little brown bat maternity colonies. The black line shows colony size estimates and the dashed gray line indicates the start of the population projection. Management scenarios included “no action” (maintaining status quo), increasing juvenile (J) survival, increasing adult (A) survival, and increasing both juvenile and adult survival. Increases in survival were 10% on the log scale. The purple ribbon shows 95% credible intervals for the “no action” strategy with no additional human intervention beyond current measures.

LITERATURE CITED

- Abadi, F., O. Gimenez, R. Arlettaz, and M. Schaub. 2010. An assessment of integrated population models: bias, accuracy, and violation of the assumption of independence. *Ecology* 91:7–14.
- Adams, R. A. 1992. Comparative skeletogenesis of the forearm of the little brown bat (*Myotis lucifugus*) and the Norway rat (*Rattus norvegicus*). *Journal of Morphology* 214:251–260.
- Allander, K., and G. F. Bennett. 1995. Retardation of breeding onset in Great tits (*Parus major*) by blood parasites. *Functional Ecology* 9:677–682.
- Anchelin, M., L. Murcia, F. Alcaraz-Pérez, E. M. García-Navarro, and M. L. Cayuela. 2011. Behaviour of telomere and telomerase during aging and regeneration in zebrafish. *PLoS ONE* 6:e16955.
- Anthony, E. L. P., and T. H. Kunz. 1977. Feeding strategies of the little brown bat, *Myotis lucifugus*, in southern New Hampshire. *Ecology* 58:775–786.
- Anthony, E. L. P., M. H. Stack, and T. H. Kunz. 1981. Night roosting and the nocturnal time budget of the little brown bat, *Myotis lucifugus*: Effects of reproductive status, prey density, and environmental conditions. *Oecologia* 51:151–156.
- Archie, E. A. 2013. Wound healing in the wild: stress, sociality, and energetic costs affect wound healing in natural populations. *Parasite Immunology* 35:374–385.
- Arlettaz, R., P. Christe, A. Lugon, N. Perrin, and P. Vogel. 2001. Food availability dictates the timing of parturition in insectivorous mouse-eared bats. *Oikos* 95:105–111.
- Asghar, M., D. Hasselquist, B. Hansson, P. Zehindjiev, H. Westerdahl, and S. Bensch. 2015. Hidden costs of infection: chronic malaria accelerates telomere degradation and senescence in wild birds. *Science* 347:436–438.
- Asghar, M., V. Yman, M. V. Homann, K. Sondén, U. Hammar, D. Hasselquist, and A. Färnert. 2018. Cellular aging dynamics after acute malaria infection: A 12-month longitudinal study. *Aging Cell* 17:e12702.
- Audet, D., and M. B. Fenton. 1988. Heterothermy and the use of torpor by the bat *Eptesicus fuscus* (Chiroptera: Vespertilionidae): A field study. *Physiological Zoology* 61:197–204.
- Auteri, G. G., and L. L. Knowles. 2020. Decimated little brown bats show potential for adaptive change. *Nature Publishing Group* 10:3023.
- Baptista, T. L., C. S. Richardson, and T. H. Kunz. 2000. Postnatal growth and age estimation in free-ranging bats: a comparison of longitudinal and cross-sectional sampling methods. *Journal of Mammalogy* 81:709–718.

- Barclay, R. M. R., J. Ulmer, C. J. A. MacKenzie, M. S. Thompson, L. Olson, J. McCool, E. Cropley, and G. Poll. 2004. Variation in the reproductive rate of bats. *Canadian Journal of Zoology* 82:688–693.
- Bartón, K. 2020. MuMIn: multi-model inference. R package version 1.43.17. Retrieved from <https://CRAN.R-project.org/package=MuMIn>.
- Bates, D., M. Mächler, B. M. Bolker, and S. C. Walker. 2015. Fitting linear mixed-effects models using lme4. *Journal of Statistical Software* 67:1–48.
- Bateson, M., and D. Nettle. 2017. The telomere lengthening conundrum - it could be biology. *Aging Cell* 16:312–319.
- Beirne, C., R. Delahay, M. Hares, and A. Young. 2014. Age-related declines and disease-associated variation in immune cell telomere length in a wild mammal. *PLoS ONE* 9:e108964.
- Beissinger, S. R., and M. I. Westphal. 1998. On the use of demographic models of population viability in endangered species management. *The Journal of Wildlife Management* 62:821.
- Bergeson, S. M., T. C. Carter, and M. D. Whitby. 2015. Adaptive roosting gives little brown bats an advantage over endangered Indiana bats. *The American Midland Naturalist* 174:321–330.
- Bernardo, J., and S. J. Agosta. 2005. Evolutionary implications of hierarchical impacts of nonlethal injury on reproduction, including maternal effects. *Biological Journal of the Linnean Society* 86:309–331.
- Besbeas, P., S. N. Freeman, B. J. T. Morgan, and E. A. Catchpole. 2002. Integrating mark-recapture-recovery and census data to estimate animal abundance and demographic parameters. *Biometrics* 58:540–547.
- Besler, N. K., and H. G. Broders. 2019. Combinations of reproductive, individual, and weather effects best explain torpor patterns among female little brown bats (*Myotis lucifugus*). *Ecology and Evolution* 9:5158–5171.
- Betts, B. J. 2010. Thermoregulatory mechanisms used in a maternity colony of Townsend's big-eared bats in northeastern Oregon. *Northwestern Naturalist* 91:288–298.
- Blackburn, E. H. 1991. Structure and function of telomeres. *Nature* 350:569–573.
- Bleher, D. S., A. C. Hicks, M. Behr, C. U. Meteyer, B. M. Berlowski-Zier, E. L. Buckles, J. T. H. Coleman, S. R. Darling, A. Gargas, R. Niver, J. C. Okoniewski, R. J. Rudd, and W. B. Stone. 2009. Bat white-nose syndrome: an emerging fungal pathogen? *Science* 323:227–227.
- Boston, E. S. M., S. J. Puechmaille, D. D. Scott, D. J. Buckley, M. G. Lundy, I. W. Montgomery, P. A. Prodöhl, and E. C. Teeling. 2012. Empirical assessment of non-invasive population genetics in bats: comparison of DNA quality from faecal and tissue samples. *Acta Chiropterologica* 14:45–52.

- Brenner, F. J. 1968. A three-year study of two breeding colonies of the big brown bat, *Eptesicus fuscus*. *Journal of Mammalogy* 49:775–778.
- Brooks, R. T. 2011. Declines in summer bat activity in central New England 4 years following the initial detection of white-nose syndrome. *Biodiversity and Conservation* 20:2537–2541.
- Brown, J. C. L., G. B. McClelland, P. A. Faure, J. M. Klaiman, and J. F. Staples. 2009. Examining the mechanisms responsible for lower ROS release rates in liver mitochondria from the long-lived house sparrow (*Passer domesticus*) and big brown bat (*Eptesicus fuscus*) compared to the short-lived mouse (*Mus musculus*). *Mechanisms of Ageing and Development* 130:467–476.
- Brunet-Rossinni, A. K. 2004. Reduced free-radical production and extreme longevity in the little brown bat (*Myotis lucifugus*) versus two non-flying mammals. *Mechanisms of Ageing and Development* 125:11–20.
- Brunet-Rossinni, A. K., and G. S. Wilkinson. 2009. Age estimation and senescence. Pages 315–325 in T. H. Kunz and S. Parsons, editors. *Ecological and Behavioral Methods for the Study of Bats*. Second edition. The John Hopkins University Press, Baltimore, Maryland.
- Brunet-Rossinni, A. K., and S. N. Austad. 2004. Ageing studies on bats: a review. *Biogerontology* 5:211–222.
- Buchanan, G. D., and E. V. Younglai. 1986. Plasma progesterone levels during pregnancy in the little brown bat *Myotis lucifugus* (Vespertilionidae). *Biology of Reproduction* 34:878–884.
- Buchler, E. R. 1975. Food transit time in *Myotis lucifugus* (Chiroptera: Vespertilionidae). *Journal of Mammalogy* 56:252–255.
- Burles, D. W., R. M. Brigham, R. A. Ring, and T. E. Reimchen. 2009. Influence of weather on two insectivorous bats in a temperate Pacific Northwest rainforest. *Canadian Journal of Zoology* 87:132–138.
- Burnett, C. D., and P. V. August. 1981. Time and energy budgets for dayroosting in a maternity colony of *Myotis lucifugus*. *Journal of Mammalogy* 62:758–766.
- Burnett, C. D., and T. H. Kunz. 1982. Growth rates and age estimation in *Eptesicus fuscus* and comparison with *Myotis lucifugus*. *Journal of Mammalogy* 63:33–41.
- Burnham, K. P., and D. R. Anderson. 2002. *Model selection and multimodel inference: a practical information-theoretic approach*. Second edition. Springer-Verlag, New York.
- Burns, L. E., and H. G. Broders. 2014. Correlates of dispersal extent predict the degree of population genetic structuring in bats. *Conservation Genetics* 15:1371–1379.
- Burns, L. E., T. R. Frasier, and H. G. Broders. 2014. Genetic connectivity among swarming sites in the wide ranging and recently declining little brown bat (*Myotis lucifugus*). *Ecology and Evolution* 4:4130–4149.

- Cagle, F. R., and E. L. Cockrum. 1943. Notes on a summer colony of *Myotis lucifugus lucifugus*. *Journal of Mammalogy* 24:474.
- Callicott, R. J., and J. E. Womack. 2006. Real-time PCR assay for measurement of mouse telomeres. *Comparative Medicine* 56:17–22.
- Calow, P. 1979. The cost of reproduction - a physiological approach. *Biological Reviews* 54:23–40.
- Caro, T., J. Eadie, and A. Sih. 2005. Use of substitute species in conservation biology. *Conservation Biology* 19:1821–1826.
- Cassinello, J., and C. L. Alados. 1996. Female reproductive success in captive *Ammotragus lervia* (Bovidae, Artiodactyla). Study of its components and effects of hierarchy and inbreeding. *Journal of the Zoological Society of London* 239:141–153.
- Castle, K. T., T. J. Weller, P. M. Cryan, C. D. Hein, and M. R. Schirmacher. 2015. Using sutures to attach miniature tracking tags to small bats for multimonth movement and behavioral studies. *Ecology and Evolution* 5:2980–2989.
- Cawthon, R. M. 2002. Telomere measurement by quantitative PCR. *Nucleic Acids Research* 30:e47.
- Cheng, T. L., A. Gerson, M. S. Moore, J. D. Reichard, J. DeSimone, C. K. R. Willis, W. F. Frick, and A. M. Kilpatrick. 2019. Higher fat stores contribute to persistence of little brown bat populations with white-nose syndrome. *Journal of Animal Ecology* 22:245–10.
- Cheng, T. L., H. Mayberry, L. P. McGuire, J. R. Hoyt, K. E. Langwig, H. Nguyen, K. L. Parise, J. T. Foster, C. K. R. Willis, A. M. Kilpatrick, and W. F. Frick. 2016. Efficacy of a probiotic bacterium to treat bats affected by the disease white-nose syndrome. *Journal of Applied Ecology* 54:701–708.
- Choquet, R., J.-D. Lebreton, O. Gimenez, A.-M. Reboulet, and R. Pradel. 2009. U-CARE: Utilities for performing goodness of fit tests and manipulating CAPture-REcapture data. *Ecography* 32:1071–1074.
- Christian, J. J. 1956. The natural history of a summer aggregation of the big brown bat, *Eptesicus fuscus fuscus*. *The American Midland Naturalist* 55:66–95.
- Cooch, E. G., and G. C. White. 2019. Program MARK: A gentle introduction. Available online from <www.phidot.org/software/mark/docs/book/>.
- Corthals, A., A. Martin, O. M. Warsi, M. Woller-Skar, W. Lancaster, A. Russell, and L. M. Dávalos. 2015. From the field to the lab: best practices for field preservation of bat specimens for molecular analyses. *PLoS ONE* 10:e0118994.
- Coulson, T., F. Guinness, J. Pemberton, and T. Clutton-Brock. 2004. The demographic consequences of releasing a population of red deer from culling. *Ecology* 85:411–422.

- Cryan, P. M., C. A. Stricker, and M. B. Wunder. 2012. Evidence of cryptic individual specialization in an opportunistic insectivorous bat. *Journal of Mammalogy* 93:381–389.
- Cryan, P. M., C. U. Meteyer, J. G. Boyles, and D. S. Blehert. 2010. Wing pathology of white-nose syndrome in bats suggests life-threatening disruption of physiology. *BMC Biology* 8:135.
- Culina, A., D. M. Linton, R. Pradel, S. Bouwhuis, and D. W. MacDonald. 2019. Live fast, don't die young: Survival–reproduction trade-offs in long-lived income breeders. *Journal of Animal Ecology* 88:746–756.
- Czenze, Z. J., and C. K. R. Willis. 2015. Warming up and shipping out: arousal and emergence timing in hibernating little brown bats (*Myotis lucifugus*). *Journal of Comparative Physiology B* 185:575–586.
- Daniali, L., A. Benetos, E. Susser, J. D. Kark, C. Labat, M. Kimura, K. K. Desai, M. Granick, and A. Aviv. 2013. Telomeres shorten at equivalent rates in somatic tissues of adults. *Nature Communications* 4:1597.
- Daszak, P., A. A. Cunningham, and A. D. Hyatt. 2000. Emerging infectious diseases of wildlife—threats to biodiversity and human health. *Science* 287:443–449.
- Davis, W. H., and H. B. Hitchcock. 1965. Biology and migration of the bat, *Myotis lucifugus*, in New England. *Journal of Mammalogy* 46:296–313.
- Davis, W. H., and H. B. Hitchcock. 1995. A new longevity record for the bat *Myotis lucifugus*. *Bat Research News* 36:6.
- Davy, C. M., G. F. Mastromonaco, J. L. Riley, J. H. Baxter-Gilbert, H. Mayberry, and C. K. R. Willis. 2016. Conservation implications of physiological carry-over effects in bats recovering from white-nose syndrome. *Conservation Biology* 31:615–624.
- De Castro, F., and B. Bolker. 2005. Mechanisms of disease-induced extinction. *Ecology Letters* 8:117–126.
- De Paoli-Iseppi, R., B. E. Deagle, C. R. McMahon, M. A. Hindell, J. L. Dickinson, and S. N. Jarman. 2017. Measuring animal age with DNA methylation: from humans to wild animals. *Frontiers in Genetics* 8:1–8.
- Derocher, A. E., I. Stirling, and D. Andriashek. 1992. Pregnancy rates and serum progesterone levels of polar bears in western Hudson Bay. *Canadian Journal of Zoology* 70:561–566.
- Desprez, M., R. Harcourt, M. A. Hindell, S. Cubaynes, O. Gimenez, and C. R. McMahon. 2014. Age-specific cost of first reproduction in female southern elephant seals. *Biology Letters* 10:20140264.
- Dixon, M. D. 2011. Population genetic structure and natal philopatry in the widespread North American bat *Myotis lucifugus*. *Journal of Mammalogy* 92:1343–1351.

- Dlouha, D., J. Maluskova, I. Kralova Lesna, V. Lanska, and J. A. Hubacek. 2014. Comparison of the relative telomere length measured in leukocytes and eleven different human tissues. *Physiological Research* 63:S343–S350.
- Dobony, C. A., A. C. Hicks, K. E. Langwig, R. V. Linden, J. C. Okoniewski, and R. E. Rainbolt. 2011. Little brown myotis persist despite exposure to white-nose syndrome. *Journal of Fish and Wildlife Management* 2:190-195.
- Dobony, C. A., and J. B. Johnson. 2018. Observed resiliency of little brown myotis to long-term white-nose syndrome exposure. *Journal of Fish and Wildlife Management* 9:168-179.
- Dugdale, H. L., and D. S. Richardson. 2018. Heritability of telomere variation: it is all about the environment! *Philosophical Transactions of the Royal Society B: Biological Sciences* 373:20160450.
- Dunsha, G., D. Duffield, N. Gales, M. Hindell, R. S. Wells, and S. N. Jarman. 2011. Telomeres as age markers in vertebrate molecular ecology. *Molecular Ecology Resources* 11:225–235.
- Dzal, Y. A., and R. M. Brigham. 2013. The tradeoff between torpor use and reproduction in little brown bats (*Myotis lucifugus*). *Journal of Comparative Physiology B* 183:279–288.
- Dzal, Y., L. P. McGuire, N. Veselka, and M. B. Fenton. 2011. Going, going, gone: the impact of white-nose syndrome on the summer activity of the little brown bat (*Myotis lucifugus*). *Biology Letters*:392–294.
- Eberhardt, L. L. 2002. A paradigm for population analysis of long-lived vertebrates. *Ecology* 83:2841–2854.
- Ehrlenbach, S., P. Willeit, S. Kiechl, J. Willeit, M. Reindl, K. Schanda, F. Kronenberg, and A. Brandstätter. 2009. Influences on the reduction of relative telomere length over 10 years in the population-based Bruneck Study: introduction of a well-controlled high-throughput assay. *International Journal of Epidemiology* 38:1725–1734.
- Ellison, L. E., T. J. O'Shea, D. J. Neubaum, M. A. Neubaum, R. D. Pearce, and R. A. Bowen. 2007. A comparison of conventional capture versus PIT reader techniques for estimating survival and capture probabilities of big brown bats (*Eptesicus fuscus*). *Acta Chiropterologica* 9:149–160.
- Entwistle, A. C., P. A. Racey, and J. R. Speakman. 1997. Roost selection by the brown long-eared bat *Plecotus auritus*. *Journal of Applied Ecology* 34:399–408.
- Erickson, R. A., W. E. Thogmartin, and J. A. Szymanski. 2014. BatTool: an R package with GUI for assessing the effect of white-nose syndrome and other take events on *Myotis* spp. of bats. *Source Code for Biology and Medicine* 9:1–10.
- Fairlie, J., R. Holland, J. G. Pilkington, J. M. Pemberton, L. Harrington, and D. H. Nussey. 2016. Lifelong leukocyte telomere dynamics and survival in a free-living mammal. *Aging Cell* 15:140–148.

- Fenton, M. B., and R. M. R. Barclay. 1980. *Myotis lucifugus*. Mammalian Species 142:1–8.
- Finnicum, C. T., C. V. Dolan, G. Willemsen, Z. M. Weber, J. L. Petersen, J. J. Beck, V. Codd, D. I. Boomsma, G. E. Davies, and E. A. Ehli. 2017. Relative telomere repeat mass in buccal and leukocyte-derived DNA. PLoS ONE 12:e0170765.
- Fisher, M. C., D. A. Henk, C. J. Briggs, J. S. Brownstein, L. C. Madoff, S. L. McCraw, and S. J. Gurr. 2012. Emerging fungal threats to animal, plant and ecosystem health. Nature 484:186–194.
- Fletcher, Q. E., Q. M. R. Webber, and C. K. R. Willis. 2020. Modelling the potential efficacy of treatments for white-nose syndrome in bats. Journal of Applied Ecology 26:486–9.
- Foley, N. M., G. M. Hughes, Z. Huang, M. Clarke, D. Jebb, C. V. Whelan, E. J. Petit, F. Touzaline, O. Farcy, G. Jones, R. D. Ransome, J. Kacprzyk, M. J. O’Connell, G. Kerth, H. Rebelo, L. Rodrigues, S. J. Puechmaille, and E. C. Teeling. 2018. Growing old, yet staying young: The role of telomeres in bats’ exceptional longevity. Science Advances 4:eaa0926.
- Francel, K. E., M. F. W. Dale W Sparks, and J. Virgil Brack. 2012. Capture and reproductive trends in summer bat communities in West Virginia: assessing the impact of white-nose syndrome. Journal of Fish and Wildlife Management 3:33–42.
- Frank, C. L., A. D. Davis, and C. Herzog. 2019. The evolution of a bat population with white-nose syndrome (WNS) reveals a shift from an epizootic to an enzootic phase. Frontiers in Zoology 16:40.
- Frick, W. F., D. S. Reynolds, and T. H. Kunz. 2010a. Influence of climate and reproductive timing on demography of little brown myotis *Myotis lucifugus*. The Journal of Animal Ecology 79:128–136.
- Frick, W. F., J. F. Pollock, A. C. Hicks, K. E. Langwig, D. S. Reynolds, G. G. Turner, C. M. Butchkoski, and T. H. Kunz. 2010b. An emerging disease causes regional population collapse of a common North American bat species. Science 329:679–682.
- Frick, W. F., T. L. Cheng, K. E. Langwig, J. R. Hoyt, A. F. Janicki, K. L. Parise, J. T. Foster, and A. M. Kilpatrick. 2017. Pathogen dynamics during invasion and establishment of white-nose syndrome explain mechanisms of host persistence. Ecology 98:624–631.
- Fuller, N. W. 2016. Pathophysiology and recovery of *Myotis lucifugus* affected by white nose syndrome. Ph.D. dissertation. Boston University. Boston, Massachusetts.
- Fuller, N. W., J. D. Reichard, M. L. Nabhan, S. R. Fellows, L. C. Pepin, and T. H. Kunz. 2011. Free-ranging little brown Myotis (*Myotis lucifugus*) heal from wing damage associated with white-nose syndrome. EcoHealth 8:154–162.
- Fuller, N. W., L. P. McGuire, E. L. Pannkuk, T. Blute, C. G. Haase, H. W. Mayberry, T. S. Risch, and C. K. R. Willis. 2020. Disease recovery in bats affected by white-nose syndrome. The Journal of Experimental Biology 223:jeb.211912.

- Gadalla, S. M., R. Cawthon, N. Giri, B. P. Alter, and S. A. Savage. 2010. Telomere length in blood, buccal cells, and fibroblasts from patients with inherited bone marrow failure syndromes. *Aging* 2:867–874.
- Geiser, F. 2004. Metabolic rate and body temperature reduction during hibernation and daily torpor. *Annual Review of Physiology* 66:239–274.
- Gelman, A., and D. B. Rubin. 1992. Inference from iterative simulation using multiple sequences. *Statistical Science* 7:457–511.
- Gignoux-Wolfsohn, S. A., M. L. Pinsky, K. Kerwin, C. Herzog, M. Hall, A. B. Bennett, N. H. Fefferman, and B. Maslo. 2019. Genomic signatures of evolutionary rescue in bats surviving white-nose syndrome. *bioRxiv* doi: 10.1101/470294.
- Gilbert, C., D. McCafferty, Y. Le Maho, J.-M. Martrette, S. Giroud, S. Blanc, and A. Ancel. 2009. One for all and all for one: the energetic benefits of huddling in endotherms. *Biological Reviews* 85:545–569.
- Gimenez, O., J.-D. Lebreton, R. Choquet, and R. Pradel. 2018. R2ucare: an R package to perform goodness-of-fit tests for capture-recapture models. *Methods in Ecology and Evolution* 9:1749–1754.
- Gol'din, P., L. Godlevska, and M. Ghazali. 2018. Age-related changes in the teeth of two bat species: dental wear, pulp cavity and dentine growth layers. *Acta Chiropterologica* 20:519–530.
- Gomes, N. M. V., O. A. Ryder, M. L. Houck, S. J. Charter, W. Walker, N. R. Forsyth, S. N. Austad, C. Venditti, M. Pagel, J. W. Shay, and W. E. Wright. 2011. Comparative biology of mammalian telomeres: hypotheses on ancestral states and the roles of telomeres in longevity determination. *Aging Cell* 10:761–768.
- Gonzalez, A., O. Ronce, R. Ferriere, and M. E. Hochberg. 2013. Evolutionary rescue: an emerging focus at the intersection between ecology and evolution. *Philosophical Transactions of the Royal Society B: Biological Sciences* 368:20120404.
- Green, W. C. H., and A. Rothstein. 1991. Trade-offs between growth and reproduction in female bison. *Oecologia* 86:521–527.
- Grenier, M. B., D. B. McDonald, and S. W. Buskirk. 2007. Rapid population growth of a critically endangered carnivore. *Science* 317:779.
- Greville, L. J., A. Ceballos-Vasquez, R. Valdizón-Rodríguez, J. R. Caldwell, and P. A. Faure. 2018. Wound healing in wing membranes of the Egyptian fruit bat (*Rousettus aegyptiacus*) and big brown bat (*Eptesicus fuscus*). *Journal of Mammalogy* 99:974–982.
- Griffin, D. R. 1940. Migrations of New England bats. *Bulletin of the American Museum of Natural History* 86:217–246.

- Grindal, S. D., T. S. Collard, R. M. Brigham, and R. M. R. Barclay. 1992. The influence of precipitation on reproduction by myotis bats in British Columbia. *American Midland Naturalist* 128:339–344.
- Grinevitch, L., S. L. Holroyd, and R. M. R. Barclay. 1995. Sex differences in the use of daily torpor and foraging time by big brown bats (*Eptesicus fuscus*) during the reproductive season. *Journal of the Zoological Society of London* 235:301–309.
- Gustafsson, L., and T. Pärt. 1990. Acceleration of senescence in the collared flycatcher *Ficedula albicollis* by reproductive costs. *Nature* 347:279–281.
- Hall, J. S., R. J. Cloutier, and D. R. Griffin. 1957. Longevity records and notes on tooth wear of bats. *Journal of Mammalogy* 38:407–409.
- Hammers, M., S. A. Kingma, K. Bebbington, J. van de Crommenacker, L. G. Spurgin, D. S. Richardson, T. Burke, H. L. Dugdale, and J. Komdeur. 2015. Senescence in the wild: insights from a long-term study on Seychelles warblers. *Experimental Gerontology* 71:69–79.
- Hausmann, M. F., and N. M. Marchetto. 2010. Telomeres: linking stress and survival, ecology and evolution. *Current Zoology* 56:714–727.
- Heideman, P. D., and R. C. Utzurrum. 2003. Seasonality and synchrony of reproduction in three species of nectarivorous Philippines bats. *BMC Ecology* 3:1–14.
- Henry, M., D. W. Thomas, R. Vaudrym, and M. Carrier. 2002. Foraging distances and home range of pregnant and lactating little brown bats (*Myotis lucifugus*). *Journal of Mammalogy* 83:767–774.
- Hinnebusch, J., S. Bergström, and A. G. Barbour. 1990. Cloning and sequence analysis of linear plasmid telomeres of the bacterium *Borrelia burgdorferi*. *Molecular Microbiology* 4:811–820.
- Hitchcock, H. B. 1965. Twenty-three years of bat banding in Ontario and Quebec. *The Canadian Field-Naturalist* 79:4–14.
- Hoelzl, F., J. S. Cornils, S. Smith, Y. Moodley, and T. Ruf. 2016a. Telomere dynamics in free-living edible dormice (*Glis glis*): the impact of hibernation and food supply. *The Journal of Experimental Biology* 219:2469–2474.
- Hoelzl, F., S. Smith, J. S. Cornils, D. Aydinonat, C. Bieber, and T. Ruf. 2016b. Telomeres are elongated in older individuals in a hibernating rodent, the edible dormouse (*Glis glis*). *Scientific Reports* 6:36856.
- Hood, W. R., J. Bloss, and T. H. Kunz. 2002. Intrinsic and extrinsic sources of variation in size at birth and rates of postnatal growth in the big brown bat *Eptesicus fuscus* (Chiroptera: Vespertilionidae). *Journal of Zoology* 258:355–363.

- Hothorn, T., F. Bretz, and P. Westfall. 2008. Simultaneous inference in general parametric models. *Biometrical Journal* 50:346–363.
- Houston, D. B., and V. Stevens. 1998. Resource limitation in mountain goats: a test by experimental cropping. *Canadian Journal of Zoology* 66:228–238.
- Hoyt, J. R., K. E. Langwig, J. Okoniewski, W. F. Frick, W. B. Stone, and A. M. Kilpatrick. 2015a. Long-term persistence of *Pseudogymnoascus destructans*, the causative agent of white-nose syndrome, in the absence of bats. *EcoHealth* 12:330-333.
- Hoyt, J. R., K. E. Langwig, J. P. White, H. M. Kaarakka, J. A. Redell, K. L. Parise, W. F. Frick, J. T. Foster, and A. M. Kilpatrick. 2019. Field trial of a probiotic bacteria and a chemical, chitosan, to protect bats from white-nose syndrome. *Scientific Reports* 9:9158.
- Hoyt, J. R., T. L. Cheng, K. E. Langwig, M. M. Hee, W. F. Frick, and A. M. Kilpatrick. 2015b. Bacteria isolated from bats inhibit the growth of *Pseudogymnoascus destructans*, the causative agent of white-nose syndrome. *PLoS ONE* 10:e0121329.
- Huggins, R. M. 1989. On the statistical analysis of capture experiments. *Biometrika* 76:133–140.
- Humphrey, S. R. 1971. Population ecology of the little brown bat, *Myotis lucifugus*, in Indiana and north-central Kentucky. Ph.D. dissertation. Oklahoma State University. Stillwater, Oklahoma.
- Humphrey, S. R., and J. B. Cope. 1976. Population Ecology of the little brown bat, *Myotis lucifugus*, in Indiana and North-Central Kentucky. Special Publication No. 4. The American Society of Mammalogists. 81 pp.
- Ibáñez-Álamo, J. D., J. Pineda-Pampliega, R. L. Thomson, J. I. Aguirre, A. Díez-Fernández, B. Faivre, J. Figuerola, and S. Verhulst. 2018. Urban blackbirds have shorter telomeres. *Biology Letters* 14:20180083.
- Ilmonen, P., A. Kotrschal, and D. J. Penn. 2008. Telomere attrition due to infection. *PLoS ONE* 3:e2143.
- Ineson, K. M., T. J. O'Shea, C. W. Kilpatrick, K. L. Parise, and J. T. Foster. *In press*. Ambiguities in using telomere length for age determination in two North American bat species. *Journal of Mammalogy*.
- Jarman, S. N., A. M. Polanowski, C. E. Faux, J. Robbins, R. De Paoli-Iseppi, M. Bravington, and B. E. Deagle. 2015. Molecular biomarkers for chronological age in animal ecology. *Molecular Ecology* 24:4826–4847.
- Johnson, D. S., R. P. Barry, and R. T. Bowyer. 2004. Estimating timing of life-history events with coarse data. *Journal of Mammalogy* 85:932–939.

- Johnson, H. E., L. S. Mills, T. R. Stephenson, and J. D. Wehausen. 2010. Population-specific vital rate contributions influence management of an endangered ungulate. *Ecological Applications* 20:1753–1765.
- Johnson, J. S., J. J. Treanor, A. C. Slusher, and M. J. Lacki. 2019. Buildings provide vital habitat for little brown myotis (*Myotis lucifugus*) in a high-elevation landscape. *Ecosphere* 10:e02925.
- Jones, M. E., A. Cockburn, R. Hamede, C. Hawkins, H. Hesterman, S. Lachish, D. Mann, H. McCallum, and D. Pemberton. 2008. Life-history change in disease-ravaged Tasmanian devil populations. *Proceedings of the National Academy of Sciences* 105:10023–10027.
- Keen, R., and H. B. Hitchcock. 1980. Survival and longevity of the little brown bat (*Myotis lucifugus*) in Southeastern Ontario. *Journal of Mammalogy* 61:1–7.
- Kendall, W. L. 2018. The “robust design.” Chapter 15 in *Program MARK: A gentle introduction*. Available online from <www.phidot.org/software/mark/docs/book/>.
- Kendall, W. L., and J. D. Nichols. 1995. On the use of secondary capture-recapture samples to estimate temporary emigration and breeding proportions. *Journal of Applied Statistics* 22:751–762.
- Kendall, W. L., J. D. Nichols, and J. E. Hines. 1997. Estimating temporary emigration using capture-recapture data with Pollock's robust design. *Ecology* 78:563–578.
- Kéry, M., and M. Schaub. 2012. *Bayesian population analysis using WinBUGS: a hierarchical perspective*. First edition. Academic Press, Burlington.
- Kilpatrick, A. M. 2006. Facilitating the evolution of resistance to avian malaria in Hawaiian birds. *Biological Conservation* 128:475–485.
- Kunz, T. H. 1973. Population studies of the cave bat (*Myotis velifer*): reproduction, growth, and development. *Occasional Papers of the Museum of Natural History, The University of Kansas*:1–43.
- Kunz, T. H. 2003. Censusing bats: challenges, solutions, and sampling biases. Pages 9–19 in *Monitoring trends in bat populations of the United States and territories problems and prospects*. U.S. Geological Survey. 274 pp.
- Kunz, T. H., and D. S. Reynolds. 2003. Bat colonies in buildings. Pages 91–102 in *Monitoring trends in bat populations of the United States and territories: problems and prospects*:1–12. U.S. Geological Survey. 274 pp.
- Kunz, T. H., and E. L. P. Anthony. 1982. Age estimation and post-natal growth in the bat *Myotis lucifugus*. *Journal of Mammalogy* 63:23–32.

- Kunz, T. H., and E. L. P. Anthony. 1996. Variation in the timing of nightly emergence behavior in the little brown bat, *Myotis lucifugus* (Chiroptera: Vespertilionidae). *Contributions in Mammalogy: A Memorial Volume Honoring Dr. J. Knox Jones, Jr.*:225–235.
- Kunz, T. H., E. Bicer, W. R. Hood, M. J. Axtell, W. R. Harrington, B. A. Silvia, and E. P. Widmaier. 1999. Plasma leptin decreases during lactation in insectivorous bats. *Journal of Comparative Physiology B* 169:61–66.
- Kunz, T. H., J. A. Wrazen, and C. D. Burnett. 1998. Changes in body mass and fat reserves in prehibernating little brown bats (*Myotis lucifugus*). *Écoscience* 5:8–17.
- Kunz, T. H., R. A. Adams, and W. R. Hood. 2009. Methods for assessing size at birth and postnatal growth and development in bats. Pages 273–315 *in* *Ecological and Behavioral Methods for the Study of Bats*. The John Hopkins University Press, Baltimore.
- Kurta, A. 1985. External insulation available to a non-nesting mammal, the little brown bat (*Myotis lucifugus*). *Comparative Biochemistry and Physiology* 82A:413–420.
- Kurta, A., G. P. Bell, K. A. Nagy, and T. H. Kunz. 1989. Energetics of pregnancy and lactation in freeranging little brown bats (*Myotis lucifugus*). *Physiological Zoology* 62:804–818.
- Laake, J. L. 2013. RMark: An R Interface for analysis of capture-recapture data with MARK. AFSC Processed Rep. 2013-01, 25 p. Alaska Fisheries Science Center, National Oceanic and Atmospheric Administration, National Marine Fisheries Service, 7600 Sand Point Way NE, Seattle WA 98115.
- Laake, J., and E. Rexstad. 2017. RMark - an alternative approach to building linear models in MARK. Appendix C *in* Program MARK: a gentle introduction. Available online from <www.phidot.org/software/mark/docs/book/>.
- Lachish, S., H. McCallum, and M. Jones. 2009. Demography, disease and the devil: life-history changes in a disease-affected population of Tasmanian devils (*Sarcophilus harrisi*). *Journal of Animal Ecology* 78:427–436.
- Lampo, M., S. J. Celsa, A. Rodríguez-Contreras, F. Rojas-Runjaic, and C. Z. García. 2011. High turnover rates in remnant populations of the Harlequin frog *Atelopus cruciger* (Bufonidae): low risk of extinction? *Biotropica* 44:420–426.
- Langwig, K. E., J. R. Hoyt, K. L. Parise, W. F. Frick, J. T. Foster, and A. M. Kilpatrick. 2017. Resistance in persisting bat populations after white-nose syndrome invasion. *Philosophical Transactions of the Royal Society B: Biological Sciences* 372:20160044.
- Langwig, K. E., J. Voyles, M. Q. Wilber, W. F. Frick, K. A. Murray, B. M. Bolker, J. P. Collins, T. L. Cheng, M. C. Fisher, J. R. Hoyt, D. L. Lindner, H. I. McCallum, R. Puschendorf, E. B. Rosenblum, M. Toothman, C. K. Willis, C. J. Briggs, and A. M. Kilpatrick. 2015a. Context-dependent conservation responses to emerging wildlife diseases. *Frontiers in Ecology and the Environment* 13:195–202.

- Langwig, K. E., W. F. Frick, J. T. Bried, A. C. Hicks, T. H. Kunz, and A. Marm Kilpatrick. 2012. Sociality, density-dependence and microclimates determine the persistence of populations suffering from a novel fungal disease, white-nose syndrome. *Ecology Letters* 15:1050–1057.
- Langwig, K. E., W. F. Frick, R. Reynolds, K. L. Parise, K. P. Drees, J. R. Hoyt, T. L. Cheng, T. H. Kunz, J. T. Foster, and A. M. Kilpatrick. 2015b. Host and pathogen ecology drive the seasonal dynamics of a fungal disease, white-nose syndrome. *Proceedings of the Royal Society B: Biological Sciences* 282:20142335.
- Lazenby, B. T., M. W. Tobler, W. E. Brown, C. E. Hawkins, G. J. Hocking, F. Hume, S. Huxtable, P. Iles, M. E. Jones, C. Lawrence, S. Thalmann, P. Wise, H. Williams, S. Fox, and D. Pemberton. 2018. Density trends and demographic signals uncover the long-term impact of transmissible cancer in Tasmanian devils. *Journal of Applied Ecology* 55:1368–1379.
- Lenihan, C., and D. Van Vuren. 1996. Growth and survival of juvenile yellow-bellied marmots. *Canadian Journal of Zoology* 74:297–302.
- Lilley, T. M., I. W. Wilson, K. A. Field, D. M. Reeder, M. E. Vodzak, G. G. Turner, A. Kurta, A. S. Blomberg, S. Hoff, C. J. Herzog, B. J. Sewall, and S. Paterson. 2020. Genome-wide changes in genetic diversity in a population of *Myotis lucifugus* affected by white-nose syndrome. *G3: Genes, Genomes, Genetics* 10:2007–2020.
- Lilley, T. M., J. S. Johnson, L. Ruokolainen, E. J. Rogers, C. A. Wilson, S. M. Schell, K. A. Field, and D. M. Reeder. 2016. White-nose syndrome survivors do not exhibit frequent arousals associated with *Pseudogymnoascus destructans* infection. *Frontiers in Zoology* 13:1–8.
- Lin, J.-W., H.-Y. Lo, H.-C. Wang, and P.-J. L. Shaner. 2014. The effects of mite parasitism on the reproduction and survival of the Taiwan field mice (*Apodemus semotus*). *Zoological Studies* 53:79.
- Lindner, D. L., A. Gargas, J. M. Lorch, M. T. Banik, J. Glaeser, T. H. Kunz, and D. S. Blehert. 2011. DNA-based detection of the fungal pathogen *Geomyces destructans* in soils from bat hibernacula. *Mycologia* 103:241–246.
- Linton, D. M., and D. W. MacDonald. 2018. Spring weather conditions influence breeding phenology and reproductive success in sympatric bat populations. *Journal of Animal Ecology* 87:1080–1090.
- Lorch, J. M., C. U. Meteyer, M. J. Behr, J. G. Boyles, P. M. Cryan, A. C. Hicks, A. E. Ballmann, J. T. H. Coleman, D. N. Redell, D. M. Reeder, and D. S. Blehert. 2011. Experimental infection of bats with *Geomyces destructans* causes white-nose syndrome. *Nature* 480:376–378.

- Lorch, J. M., L. K. Muller, R. E. Russell, M. O'Connor, D. L. Lindner, and D. S. Blehert. 2013. Distribution and environmental persistence of the causative agent of white-nose syndrome, *Geomyces destructans*, in bat hibernacula of the eastern United States. *Applied and Environmental Microbiology* 79:1293–1301.
- Lučan, R. K., M. Weiser, and V. Hanák. 2013. Contrasting effects of climate change on the timing of reproduction and reproductive success of a temperate insectivorous bat. *Journal of Zoology* 290:151–159.
- Lund, T. C., T. J. Glass, J. Tolar, and B. R. Blazar. 2009. Expression of telomerase and telomere length are unaffected by either age or limb regeneration in *Danio rerio*. *PLoS ONE* 4:e7688.
- Ma, S., A. Upneja, A. Galecki, Y.-M. Tsai, C. F. Burant, S. Raskind, Q. Zhang, Z. D. Zhang, A. Seluanov, V. Gorbunova, C. B. Clish, R. A. Miller, and V. N. Gladyshev. 2016. Cell culture-based profiling across mammals reveals DNA repair and metabolism as determinants of species longevity. *eLife* 5:e19130.
- Maslo, B., and N. H. Fefferman. 2015. A case study of bats and white-nose syndrome demonstrating how to model population viability with evolutionary effects. *Conservation Biology* 29:1176–1185.
- Maslo, B., M. Valent, J. F. Gumbs, and W. F. Frick. 2015. Conservation implications of ameliorating survival of little brown bats with white-nose syndrome. *Ecological Applications* 25:1832–1840.
- Mason, M. K., D. Hockman, D. S. Jacobs, and N. Illing. 2010. Evaluation of maternal features as indicators of asynchronous embryonic development in *Miniopterus natalensis*. *Acta Chiropterologica* 12:161–171.
- McGuire, L. P., H. W. Mayberry, Q. E. Fletcher, and C. K. R. Willis. 2019. An experimental test of energy and electrolyte supplementation as a mitigation strategy for white-nose syndrome. *Conservation Physiology* 7:89–8.
- McGuire, L. P., M. B. Fenton, and C. G. Guglielmo. 2009. Effect of age on energy storage during prehibernation swarming in little brown bats (*Myotis lucifugus*). *Canadian Journal of Zoology* 87:515–519.
- McKnight, D. T., L. Schwarzkopf, R. A. Alford, D. S. Bower, and K. R. Zenger. 2017. Effects of emerging infectious diseases on host population genetics: a review. *Conservation Genetics* 18:1235–1245.
- McLennan, D., J. D. Armstrong, D. C. Stewart, S. Mckelvey, W. Boner, P. Monaghan, and N. B. Metcalfe. 2016. Interactions between parental traits, environmental harshness and growth rate in determining telomere length in wild juvenile salmon. *Molecular Ecology* 25:5425–5438.

- Meteyer, C. U., D. Barber, and J. N. Mandl. 2012. Pathology in euthermic bats with white nose syndrome suggests a natural manifestation of immune reconstitution inflammatory syndrome. *Virulence* 3:583–588.
- Meteyer, C. U., M. Valent, J. Kashmer, E. L. Buckles, J. M. Lorch, D. S. Blehert, A. Lollar, D. Berndt, E. Wheeler, C. L. White, and A. E. Ballmann. 2011. Recovery of little brown bats (*Myotis lucifugus*) from natural infection with *Geomyces destructans*, white-nose syndrome. *Journal of Wildlife Diseases* 47:618–626.
- Meyer, G. A., J. A. Senulis, and J. A. Reinartz. 2016. Effects of temperature and availability of insect prey on bat emergence from hibernation in spring. *Journal of Mammalogy* 97:1623–1633.
- Mills, L. S. 2013. *Conservation of Wildlife Populations*. Second edition. Wiley-Blackwell, Chichester, UK.
- Monaghan, P. 2010. Telomeres and life histories: the long and the short of it. *Annals of the New York Academy of Sciences* 1206:130–142.
- Moore, M. S., J. D. Reichard, T. D. Murtha, M. L. Nabhan, R. E. Pian, J. S. Ferreira, and T. H. Kunz. 2013. Hibernating little brown *Myotis (Myotis lucifugus)* show variable immunological responses to white-nose syndrome. *PLoS ONE* 8:e58976.
- Morgan, C. C., A. M. McCartney, M. T. Donoghue, N. B. Loughran, C. Spillane, E. C. Teeling, and M. J. O’Connell. 2013. Molecular adaptation of telomere associated genes in mammals. *BMC Evolutionary Biology* 13:251.
- Morris, W. F., and D. F. Doak. 2002. *Quantitative Conservation Biology: Theory and Practice of Population Viability Analysis*. Sinauer Associates, Inc., Sunderland, MA.
- Muller, L. K., J. M. Lorch, D. L. Lindner, M. O’Connor, A. Gargas, and D. S. Blehert. 2013. Bat white-nose syndrome: a real-time TaqMan polymerase chain reaction test targeting the intergenic spacer region of *Geomyces destructans*. *Mycologia* 105:253–259.
- Mulvey, M., J. M. Aho, and O. E. Rhodes Jr. 1994. Parasitism and white-tailed deer: timing and components of female reproduction. *Oikos* 70:177–182.
- Murray, D. L., E. W. Cox, W. B. Ballard, H. A. Whitlaw, M. S. Lenarz, T. W. Custer, T. Barnett, and T. K. Fuller. 2006. Pathogens, nutritional deficiency, and climate influences on a declining moose population. *Wildlife Monographs* 166:1–30.
- Muths, E., R. D. Scherer, and D. S. Pilliod. 2011. Compensatory effects of recruitment and survival when amphibian populations are perturbed by disease. *Journal of Applied Ecology* 48:873–879.
- Møller, A. P., E. Flensted-Jensen, and W. Mardal. 2006. Rapidly advancing laying date in a seabird and the changing advantage of early reproduction. *Journal of Animal Ecology* 75:657–665.

- Nakagawa, S., N. J. Gemmell, and T. Burke. 2004. Measuring vertebrate telomeres: applications and limitations. *Molecular Ecology* 13:2523–2533.
- Neubaum, D. J. 2018. Unsuspected retreats: autumn transitional roosts and presumed winter hibernacula of little brown myotis in Colorado. *Journal of Mammalogy* 99:1294–1306.
- Neubaum, D. J., K. R. Wilson, and T. J. O'Shea. 2007. Urban maternity-roost selection by big brown bats in Colorado. *Journal of Wildlife Management* 71:728–736.
- Newell, D. A., R. L. Goldingay, and L. O. Brooks. 2013. Population recovery following decline in an endangered stream-breeding frog (*Mixophyes fleayi*) from subtropical Australia. *PLoS ONE* 8:e58559.
- Norquay, K. J. O., and C. K. R. Willis. 2014. Hibernation phenology of *Myotis lucifugus*. *Journal of Zoology* 294:85–92.
- Norquay, K. J. O., F. Martinez-Nuñez, J. E. Dubois, K. M. Monson, and C. K. R. Willis. 2013. Long-distance movements of little brown bats (*Myotis lucifugus*). *Journal of Mammalogy* 94:506–515.
- Nussey, D. H., D. Baird, E. Barrett, W. Boner, J. Fairlie, N. Gemmell, N. Hartmann, T. Horn, M. Haussmann, M. Olsson, C. Turbill, S. Verhulst, S. Zahn, and P. Monaghan. 2014. Measuring telomere length and telomere dynamics in evolutionary biology and ecology. *Methods in Ecology and Evolution* 5:299–310.
- O'Farrell, M. J., and E. H. Studier. 1973. Reproduction, growth, and development in *Myotis thysanodes* and *M. lucifugus*. *Ecology* 54:18–30.
- O'Shea, T. J., L. E. Ellison, and T. R. Stanley. 2011. Adult survival and population growth rate in Colorado big brown bats (*Eptesicus fuscus*). *Journal of Mammalogy* 92:433–443.
- Olsen, E. M., M. Heino, G. R. Lilly, M. J. Morgan, J. Brattey, B. Ernande, and U. Dieckmann. 2004. Maturation trends indicative of rapid evolution preceded the collapse of northern cod. *Nature* 428:932–935.
- Olson, C. R., and R. M. R. Barclay. 2013. Concurrent changes in group size and roost use by reproductive female little brown bats (*Myotis lucifugus*). *Canadian Journal of Zoology* 91:149–155.
- Oyler-McCance, S. J., J. A. Fike, P. M. Lukacs, D. W. Sparks, T. J. O'Shea, and J. O. Whitaker Jr. 2018. Genetic mark-recapture improves estimates of maternity colony size for Indiana bats. *Journal of Fish and Wildlife Management* 9:25–35.
- Padhi, S., I. Dias, V. Korn, and J. Bennett. 2018. *Pseudogymnoascus destructans*: causative agent of white-nose syndrome in bats is inhibited by safe volatile organic compounds. *Journal of Fungi* 4:48–12.

- Palmer, J. M., K. P. Drees, J. T. Foster, and D. L. Lindner. 2017. Extreme sensitivity to ultraviolet light in the fungal pathogen causing white-nose syndrome of bats. *Nature Communications*:1–10.
- Paradiso, J. L., and A. M. Greenhall. 1967. Longevity records for American bats. *The American Midland Naturalist* 78:251–252.
- Pearson, O. P., M. R. Koford, and A. K. Pearson. 1952. Reproduction of the lump-nosed bat (*Corynorhinus rafinesquei*) in California. *Journal of Mammalogy* 33:273–320.
- Pfaffl, M. W. 2001. A new mathematical model for relative quantification in real-time RT–PCR. *Nucleic Acids Research* 29:e45.
- Phillips, C. J., B. Steinberg, and T. H. Kunz. 1982. Dentin, cementum, and age determination in bats: a critical evaluation. *Journal of Mammalogy* 63:197–207.
- Plummer, M. 2003. JAGS: A program for analysis of Bayesian graphical models using Gibbs sampling. *Proceedings of the 3rd International Workshop on Distributed Statistical Computing*:1–10.
- Pollock, T., C. R. Moreno, L. Sánchez, A. Ceballos-Vasquez, P. A. Faure, and E. C. Mora. 2015. Wound healing in the flight membranes of wild big brown bats. *The Journal of Wildlife Management* 80:19–26.
- Pradel, R., J. E. Hines, J.-D. Lebreton, and J. D. Nichols. 1997. Capture-recapture survival models taking account of transients. *Biometrics* 53:60–72.
- Price, T., M. Kirkpatrick, and S. J. Arnold. 1988. Directional selection and the evolution of breeding date in birds. *Science* 240:798–799.
- Puechmaille, S. J., G. Mathy, and E. J. Petit. 2007. Good DNA from bat droppings. *Acta Chiropterologica* 9:269–276.
- R Core Team. 2018. R: a language and environment for statistical computing. R Foundation for Statistical Computing, Vienna, Austria.
- Racey, P. A. 1969. Diagnosis of pregnancy and experimental extension of gestation in the Pipistrelle bat, *Pipistrellus pipistrellus*. *Journal of Reproduction and Fertility* 19:465–474.
- Racey, P. A. 1973. Environmental factors affecting the length of gestation in heterothermic bats. *Journal of Reproduction and Fertility* 19:175–189.
- Racey, P. A. 2009. Reproductive assessment of bats. Pages 249–264 *in* T. H. Kunz and S. Parsons, editors. *Ecological and Behavioral Methods for the Study of Bats*. Second edition. The John Hopkins University Press, Baltimore, Maryland.
- Racey, P. A., and A. C. Entwistle. 2000. Life-history and reproductive strategies of bats. Pages 363–414 *in* *Reproductive Biology of Bats*. Academic Press, San Diego, CA.

- Racey, P. A., and S. M. Swift. 1981. Variations in gestation length in a colony of pipistrelle bats (*Pipistrellus pipistrellus*) from year to year. *Journal of Reproduction and Fertility* 61:123–129.
- Racey, P. A., J. R. Speakman, and S. M. Swift. 1987. Reproductive adaptations of heterothermic bats at the northern borders of their distribution. *South African Journal of Science* 33:635–638.
- Ramón-Laca, A., L. Soriano, D. Gleeson, and J. A. Godoy. 2015. A simple and effective method for obtaining mammal DNA from faeces. *Wildlife Biology* 21:195–203.
- Ransome, R. D. 1989. Population changes of Greater horseshoe bats studied near Bristol over the past twenty-six years. *Biological Journal of the Linnean Society* 38:71–82.
- Ransome, R. D. 1995. Earlier breeding shortens life in female greater horseshoe bats. *Philosophical Transactions of the Royal Society B: Biological Sciences* 350:153–161.
- Ransome, R. D., and T. P. McOwat. 1994. Birth timing and population changes in greater horseshoe bat colonies (*Rhinolophus ferrumequinum*) are synchronized by climatic temperature. *Zoological Journal of the Linnean Society* 112:337–351.
- Reeder, D. M., C. L. Frank, G. G. Turner, C. U. Meteyer, A. Kurta, E. R. Britzke, M. E. Vodzak, S. R. Darling, C. W. Stihler, A. C. Hicks, R. Jacob, L. E. Grieneisen, S. A. Brownlee, L. K. Muller, and D. S. Blehert. 2012. Frequent arousal from hibernation linked to severity of infection and mortality in bats with white-nose syndrome. *PLoS ONE* 7:e38920.
- Reichard, J. D., and T. H. Kunz. 2009. White-nose syndrome inflicts lasting injuries to the wings of little brown myotis (*Myotis lucifugus*). *Acta Chiropterologica* 11:457–464.
- Reichard, J. D., L. E. Gonzalez, C. M. Casey, L. C. Allen, N. I. Hristov, and T. H. Kunz. 2009. Evening emergence behavior and seasonal dynamics in large colonies of Brazilian free-tailed bats. *Journal of Mammalogy* 90:1478–1486.
- Reichard, J. D., N. W. Fuller, A. B. Bennett, S. R. Darling, M. S. Moore, K. E. Langwig, E. D. Preston, S. V. Oettingen, C. S. Richardson, and D. Scott Reynolds. 2014. Interannual survival of *Myotis lucifugus* (Chiroptera: Vespertilionidae) near the epicenter of white-nose syndrome. *Northeastern Naturalist* 21:N56–N59.
- Reichert, S., F. Criscuolo, E. Verinaud, S. Zahn, and S. Massemin. 2013. Telomere length correlations among somatic tissues in adult zebra finches. *PLoS ONE* 8:e81496.
- Reiter, J., and B. J. Le Boeuf. 1991. Life history consequences of variation in age at primiparity in northern elephant seals. *Behavioral Ecology and Sociobiology* 28:153–160.
- Reynolds, D. S. 1999. Variation in life history traits in the little brown bat, *Myotis lucifugus* (Chiroptera: Vespertilionidae). Ph.D. dissertation. Boston University. Boston, Massachusetts.

- Richardson, C. S., T. Heeren, E. P. Widmaier, and T. H. Kunz. 2009. Macro- and microgeographic variation in metabolism and hormone correlates in big brown bats (*Eptesicus fuscus*). *Physiological and Biochemical Zoology* 82:798–811.
- Riecke, T. V., P. J. Williams, T. L. Behnke, D. Gibson, A. G. Leach, B. S. Sedinger, P. A. Street, and J. S. Sedinger. 2019. Integrated population models: model assumptions and inference. *Methods in Ecology and Evolution* 10:1072–1082.
- Roach, D. A., and J. R. Carey. 2014. Population biology of aging in the wild. *Annual Review of Ecology, Evolution, and Systematics* 45:421–443.
- Rocke, T. E., B. Kingstad-Bakke, M. Wüthrich, Ben Stading, R. C. Abbott, M. Isidoro-Ayza, H. E. Dobson, L. dos Santos Dias, K. Galles, J. S. Lankton, E. A. Falendysz, J. M. Lorch, J. S. Fites, J. Lopera-Madrid, J. P. White, B. Klein, and J. E. Osorio. 2019. Virally-vectored vaccine candidates against white-nose syndrome induce anti-fungal immune response in little brown bats (*Myotis lucifugus*). *Scientific Reports* 9:6788.
- Rollings, N., E. J. Uhrig, R. W. Krohmer, H. L. Wayne, R. T. Mason, M. Olsson, C. M. Whittington, and C. R. Friesen. 2017. Age-related sex differences in body condition and telomere dynamics of red-sided garter snakes. *Proceedings of the Royal Society of London B: Biological Sciences* 284:20162146.
- Ruijter, J. M., C. Ramakers, W. M. H. Hoogaars, Y. Karlen, O. Bakker, M. J. B. van den Hoff, and A. F. M. Moorman. 2009. Amplification efficiency: linking baseline and bias in the analysis of quantitative PCR data. *Nucleic Acids Research* 37:e45.
- Russell, R. E., W. E. Thogmartin, R. A. Erickson, J. Szymanski, and K. Tinsley. 2015. Estimating the short-term recovery potential of little brown bats in the eastern United States in the face of White-nose syndrome. *Ecological Modelling* 314:111–117.
- Rydell, J. 1989. Feeding activity of the northern bat *Eptesicus nilssoni* during pregnancy and lactation. *Oecologia* 80:562–565.
- Salmón, P., J. F. Nilsson, H. Watson, S. Bensch, and C. Isaksson. 2017. Selective disappearance of great tits with short telomeres in urban areas. *Proceedings of the Royal Society of London B: Biological Sciences* 284:20171349.
- Sapsford, S. J., M. J. Voordouw, R. A. Alford, and L. Schwarzkopf. 2015. Infection dynamics in frog populations with different histories of decline caused by a deadly disease. *Oecologia* 179:1099–1110.
- Schaub, M., and F. Abadi. 2010. Integrated population models: a novel analysis framework for deeper insights into population dynamics. *Journal of Ornithology* 152:227–237.
- Scheele, B. C., L. F. Skerratt, L. F. Grogan, D. A. Hunter, N. Clemann, M. McFadden, D. Newell, C. J. Hoskin, G. R. Gillespie, G. W. Heard, L. Brannelly, A. A. Roberts, and L. Berger. 2017. After the epidemic: ongoing declines, stabilizations and recoveries in amphibians afflicted by chytridiomycosis. *Biological Conservation* 206:37–46.

- Schmidt, J. E., A. E. Sirman, J. D. Kittilson, M. E. Clark, W. L. Reed, and B. J. Heidinger. 2016. Telomere correlations during early life in a long-lived seabird. *Experimental Gerontology* 85:28–32.
- Schowalter, D. B., J. R. Gunson, and L. D. Harder. 1979. Life history characteristics of little brown bats (*Myotis lucifugus*) in Alberta. *The Canadian Field-Naturalist* 93:243–251.
- Scott, M. E. 1988. The impact of infection and disease on animal populations: implications for conservation biology. *Conservation Biology* 2:40–56.
- Seber, G. A. F. 1982. The estimation of animal abundance and related parameters. Second edition. MacMillan Press, New York, New York.
- Sedgeley, J. A. 2001. Quality of cavity microclimate as a factor influencing selection of maternity roosts by a tree-dwelling bat, *Chalinolobus tuberculatus*, in New Zealand. *Journal of Applied Ecology* 38:425–438.
- Sikes, R. S., and W. L. Gannon. 2011. Guidelines of the American Society of Mammalogists for the use of wild mammals in research. *Journal of Mammalogy* 92:235–253.
- Sikes, R. S., and the Animal Care and Use Committee of the American Society of Mammalogists. 2016. Guidelines of the American Society of Mammalogists for the use of wild mammals in research and education. *Journal of Mammalogy* 97:663–688.
- Smith, S., C. Turbill, and D. J. Penn. 2011. Chasing telomeres, not red herrings, in evolutionary ecology. *Heredity* 107:372–373.
- Solick, D. I., and R. M. R. Barclay. 2007. Geographic variation in the use of torpor and roosting behaviour of female western long-eared bats. *Journal of Zoology* 272:358–366.
- Spurgin, L. G., K. Bebbington, E. A. Fairfield, M. Hammers, J. Komdeur, T. Burke, H. L. Dugdale, and D. S. Richardson. 2017. Spatio-temporal variation in lifelong telomere dynamics in a long-term ecological study. *Journal of Animal Ecology* 87:187–198.
- Squier, C. A., and M. J. Kremer. 2001. Biology of oral mucosa and esophagus. *Journal of the National Cancer Institute Monographs* 29:7–15.
- Stearns, S. C. 1989. Trade-offs in life-history evolution. *Functional Ecology* 3:259–268.
- Stearns, S. C. 1992. *The Evolution of Life Histories*. Oxford University Press, Oxford, United Kingdom.
- Steenstrup, T., J. V. B. Hjelmborg, J. D. Kark, K. Christensen, and A. Aviv. 2013. The telomere lengthening conundrum—artifact or biology? *Nucleic Acids Research* 41:e131.
- Studier, E. H., and M. J. O'Farrell. 1972. Biology of *Myotis thysanodes* and *M. lucifugus* (Chiroptera: Vespertilionidae) - I. Thermoregulation. *Comparative Biochemistry and Physiology* 41A:567–595.

- Su, Y.-S., and M. Yajima. 2020. R2jags: Using R to Run “JAGS.” R Package version 0.6-1. Retrieved from <<https://cran.r-project.org/web/packages/R2jags/>>.
- Taberlet, P., L. P. Waits, and G. Luikart. 1999. Noninvasive genetic sampling: look before you leap. *Trends in Ecology & Evolution* 14:323–327.
- Theda, C., S. H. Hwang, A. Czajko, Y. J. Loke, P. Leong, and J. M. Craig. 2018. Quantitation of the cellular content of saliva and buccal swab samples. *Scientific Reports* 8:6944.
- Thomas, D. W. 1995. Hibernating bats are sensitive to nontactile human disturbance. *Journal of Mammalogy* 76:940–946.
- Thomas, P., N. J. O'Callaghan, and M. Fenech. 2008. Telomere length in white blood cells, buccal cells and brain tissue and its variation with ageing and Alzheimer's disease. *Mechanisms of Ageing and Development* 129:183–190.
- Tian, X., A. Seluanov, and V. Gorbunova. 2017. Molecular mechanisms determining lifespan in short- and long-lived species. *Trends in Endocrinology & Metabolism* 28:722–734.
- Tian, X., K. Doerig, R. Park, A. Can Ran Qin, C. Hwang, A. Neary, M. Gilbert, A. Seluanov, and V. Gorbunova. 2018. Evolution of telomere maintenance and tumour suppressor mechanisms across mammals. *Philosophical Transactions of the Royal Society B: Biological Sciences* 373:20160443.
- Turbill, C., S. Smith, C. Deimel, and T. Ruf. 2012. Daily torpor is associated with telomere length change over winter in Djungarian hamsters. *Biology Letters* 8:304–307.
- Turner, G. G., D. A. Reeder, and J. T. H. Coleman. 2011. A five-year assessment of mortality and geographic spread of white-nose syndrome in North American Bats and a look to the future. *Bat Research News* 52:13–27.
- Tuttle, M. D. 1976. Population ecology of the gray bat (*Myotis grisescens*): factors influencing growth and survival of newly volant young. *Ecology* 57:587–595.
- Ujvari, B., P. A. Biro, J. E. Charters, G. Brown, K. Heasman, C. Beckmann, and T. Madsen. 2017. Curvilinear telomere length dynamics in a squamate reptile. *Functional Ecology* 31:753–759.
- van de Pol, M., and J. Wright. 2009. A simple method for distinguishing within- versus between-subject effects using mixed models. *Animal Behaviour* 77:753–758.
- van Lieshout, S. H. J., A. Bretman, C. Newman, C. D. Buesching, D. W. MacDonald, and H. L. Dugdale. 2019. Individual variation in early-life telomere length and survival in a wild mammal. *Molecular Ecology* 28:4152–4165.
- Vitková, M., J. Král, W. Traut, J. Zrzavý, and F. Marec. 2005. The evolutionary origin of insect telomeric repeats, (TTAGG)_n. *Chromosome Research* 13:145–156.

- von Zglinicki, T. 2002. Oxidative stress shortens telomeres. *Trends in Biochemical Sciences* 27:339–344.
- Vonhof, M. J., A. L. Russell, and C. M. Miller-Butterworth. 2015. Range-wide genetic analysis of little brown bat (*Myotis lucifugus*) populations: estimating the risk of spread of white-nose syndrome. *PLoS ONE* 10:e0128713–23.
- Voyles, J., D. C. Woodhams, V. Saenz, A. Q. Byrne, R. Perez, G. Rios-Sotelo, M. J. Ryan, M. C. Bletz, F. A. Sobell, S. McLetchie, L. Reinert, E. B. Rosenblum, L. A. Rollins-Smith, R. Ibáñez, J. M. Ray, E. J. Griffith, H. Ross, and C. L. Richards-Zawacki. 2018. Shifts in disease dynamics in a tropical amphibian assemblage are not due to pathogen attenuation. *Science* 359:1517–1519.
- Walker, F. M., C. H. D. Williamson, D. E. Sanchez, C. J. Sobek, and C. L. Chambers. 2016. Species from feces: order-wide identification of Chiroptera from guano and other non-invasive genetic samples. *PLoS ONE* 11:e0162342.
- Warnecke, L., J. M. Turner, T. K. Bollinger, J. M. Lorch, V. Misra, P. M. Cryan, G. Wibbelt, D. S. Blehert, and C. K. R. Willis. 2012. Inoculation of bats with European *Geomyces destructans* supports the novel pathogen hypothesis for the origin of white-nose syndrome. *Proceedings of the National Academy of Sciences of the United States of America* 109:6999–7003.
- Wasser, S. K., and D. P. Barash. 1983. Reproductive suppression among female mammals: Implications for biomedicine and sexual selection theory. *The Quarterly Review of Biology* 58:513–538.
- Weaver, K. N., S. E. Alfano, A. R. Kronquist, and D. M. Reeder. 2009. Healing rates of wing punch wounds in free-ranging little brown *Myotis (Myotis lucifugus)*. *Acta Chiropterologica* 11:220–223.
- Webb, P. I., J. R. Speakman, and P. A. Racey. 1996. Population dynamics of a maternity colony of the pipistrelle bat (*Pipistrellus pipistrellus*) in north-east Scotland. *Journal of the Zoological Society of London* 240:777–780.
- White, G. C., and K. P. Burnham. 1999. Program MARK: survival estimation from populations of marked animals. *Bird Study* 46:S120–S139.
- White, J. P., G. E. Nordquist, and H. M. Kaarakka. 2019. Longevity records of five male little brown bats (*Myotis lucifugus*) in Northwest Wisconsin. *Northeastern Naturalist* 26:N43–N46.
- Wilcox, A., and C. K. R. Willis. 2016. Energetic benefits of enhanced summer roosting habitat for little brown bats (*Myotis lucifugus*) recovering from white-nose syndrome. *Conservation Physiology* 4:cov070.

- Wilder, A. P., T. H. Kunz, and M. D. Sorenson. 2015. Population genetic structure of a common host predicts the spread of white-nose syndrome, an emerging infectious disease in bats. *Molecular Ecology* 24:5495–5506.
- Wilkinson, G. S., and D. M. Adams. 2019. Recurrent evolution of extreme longevity in bats. *Biology Letters* 15:20180860.
- Wilkinson, G. S., and J. M. South. 2002. Life history, ecology and longevity in bats. *Aging Cell* 1:124–131.
- Willis, C. K. R., and R. M. Brigham. 2007. Social thermoregulation exerts more influence than microclimate on forest roost preferences by a cavity-dwelling bat. *Behavioral Ecology and Sociobiology* 62:97–108.
- Wimsatt, W. A. 1945. Notes on breeding behavior, pregnancy, and parturition in some vespertilionid bats of the eastern United States. *Journal of Mammalogy* 26:23–33.
- Wojciechowski, M. S., M. Jefimow, and E. Tęgowska. 2007. Environmental conditions, rather than season, determine torpor use and temperature selection in large mouse-eared bats (*Myotis myotis*). *Comparative Biochemistry and Physiology Part A: Molecular & Integrative Physiology* 147:828–840.
- Wright, P. G. R., F. Mathews, H. Schofield, C. Morris, J. Burrage, A. Smith, E. L. Dempster, and P. B. Hamilton. 2018. Application of a novel molecular method to age free-living wild Bechstein's bats. *Molecular Ecology Resources* 18:1374–1380.
- Yap, T. A., M. S. Koo, R. F. Ambrose, D. B. Wake, and V. T. Vredenburg. 2015. Averting a North American biodiversity crisis. *Science* 349:481–482.
- Zahn, A. 1999. Reproductive success, colony size and roost temperature in attic-dwelling bat *Myotis myotis*. *Journal of Zoology London* 247:275–280.
- Zipkin, E. F., and S. P. Saunders. 2018. Synthesizing multiple data types for biological conservation using integrated population models. *Biological Conservation* 217:240–250.

APPENDIX A

IACUC Approval for use of Animals in Research

University of New Hampshire

Research Integrity Services, Service Building
51 College Road, Durham, NH 03824-3585
Fax: 603-862-3564

04-Feb-2016

Foster, Jeffrey T
MCBS, Rudman Hall
Durham, NH 03824

IACUC #: 160105

Project: Comparative Genomics and Demographics to Assess the Evolution of Resistance to and the Impacts of White-Nose Syndrome in North American Bats

Approval Date: 26-Jan-2016

The Institutional Animal Care and Use Committee (IACUC) reviewed and approved the protocol submitted for this study under Category D on Page 5 of the Application for Review of Vertebrate Animal Use in Research or Instruction - *Animal use activities that involve accompanying pain or distress to the animals for which appropriate anesthetic, analgesic, tranquilizing drugs or other methods for relieving pain or distress are used.*

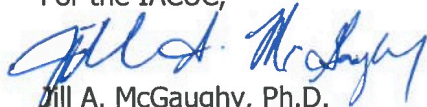
Approval is granted for a period of three years from the approval date above. Continued approval throughout the three year period is contingent upon completion of annual reports on the use of animals. At the end of the three year approval period you may submit a new application and request for extension to continue this project. Requests for extension must be filed prior to the expiration of the original approval.

Please Note:

1. All cage, pen, or other animal identification records must include your IACUC # listed above.
2. Use of animals in research and instruction is approved contingent upon participation in the UNH Occupational Health Program for persons handling animals. Participation is mandatory for all principal investigators and their affiliated personnel, employees of the University and students alike. Information about the program, including forms, is available at <http://unh.edu/research/occupational-health-program-animal-handlers>.

If you have any questions, please contact either Dean Elder at 862-4629 or Julie Simpson at 862-2003.

For the IACUC,


Jill A. McGaughy, Ph.D.
Chair

cc: File

University of New Hampshire

Research Integrity Services, Service Building
51 College Road, Durham, NH 03824-3585
Fax: 603-862-3564

26-Feb-2019

Foster, Jeffrey T
Molecular Cellular & Biomedical Sci
Rudman Hall Rm 291
Durham, NH 03824-2618

IACUC #: 181209

Project: Comparative Genomics and Demographics to Assess the Impacts of White-Nose Syndrome in North American Bats

Approval Date: 28-Jan-2019

The Institutional Animal Care and Use Committee (IACUC) reviewed and approved the protocol submitted for this study under Category D in Section V of the Application for Review of Vertebrate Animal Use in Research or Instruction - *Animal use activities that involve accompanying pain or distress to the animals for which appropriate anesthetic, analgesic, tranquilizing drugs or other methods for relieving pain or distress are used.*

Approval is granted for a period of three years from the approval date above. Continued approval throughout the three year period is contingent upon completion of annual reports on the use of animals. At the end of the three year approval period you may submit a new application and request for extension to continue this project. Requests for extension must be filed prior to the expiration of the original approval.

Please Note:

1. All cage, pen, or other animal identification records must include your IACUC # listed above.
2. Use of animals in research and instruction is approved contingent upon participation in the UNH Occupational Health Program for persons handling animals. Participation is mandatory for all principal investigators and their affiliated personnel, employees of the University and students alike. Information about the program, including forms, is available at <http://unh.edu/research/occupational-health-program-animal-handlers>.

If you have any questions, please contact either Dean Elder at 862-4629 or Julie Simpson at 862-2003.

For the IACUC,



Rebecca Rowe, Ph.D.
Chair

cc: File

APPENDIX B

Supplementary Figures for Chapter 1

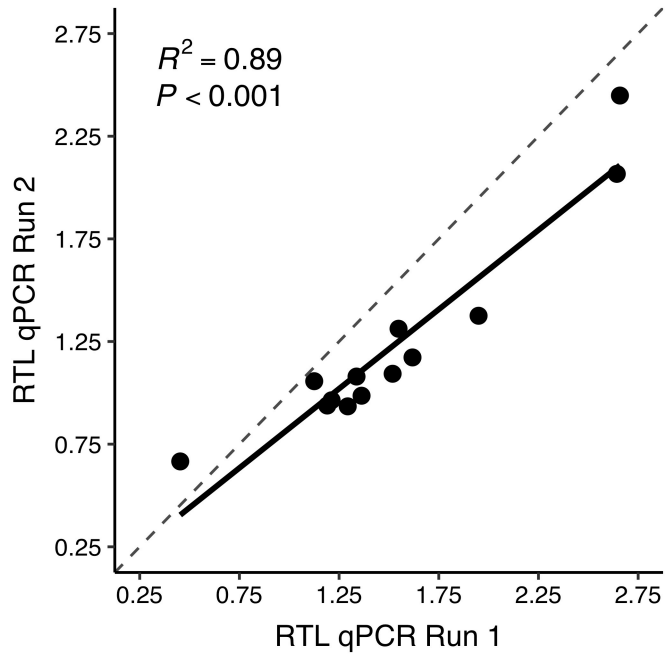


Figure B1. Plot showing repeatability in relative telomere length (RTL) measurements between qPCR runs of identical samples from little brown bat (*Myotis lucifugus*) wing tissue collected in New England, 2016–2019. The dashed line indicates a 1:1 reference line.

Table B1. Summary of linear mixed models of relative telomere length and predictor variables in little brown bats (*Myotis lucifugus*) sampled in New England, 2016–2019, with only 1- and 2-year-old bats included. Linear and quadratic age terms were considered along with reproductive status (Rep) and wing score (WS) at the time of capture. Coefficient estimates are shown for each model. K = number of parameters; logLik = log likelihood, w_i = model weight.

Model	Intercept	Age	Age ²	WS	Rep	K	logLik	AICc	Δ AICc	w_i
WS	1.239			-0.127		4	-25.64	62.1	0.00	0.52
Age + WS	1.258	-0.016		-0.127		5	-25.62	64.3	2.28	0.17
Null	1.150					3	-28.11	64.7	2.67	0.14
Rep	1.221				+	7	-24.26	66.5	4.14	0.06
Age	1.180	-0.024				4	-28.06	66.9	4.84	0.05
Rep + WS	1.255			-0.073	+	8	-23.71	67.9	5.83	0.03
Age ²	1.310	-0.258	0.090			5	-27.66	68.4	6.36	0.02
Age + Rep	1.197	-0.020			+	8	-24.23	68.9	6.88	0.02
Age + Rep + WS	1.226	-0.024		-0.073	+	9	-23.67	70.4	8.34	0.01